Ana Catarina Barros Lopes

Small Chiral Molecules Modulators of P-gp: Synthesis and Studies of Enantioselectivity

Dissertação do 2º Ciclo de Estudos Conducente ao Grau de Mestre em Toxicologia Analítica, Clínica e Forense

Trabalho realizado sobre a orientação das professoras:

Prof. Doutora Carla Sofia Garcia Fernandes
Doutora Renata Sofia Araújo da Silva

novembro 2016

Elaborated under supervision of:

- Prof. Doutora Carla Sofia Garcia Fernandes
  Faculdade de Farmácia da Universidade do Porto/ Centro Interdisciplinar de Investigação Marinha e Ambiental (CIIMAR), Universidade do Porto

- Doutora Renata Sofia Araújo da Silva
  Faculdade de Farmácia da Universidade do Porto/ UCIBIO-REQUIMTE, Laboratório de Toxicologia, Departamento de Ciências Biológicas, Universidade do Porto

This work was developed in Laboratório de Química Orgânica e Farmacêutica, Departamento de Ciências Químicas and Laboratório de Toxicologia, Departamento de Ciências Biológicas, Faculdade de Farmácia da Universidade do Porto. This research was partially supported through national funds provided by FCT – Foundation for Science and Technology and European Regional Development Fund (ERDF) and COMPETE under the projects PEst-C/MAR/LA0015/2013, PTDC/MAR-BIO/4694/2014, and INNOVMAR - Innovation and Sustainability in the Management and Exploitation of Marine Resources, reference NORTE-01-0145-FEDER-000035, Research Line NOVELMAR.

The results presented in this dissertation are part of the following scientific communications:

Poster Communications

A. Lopes*, S. Long, C. Fernandes, M. Pinto, E. Sousa. “Synthesis of new thioxanthone derivatives”. 9th Meeting of Young Researches of University of Porto, Porto, Portugal. 17-19 February 2016.

A. Lopes*, R. Silva, C. Fernandes, F. Remião, M. Pinto, E. Sousa. “Chiral Thioxanthones as Promising P-glycoprotein Modulators”. 5th Portuguese Young Chemists Meeting and 1st European Young Chemists Meeting, Guimarães, Portugal. 26-29 April 2016.

A. Lopes*, Martyna Piskorska, R. Silva, C. Fernandes, A. Palmeira, F. Remião, M. M.M. Pinto, E. Sousa. "Studying the influence of stereochemistry in P-gp modulation: case-study with newly synthetized thioxanthones ". 1º Encontro Anual do Departamento de Ciências Biológicas da Faculdade de Farmácia da Universidade do Porto, Porto, Portugal. 19 July 2016.

* presenting author

Agradecimentos

Quero aproveitar para agradecer a todas as pessoas que me acompanharam ao longo destes dois anos e que me permitiram concluir o mestrado com sucesso, em especial:

Às minhas orientadoras, Prof. Carla Fernandes, Prof. Emília Sousa e Prof. Renata Silva, por me concederem a oportunidade de fazer parte deste trabalho de investigação, que me permitiu obter experiência em duas áreas muito interessantes que, apesar de serem bastante distintas, se complementam na perfeição. Agradeço também por todos os conhecimentos que me transmitiram e por toda a disponibilidade, apoio e incentivo proporcionados.

À Prof Maria de Lurdes Bastos, diretora do Mestrado em Toxicologia Analítica, Clínica e Forense, e a todos os professores que lecionaram neste mestrado pela transmissão de conhecimentos e pela disponibilidade prestada.

À Dr. Sara Cravo por toda a ajuda prestada, desde o primeiro dia, no laboratório de Química Orgânica e Farmacêutica e por realizar a análise de HPLC dos meus compostos.

À Maria Letícia Carraro e à Eva Martins pela ajuda e apoio disponibilizados ao longo do meu percurso no Laboratório de Química Orgânica e Farmacêutica e no Laboratório de Toxicologia, respetivamente. Agradeço também a amabilidade e simpatia com que sempre me trataram.

A todos os meus colegas de laboratório pelo espírito de entreajuda, pelo apoio e pelo ambiente harmonioso criado no laboratório, em especial à Cecília, à Daniela, ao Bruno e ao Phyo pelo companheirismo e incentivo prestados não só no laboratório, mas também fora dele.

A todos os meus amigos, e em especial à Andreia, à Ana, à Mariana, à Tânia e ao Jorge pelo companheirismo, apoio e motivação.

Aos meus pais por me apoiarem e me darem a oportunidade de me dedicar exclusivamente ao mestrado.

Abstract

The P-glycoprotein is an efflux pump belonging to the superfamily of ABC transporters, and promotes the outward transport of a wide range of structurally unrelated compounds, thus playing important physiological functions. Though its primary function is the protection of cells against toxic xenobiotics and endogenous metabolites, this membrane transporter also plays a relevant role in drug pharmacokinetic processes.

Recently, our group showed that newly synthesized thioxanthonic derivatives protected against toxic P-gp substrates, acting as potent inducers/activators of this transporter. Therefore, it is essential to discover new P-gp modulators and enlightening the stereoselectivity of this ABC transporter face to this class of modulators. In this dissertation, eight chiral thioxanthonic derivatives (ATx's **1-8**) were synthesized by Ullmann cross coupling reaction between the thioxanthone derivative 1-chloro-4-propoxy-9*H*-thioxanthen-9-one (**Tx**) and eight enantiomerically pure building blocks (A **9-16**). The structure elucidation of all synthesized compounds was carried out by spectroscopic methods, including IR, NMR (^{1}H, ^{13}C, HMBC and HSQC), and their purity evaluated by HPLC.

The evaluation of P-gp modulation of all the synthesized chiral thioxanthonic derivatives was, then, performed *in vitro*, in order to study the influence of the stereochemistry on P-gp induction and activation. Several biological activity assays were performed using Caco-2 cells as an *in vitro* model of the human intestinal epithelium.

The data from P-gp expression showed that ATx **2** and ATx **6** were the only thioxanthones which significantly increased P-gp expression, when compared to control cells. However, all the tested compounds significantly decreased the RHO 123 intracellular accumulation, that was evaluated in the presence of the tested ATx's, thus reflecting a significantly increased P-gp activity. Since this assay allows the evaluation of potential immediate effects of the compounds on P-gp activity, as a result of a direct activation of the pump, it was possible to conclude that ATx's **1-8** were P-gp activators. The RHO 123 accumulation assay in Caco-2 cells pre-exposed to the tested ATx's for 24 hours, demonstrated a significant decrease in RHO 123 intracellular accumulation for all compounds, with exception of ATx **3**, thus also reflecting an increased P-gp activity. Since ATx **1**, ATx **4**, ATx **5**, ATx **7** and ATx **8** were not able to significantly increase P-gp expression, the increase in its activity may result from a direct pump activation.

No significant differences in the levels of P-gp expression and activity were observed between the isomers (*R*) and (*S)* of each enantiomeric pair, suggesting that P-gp modulation may not be significantly affected by enantioselectivity concerning this class of compounds

Keywords: biological activity, enantioselectivity, P-glycoprotein, P-gp modulation, pharmacokinetic, thioxanthones.

Resumo

A glicoproteína-P (P-gp) promove o transporte para o exterior das células de uma vasta gama de compostos estruturalmente não relacionados, desempenhando assim importantes funções fisiológicas. Embora a sua principal função seja proteger as células contra xenobióticos tóxicos e metabolitos endógenos, este transportador de membrana desempenha também um papel relevante nos processos farmacocinéticos.

O nosso grupo demonstrou recentemente que novos derivados tioxantónicos obtidos por síntese protegem contra substratos tóxicos da P-gp agindo como indutores/ativadores potentes deste transportador.

Portanto, é essencial descobrir novos moduladores da P-gp e esclarecer a estereoselectividade deste transportador ABC relativamente a esta classe de moduladores. Neste trabalho, oito derivados tioxantónicos quirais (ATx's **1-8**) foram sintetizados por reação de acoplamento de Ullmann entre a 1-cloro-4-propoxi-9*H*-tioxanten-9-ona (**Tx**) e oito blocos construtores enantiomericamente puros (A **9-16**). A elucidação estrutural de todos os compostos sintetizados foi realizada por métodos espectroscópicos, incluindo IV, RMN (^{1}H, ^{13}C, HMBC e HSQC), e a sua pureza foi avaliada por HPLC.

A avaliação da modulação da P-gp por parte dos compostos sintetizados foi, em seguida, realizada *in vitro,* a fim de estudar a influência da estereoquímica na indução e ativação da P-gp. Vários ensaios de atividade biológica foram realizados utilizando células Caco-2 como modelo *in vitro* do epitélio intestinal humano. Os resultados de expressão da P-gp mostraram que ATx **2** e ATx **6** foram as únicas tioxantonas testadas que aumentaram significativamente a expressão da P-gp, quando comparados com os resultados obtidos com as células controlo. No entanto, todos os compostos diminuíram os níveis intracelulares de RHO 123, que foram avaliados na presença das ATx's testadas, refletindo assim um aumento significativo na atividade da P-gp. Uma vez que este ensaio permite avaliar o potencial efeito imediato dos compostos testados na atividade da P-gp, como resultado de uma ativação direta da bomba, foi possível concluir que as ATx's **1-8** são ativadoras da P-gp. O ensaio de acumulação de RHO 123 em células Caco-2 pré-expostas às tioxantonas testadas durante 24 horas, demonstrou uma diminuição significativa na acumulação intracelular de RHO 123 para todos os compostos, com a exceção da ATx **3**, refletindo igualmente um aumento significativo da atividade da P-gp. Visto que ATx **1**, ATx **4**, ATx **5**, ATx **7** e ATx **8** não foram capazes de aumentar significativamente a expressão da P-gp, o aumento na sua atividade pode resultar de uma ativação direta da bomba.

Não foram observadas diferenças significativas nos níveis de expressão e atividade da P-gp para os isómeros (*R*) e (*S*) de cada par enantiomérico; portanto a modulação da P-gp parece

não ser significativamente afetada pela enantioselectividade no que respeita a esta classe de compostos.

Palavras-chave: atividade biológica, enantiosselectividade, farmacocinética, glicoproteína-P, modulação da P-gp, tioxantonas.

Index

Index of Figures

Index of Tables

Abbreviations and Symbols

$[\propto]_D^{25℃}$ – Specific rotation (°)

δC – Chemical shift of Carbons

δH – Chemical shift of protons

^{13}C NMR – Carbon nuclear magnetic resonance

^{1}H NMR – Proton nuclear magnetic resonance

A – Amino alcohol

ABC – ATP-binding cassette

ABCB1 – ATP-binding cassette sub-family B member 1

ADME – Absorption, distribution, metabolism and excretion

ADP – Adenosine 5'-diphosphate

ATP – Adenosine 5'-triphosphate

ATx – Aminated Thioxanthones

ATx 1 – (*S*)-1-((1-hydroxypropan-2-yl)amino)-4-propoxy-9*H*-thioxanthen-9-one

ATx 2 – (*R*)-1-((1-hydroxypropan-2-yl)amino)-4-propoxy-9*H*-thioxanthen-9-one

ATx 3 – (*S*)-1-((2-hydroxypropyl)amino)-4-propoxy-9*H*-thioxanthen-9-one

ATx 4 – (*R*)-1-((2-hydroxypropyl)amino)-4-propoxy-9*H*-thioxanthen-9-one

ATx 5 – (*S*)-1-((1-hydroxy-4-methylpentan-2-yl)amino)-4-propoxy-9*H*-thioxanthen-9-one

ATx 6 – (*R*)-1-((1-hydroxy-4-methylpentan-2-yl)amino)-4-propoxy-9*H*-thioxanthen-9-one

ATx 7 – *(S)*-1-((1-hydroxy-3-methylbutan-2-yl)amino)-4-propoxy-9*H*-thioxanthen-9-one

ATx 8 – (*R*)-1-((1-hydroxy-3-methylbutan-2-yl)amino)-4-propoxy-9*H*-thioxanthen-9-one

BBB – Blood brain barrier

BCRP – Breast cancer resistance protein (ABCG2)

C - Concentration

CIP – Cahn-Ingold-Prelog

CLA – Clausenamide

CNS – Central nervous system

d – Doublet

dd – Double doublet

DAD – Diode-array detection

DMEM - Dulbecco's modified Eagle's medium

FBS - Fetal bovine serum

HBSS - Hanks balanced salt solution

HMBC – Heteronuclear multiple bond correlation

HPLC – High performance liquid chromatography

HSQC – Heteronuclear single quantum coherence

IR – Infrared spectroscopy

J – Coupling constant

m – Multiplet

MDR – Multidrug resistance

MFI – Mean fluorescence intensity

MFI_{IA} - Mean fluorescence intensity in the presence of the P-gp inhibitor (IA – Inhibited accumulation)
MFI_{NA} - Mean fluorescence intensity in the absence of the P-gp inhibitor (NA – normal accumulation)
m.p. – Melting point

MRP – Multidrug resistance protein

NBD – Nucleotide binding domain

NEAA - Nonessential amino acids

NMR – Nuclear magnetic ressonance

nm – Nanometers

NR - Neutral red

PE - Phycoerythrin

P-gp – P-glycoprotein

RHO 123 – Rhodamine 123

RLU – Relative light units

s – Singlet

SPE – Solid phase extraction

TLC – Thin-layer chromatography

TMD – Transmembrane domains

TMHs – Transmembrane α-helices

Tx – Thioxanthone

UV – Ultraviolet

General and Specific Objectives

The main objective of this dissertation was the synthesis of new small chiral molecules and their evaluation as potential modulators of P-glycoprotein.

The specific objectives of this dissertation were:

- To synthesize a library of thioxanthones in an enantiomerically pure form by coupling reactions of a suitable functionalize thioxanthone with chiral building blocks;
- The structure elucidation of the chiral thioxanthones;
- To evaluate the purity of the synthesized chiral thioxanthones by high performance liquid chromatography;
- Screening the potential modulatory effect on P-gp expression and activity, in order to evaluate the *in vitro* behaviour for both enantiomers. A P-gp ATPase assay was performed for characterize the compounds that interact with P-gp, namely the stimulators and inhibitors of its ATPase activity.

Structure and Organization of the Dissertation

The present dissertation is structured in six chapters.

Chapter 1 - Introduction

The first chapter deals with the theoretical background that supports the developed work, and is sub-divided into 3 subchapters. A brief introduction on P-glycoprotein (P-gp) structure and function, on the known P-gp modulators and on the importance of this efflux pump in drug pharmacokinetics is presented. Also, this chapter introduces thioxanthones, with representative modulators, and highlights the importance of studying chirality issues in what concerns to this transporter.

Chapter 2 – Results and Discussion

This chapter focuses on the results and discussion of the developed research work, being sub-divided into two parts, concerning the synthesis and structure elucidation of the synthesized chiral thioxanthones, and their biological evaluation.

Chapter 3 – Experimental

The third chapter describes the experimental methodologies used in this work and is divided in two parts; the first related with the synthesis, structure elucidation and determination of the purity by liquid chromatography, and the second concerning the methods used to study the potential modulation of P-pg.

Chapter 4 – Conclusions

The fourth chapter focuses on the main conclusions of the developed work, based on the proposed objectives.

Chapter 5 – References

In this chapter, the references cited throughout the dissertation, as well as the browsers used, are presented.

Chapter 6 – Appendixes

Chapter 6 is composed by one table, Table 14, which comprises the chemical structures of the synthesized chiral thioxanthones.

CHAPTER 1:

INTRODUCTION

1. ATP-binding cassette transporters

The family of ATP-binding cassette (ABC) transporters is the largest group of transmembrane proteins, with 49 transporters identified in humans. These membrane transporters are responsible for the active transport of diverse endogenous molecules (e.g., lipids, proteins, and products of the metabolism) and xenobiotics (e.g. drugs) out of the cell, which is driven by adenosine 5'-triphosphate (ATP) hydrolysis (1, 2).

Structurally, the transporters belonging to ABC family are similar and typically consist of four domains (3-5). They include a pair of ATP-binding domains, also known as nucleotide binding domains (NBD), located in the cytoplasm, and two transmembrane domains (TMD), normally containing six membrane-spanning α-helices (Figure 1 -topology of a prototype ABC protein) (4, 6).

Two sequence motifs in each NBD, designated Walker A and Walker B, are conserved among all ABC transporter superfamily members, as well a third motif, referred to as the ABC signature motif (or C motif) (5, 7). These motifs play a vital role in the hydrolysis of ATP to adenosine 5'-diphosphate (ADP) + Pi, thus providing the energy for translocation or efflux of endobiotic and xenobiotic substrates (3, 7). On the other hand, the hydrophobic TMDs are structurally diverse, and have an essential role in recognition and transport of various substrates (3, 5). The general structure of the ABC transporters and of these domains functions in transporter-mediated translocation of substrates are evidenced in Figure 1.

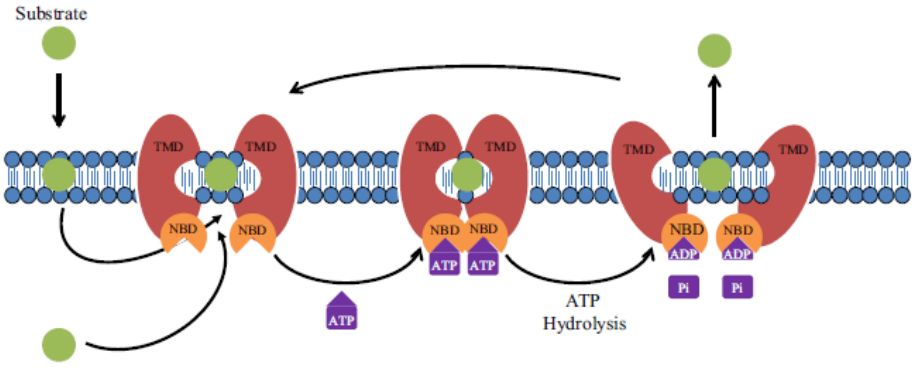

Figure 1 - Structure and mechanisms of efflux of ABC transporters (3).

The members of this superfamily of transporters are essential for many cells and, collectively, play important roles in absorption from the gastrointestinal tract and elimination into bile or into urine for a wide range of xenobiotics (1, 3, 8). They also play a major role in the disposition and toxicity of xenobiotics since they are critical to maintain

the barrier function of numerous tissues, such as the blood–brain barrier (BBB), the blood–testis barrier, and the maternal–fetal barrier or placenta (8).

P-glycoprotein (P-gp), breast cancer resistance protein (BCRP), and multidrug resistance proteins (MRPs), are some members of this family of carriers, and are known to have enantioselectivity for their substrates (9). Consequently, it is essential to study how these pumps participate in the active transport of chiral substrates, in order to better know the implications that could result from stereoselectivity (10-12).

1.1. P-glycoprotein (P-gp)

P-gp is the most studied and better characterized efflux pump belonging to superfamily of ABC transporters (13-15). The structure of P-gp complies with the characteristics described for the ABC transporters, being a polypeptide made up of two homologous halves that arose from gene duplication (16). Each half contains a TMD, formed of six membrane-spanning α helices (TMHs), and a NBD, located at the cytoplasmatic face of the membrane (Figure 2) (4, 17-19). This 170 kDa protein, also known as ABCB1, is encoded in humans by the multidrug resistance genes *MDR1* (*ABCB1*) and *MDR3* (*ABCB4*), but the P-gp expression refers, usually, to the ABCB1 isoform (18, 20, 21).

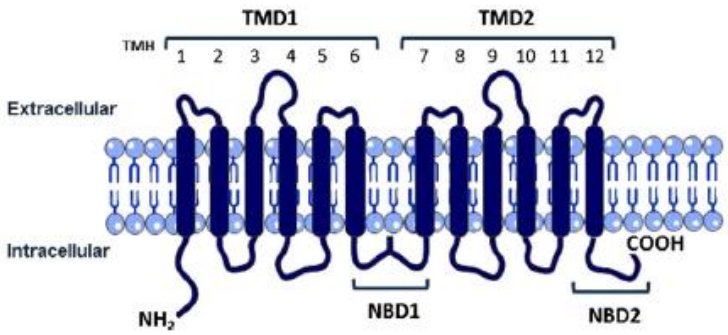

Figure 2 - Topological model of P-glycoprotein (6).

P-gp was first isolated from colchicine-resistant Chinese hamster ovary cells mutants. Consequently, since its discovery, is frequently associated with the development of multidrug resistance (MDR) in cancer cells (22). The degree of MDR is strongly correlated with changes in the drug permeability, and is largely related with the P-gp expression and activity (22, 23). Contrarily to what was initially thought, P-gp expression is not limited to cancer cells, being also widely expressed in normal tissues, including the brain, liver, small intestine, kidney and lung (7, 14, 24). This efflux pump promotes the outward transport of a wide range of structurally unrelated compounds, using the energy from the hydrolysis of ATP (16, 25, 26). Thus, it plays important physiological functions, being its primary function to protect the cells against toxic xenobiotics and endogenous metabolites (13, 16).

Furthermore, the localization of P-gp at the apical side of the cell membrane of tissues and organs like colon, kidney and liver (Figure 3), which are usually involved in absorption and excretion, suggests that this membrane transporter plays a relevant role in these pharmacokinetic processes (13, 27).

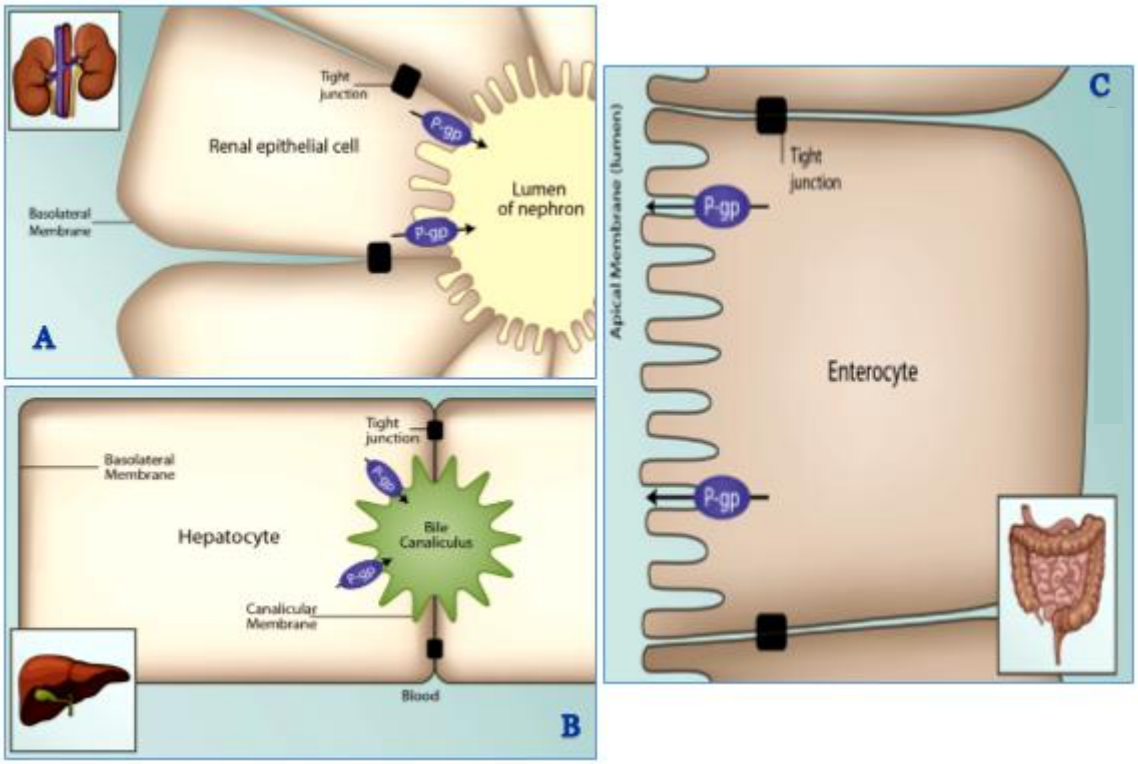

Figure 3 - Localization of P-gp on the apical membrane of renal proximal tubule cells (A), the membrane of human hepatocytes (B) and the apical membrane of intestinal epithelial cells. Figure adapted from (28).

A large number of drugs generally used in clinical treatment are modulators of P-gp. As a consequence, they can affect the expression/function of this efflux pump and, consequently, when administrated, can affect the disposition of various P-gp substrate drugs in normal tissues (26).

1.1.1. Mechanisms of drug efflux

Despite being the better characterized efflux pump, the mechanisms by which this membrane transporter combines the ATP hydrolysis with the movement of drugs across the plasma membrane is not well fully defined. Several models have been proposed to explain the mechanism of P-gp-mediated transport, but just two models, the "hydrophobic vacuum cleaner" and the "flippase" models, are in agreement with recent data related with the structure of P-gp (15, 21). These two models are illustrated in Figure 4.

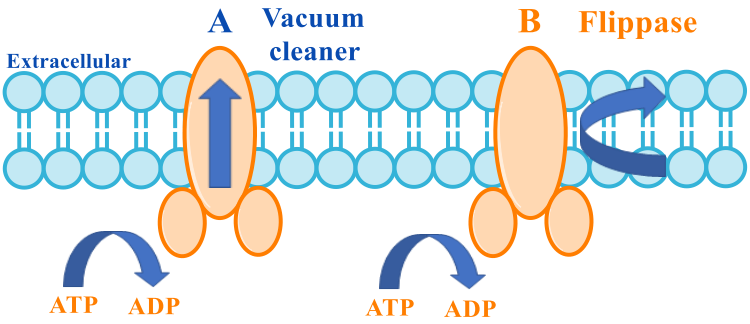

Figure 4 - Hydrophobic vacuum-cleaner (A) and flippase models of P-gp (B). Adapted from (16)

The hydrophobic vacuum-cleaner model (Figure 4 – A) was proposed by Higgins and Gottesman after performing several studies, which suggested that P-gp may interact with its substrates within the membrane and, subsequently, transport them to the extracellular medium (29). Therefore, this model described P-gp as a 'vacuum cleaner', which recognizes and 'sucks' hydrophobic compounds out of the membrane (29).

In the "flippase" model (Figure 4 – B), the P-gp substrates are flipped from the inner leaflet of the lipid bilayer to either the outer leaflet of the plasma membrane or directly to the extracellular medium, where it would passively equilibrate with the aqueous environment (29). So, considering this principle, P-gp could be seen as a translocase or 'flippase' for lipophilic molecules (16).

These two models suppose a partition of the P-gp substrates into the lipid phase prior to interacting with the protein, which may help to explain the extraordinarily broad substrate specificity of P-gp. Therefore, the key determinant of specificity seems to be the ability of a substrate to properly intercalate into the lipid bilayer, with the subsequent interaction with the substrate-binding site being of secondary importance (21).

1.1.2. P-gp substrates

P-gp substrates constitute a large group of compounds that, though chemically, structurally and pharmacologically unrelated, are recognized and transported by P-gp. Among these compounds there are many clinically important agents, as anticancer drugs, antibiotics, and anti-hypertensives, among many others, some of which are exemplified in Table 1 (15, 16, 30).

Table 1 - Different classes of agents that interact with P-gp (P-gp substrates).

Therapeutic Class	Compounds
Anticancer	Anthracyclines: doxorrubicin, daunorubicin, epirubicin, mitoxantrone, idarrubicin
	Vinca alkaloids: vincristine, vinblastine, vinorebline, vindesine
	Other alkaloids: cepharanthine, homoharringvtonine
	Taxanes: paclitaxel, docetaxel
	Antitumor antibiotics: actinomycin D, mitomycin C
	Antimetabolites: cytarabine, methotrexate, 5-fluorouracil, hydroxyurea
	Acridines: amsacrine
	Camptothecins: topotecan, irinotecan
	Epipodophyllotoxins: etoposide, teniposide
	Alkylating agents: chlorambucil, cisplatin
	Tyrosine kinase inhibitors: imatinib mesylate, gefitinib
	Others: tamoxifen, bisantrene
Antidepressants	Amitriptyline, nortriptyline, doxepin, escitalopram, levomilnacipran, vilazodone
Analgesic opioids	Morphine, pentazocine, fentanyl, loperamide
Anti-arrhythmics	Quinidine, verapamil, digoxin, lidocaine, quinidine
Anti-emetics	Ondansetron, domperidone
Antiepileptics and Anticonvulsants	Topiramate, phenytoin, carbamazepine, phenobarbital, lamotrigine, gabapentin, felbamate
Antigout agents	Colchicine
Anti-helmintics	Ivermectin
Anti-histaminics H1	Terfenadine, fexofenadine
Anti-hypertensives	Reserpine, debrisoquine, celiprolol, losartan, talinolol, prazosin
Antimicrobial agents	Erythromycin, doxycycline, itraconazole, ketoconazole, levofloxacin, rifampicin, sparfloxacin, tetracycline, grepafloxacin, clarithromycin, gramicidin A, valinomycin
Anti-human immunodeficiency virus (HIV)	Nelfinavir, ritonavir, saquinavir, amprenavir, indinavir, lopinavir

Calcium channel blockers	Nifedipine, diltiazem, azidopine, nicardipine
Calmodulin antagonists	Trifluoperazine, *trans*-flupentixol
Cardiac glycosides	Digoxin, digitoxin
Cholesterol-lowering agents	Lovastantin, simvastantin
Fluorescent dyes	Rhodamine 123, hoechst 33342, calcein acetoxymethylester
Anti-histaminics H_2	Cimetidine, ranitidine
Immunosuppressive agents	Cyclosporin A, tacrolimus, sirolimus, valspodar
Linear peptides	Leupeptin, pepstatin A
Muscle relaxant agents	Vecuronium
Neuroleptics	Chlorpromazine, phenothiazine
Steroid hormones	Aldosterone, corticosterone, dexamethasone, cortisol, hydrocortisone, methylprednisolone
Pesticides	Methylparation, endosulfan, paraquat
Natural products	Flavonoids, curcuminoids

Data was compiled from (5, 6, 16, 21, 31-35).

Most of these P-gp substrates are weakly amphipathic and relatively hydrophobic and can vary in size, structure, and function, ranging from small molecules, such as amino acids and some antibiotics, to macromolecules such as polysaccharides and proteins (16, 33). Several studies have been undertaken to elucidate the molecular attributes required for interaction between this efflux protein and its small substrates, and to identify P-gp substrates or to develop better P-gp inhibitors to overcome the problem of MDR (33). The data obtained in some of these studies highlighted the lipid solubility, cationic charge, hydrogen bonding potential, presence of an amine, molecular weight, size, surface area and the presence of aromatic ring structures as being important properties for substrate binding and functionality. The presence of an hydrogen bond acceptor (or electron donor) moiety (carbonyl, ether, hydroxyl or tertiary amine groups), with a defined spatial separation was also considered an important feature, after the screening of structurally diverse P-gp substrates using tridimensional modelling (21).

1.1.3. Modulation of P-gp

Modulators form a group of structurally unrelated compounds, which have the ability of modulating P-gp expression or activity, by inhibition or activation (16, 27). Over the years, the P-gp modulation has been seen as an important area in drug development, once P-gp

interacts with many drugs and is expressed in several organs (6, 7, 36-39). Due to the role that P-gp demonstrated to have in MDR, the first studies on this efflux pump were mostly focused on its inhibition as a therapeutic option to circumvent MDR (4, 7, 15, 31, 39). However, more recent insights showed that P-gp inhibitors might be also useful to modulate the general pharmacokinetic behavior of drugs in the organism, revealing special importance in case of central nervous system (CNS) active drugs, to allow increasing drugs brain penetration (19, 31, 32, 36). Consequently, over the years, several studies were developed in order to discover potent and safe P-gp inhibitors, and to better understand their mechanisms of inhibition (15, 19, 31, 32, 40-44).

Furthermore, some recent studies have also focused on the induction/activation of this pump, and the use of such inducers/activators to prevent the toxicity mediated by P-gp substrates has been proposed as a potential antidotal pathway(6, 20, 25, 45, 46). Accordingly, the modulation of P-gp can be applied not only in drug discovery but also in drug development, to overcome the limitations of some drugs in clinical use due their interaction with P-gp, which affects their clinical effectiveness (6, 26, 44, 45, 47, 48).
Many modulators have been identified and taking in account their different mechanisms of modulating P-gp expression and activity; they were divided in two distinct groups: inhibitors and inducers/activators (16, 21).

1.1.3.1 P-gp Inhibitors

Since the discovery of P-gp, identifying and developing selective and potent P-gp inhibitors has been a principal focus area in drug discovery (6, 26, 31, 33, 36, 49-51). The first studies focused in the clinical application of P-gp inhibitors in the treating of drug-resistant tumors, being MDR clinically important in several diseases. The P-gp inhibitors must be selectively targeted to P-gp in non-physiological tissues and must have a high propensity for binding to P-gp without inhibiting other ABC transporters (27, 49). According with their potency, selectivity and drug-drug interaction potential, the P-gp inhibitors are classified into four generations (Table 2) (19).

Table 2 - Examples of P-gp inhibitors from the four generations.

	P-gp inhibitors
First generation	Analgesics: meperidine, pentazocine
	Anesthesics: chloroform, benzyl alcohol, diethyl ether, propofol
	Antibiotics: cefoperazone, cefriaxone, salinomycin, nigericin, erythromycin, azithromycin, brefeldin A, befilomycin, clarithromycin, valinomycin

	Anticancer drugs: tamoxifen, bicalutamide, mitotane, gefitinib, lapatinib, erlotinib, lonafarnib, tipifarnib, vinblastine
	Antifungals: itraconazole, ketoconazole, econazole, dihydroptychantol A, aureobasidin A
	Anti-histaminics: benzquinamide, azelastine, tesmilifene, astemizole, terfenadine
	Anti-inflammatory drugs: zomepirac, indomethacin, curcumin, ibuprofen
	Antidepressants: amoxapine, loxapine, sertraline, paroxetine, fluoxetine
	Antimalarial drugs: quinine
	Antiprotozoal drugs: hycanthone, monensim, metronidazole
	Antiviral drugs: concanamycin A, ritonavir, nelfinavir, saquinavir
	Anxiolytics and sedative-hypnotics: midazolam
	Cardiac/ circulation drugs: amiodarone, propafenone, quinidine, verapamil, emopamil, nifedipine, nicardipine, niguldipine, nitrendipine, nimodipine, felodipine, isradipine, lomerizine, tetrandrine, mibefradil, diltiazem, bepridil, dipyridamole, reserpine, prazosin, doxazosin, carvedilol
	Cholesterol-lowering drugs: atorvastatin
	Immunosuppressants: Cyclosporin A, tacrolimus, sirolimus
	Neuroleptics and antipsychotics: trans-flupentixol, perphenazine, prochlorpromazine, trifluoperazine, perospirone, haloperidol
	Phosphodiesterase inhibitors: Vardenafil
	Steroid hormones: progesterone, medroxiprogesterone, cortisol, methylprednisolone, medroxiprogesterone 17-acetate, mifepristone, tirilazad
Second generation	Dexverapamil, dexniguldipine, cinchonine, hydro-cinchonine, quinine homodimer Q2, valspodar (PSC 833), biricodar (VX-853), toremifene, dofequidar (MS-209), stipiamide homodimer
Third generation	Zosuquidar (LY335979), taraquidar (XR9576), elacridar (G120918), laniquidar (R101933), ontogen (OC144 093), DP7, PGP-4008, CBT-1
Fourth generation	Flavonoids: quercetin, tangeretin, nobiletin, sinensetin, baicalein heptamethoxyflavone
	Alkaloids: pervilleine F, ellipticine
	Coumarins: cnidiadin, conferone, praeruptorin A, rivulobirin A, DCK
	Cannabinoids
	Taccalonolides
	Diterpenes: jolkinol B, portlanquinol, euphodendroidin D, pepluanin A
	Triterpenes: sipholenone E, uvaol, sipholenol A, oleanolic acid

	Polyenes: pentadeca-(8,13)-dien-11-yn-2one
	Lignans: schisandrin A, silibinin, nirtetralin
	Surfactants and lipids: pluronic P85, tween-20, triton X-100, cremophor EL, poly(ethylene glycol)-300 (PEG-300), Nonidet P40
	Dual ligands: aminated thioxanthones such as 1-[2-(1*H*-benzimidazol-2yl)ethanamine]-4-propoxy-9*H*-thioxanthen-9-one

Data adapted from (6, 19, 32, 52)

The first-generation of inhibitors comprises compounds pharmacologically active, which were developed and are in clinical use for other indications, but that also demonstrated to be P-gp inhibitors (15, 21, 32). This class of compounds includes channel blockers, such as verapamil, immunosuppressants, like cyclosporin A, and anti-hypertensives, as reserpine and quinidine (15), among other examples described in Table 2. The clinical use of these compounds for P-gp inhibition is limited considering the toxicity associated to the high concentrations that are needed to inhibit the pump. As a consequence, these compounds have low potency and lack of binding affinity for P-gp (15).

In order to decrease the toxicity of the first-generation of inhibitors, to increase the efficacy of the P-gp inhibitory effect and to reduce their main therapeutic activity, the second-generation was developed. It includes compounds resulting from structural modifications of the first-generation members. Therefore, the second-generation of inhibitors includes compounds analogues of the first-generation inhibitors, with a higher P-gp affinity (15, 19). The P-gp inhibitor valspodar is an example, because it inhibits the P-gp with 5-20-fold greater potency than cyclosporin A and does not possess the immunosuppressive effect of its structural analogue (21).

The third-generation of P-gp inhibitors was developed to overcome the limitations of the compounds belonging to the first- and second-generations, like the unpredictable drug-drug interactions and the associated toxicity (15). This class of compounds was developed by using quantitative structure-activity relationships (QSAR) and combinatorial chemistry, which allowed to design molecules with specific characteristics (19). Zosuquidar (LY335979), elacridar (GF120918), laniquidar (R101933), tariquidar (XR9576) and CBT-1 are some of the most studied inhibitors of third-generation of P-gp inhibitors (15, 19). This generation of P-gp inhibitors showed to be the most potent and selective inhibitors, but unexpected toxic effects were still observed clinical assays (15, 19, 49). Therefore, the development of P-gp inhibitors without toxic effects, in normal tissues, was not accomplished within the first three generations of P-gp inhibitors.

As a result, a fourth-generation of P-gp inhibitors is described as comprising compounds extracted from natural origins and their derivatives, surfactants and lipids,

peptidomimetics and agents combining transport inhibition with another beneficial biological activity (dual ligands) (6). Concerning the dual ligands, several aminated thioxanthones were reported as dual inhibitors of cell growth and P-gp, which allowed to glimpse a new opportunity for MDR reversal (6).

1.1.3.2. P-gp inducers and activators

P-gp activity can be increased by a large range of drugs, which can be classified as inducers or activators (Table 3) (6, 33). The inducers are compounds that promote an increase in the transporter's expression, which can result in an consequent increase in activity of the pump (25). However, to note that P-gp expression and activity may not be proportionally increased. For example, exposure of Caco-2 cells to doxorubicin resulted in an increased cell surface P-gp expression followed by increases in pump activity, but to a different magnitude (20). Also, colchicine increased P-gp protein expression in Caco-2 cells, with no significant changes in its activity (53). Therefore, the simultaneous evaluation of both P-gp expression and activity in the screening of P-gp inducers is of utmost importance, since an increase in the former may not be reflected in an increase in the later. Furthermore, to note that P-gp expression should not only be evaluated at the mRNA level but also at the protein level. Indeed, Takara et al. reported that P-gp transport function remained unchanged in Caco-2 cells exposed to several nonsteroidal anti-inflammatory drugs, in spite of the observed increases in MDR1 mRNA levels. Thus, it was proposed that the increased *MDR1* mRNA was not translated into increased P-gp expression (54).

On the other hand, P-gp activators are compounds that induce a conformational alteration when binding to P-gp, thus, stimulating the transport of a substrate on another binding site (6). This suggests that the efflux pump contains at least two positively cooperative sites for drug binding and transport (6, 25, 45). Moreover, the activation mechanism increases the P-gp transport function without interfering with the protein expression levels, unlike what happens with P-gp induction, being a quicker process (25).

Table 3 - Examples of inducers and/or activators of P-gp.

P-gp inducers and/or activators		
Ambrisentam	Docetaxel	Nifedipine
Amiodarone	Doxorrubicin	Norathyriol
Amprenavir	Efavirenz	Oxycodone
Avermectin	Erythromycin	Paclitaxel
Bosentan	β-Estradiol	Parthenolide

Bromocriptine	Ethinylestradiol	Pentylenetetrazole
Budesonide	Etoposide	Phenobarbital
Cadmium chloride	5-Flurouracil	Phenotiazine
Capsaicin	Hydroxyurea	Phenytoin
Carbamazepine	Hyperforin	Piperine
Catechin	Idarubicin	Probenecid
R-Cetirizine	Indinavir	Quercetin
Chlorambucil	Insulin	Quinidine
Chrysin	Ivermectin	Sirolimus
Ciclesonide	Lopinavir	Reduced rifampicin derivative
Cisplatin	LY191401	Reserpine
Clotrimazole	Mangiferin	Retinoic acid
Colchicine	Meloxicam	Ritonavir
Coticosterone	Methotrexate	Rifampicin
Curcumin	Methylprednisolone	Ritonavir
Cyanidin	Midazolam	Saquinavir
Cyclosporine A	Mitoxantrone	Sodium butyrate
Cytarabine	Morphine	SR12813
Daunorubicin	Myricetin	Tacrolimus
Dexamethasone	Nefazodone	Venlafaxine
Diltiazem	Nelfinavir	Verapamil
Digoxin	Nevirapine	Vinblastine
Dimethylsulfoxide	Nicardipine	

Data are compiled from (6, 32, 33)

1.1.4. Importance of P-gp modulation in drug pharmacokinetics

P-gp plays an important role in the absorption, elimination, disposition and toxicity of a wide range of compounds, both endobiotics and xenobiotics, since it is responsible by their transport across cell membranes. Additionally, it is important to maintain the barrier function of numerous tissues, such as the blood–brain barrier, small intestine and placenta (8, 27). Considering that many drugs used in clinical treatments are substrates of P-gp, their pharmacokinetic processes and, consequently, their effectiveness, can be greatly affected by the level of expression and functionality of this pump (16). When a drug that is a P-gp substrate is co-administrated with other drug, a P-gp inducer or inhibitor, the

pharmacokinetics and bioavailability of the P-gp substrate may be substantially altered (33).

The over-expression of P-gp, caused by a P-gp inducer, on the epithelial cells lining of the intestine combined with its substantial role in drug pumping out of these cells, after absorption, may generate a poor uptake of the drug in the intestine, thus reducing its oral bioavailability, and blocking the delivery of drugs to the brain (16, 33). This is a serious problem in drug discovery, especially when developing drugs targeted to the brain, because the efficacy of these drugs depends on their ability to cross the blood–brain barrier (16).

On the other hand, the reduced expression of P-gp can originate a decrease on its activity in the intestine, which can lead to dramatically increased drug bioavailability, and consequently, toxicity (33). The same can happen if two drugs, that are both P-gp substrates, are co-administrated, because they can compete for the transporter and, then, the drugs plasmatic levels will be higher for more time (33). Changes in expression of P-gp can also interfere with the drugs excretion, which are excreted by renal secretion or active secretion into the bile, and have their transport mediated by P-gp (23). Subsequently, the P-gp inhibition can result in the inhibition of excretion, what may induce an increased plasma concentration, and consequent side effects (23).

The level of P-gp activity, beyond its importance in drug–drug interactions, plays an essential role in the MDR phenomenon. The high expression of P-gp on the surface membranes of cancer cells causes high rates of MDR resistance in cancer cells, since P-gp transports a wide range of anticancer drugs (26). The mechanism of MDR and the importance of P-gp expression in the protection of organisms are shown in Figure 5.

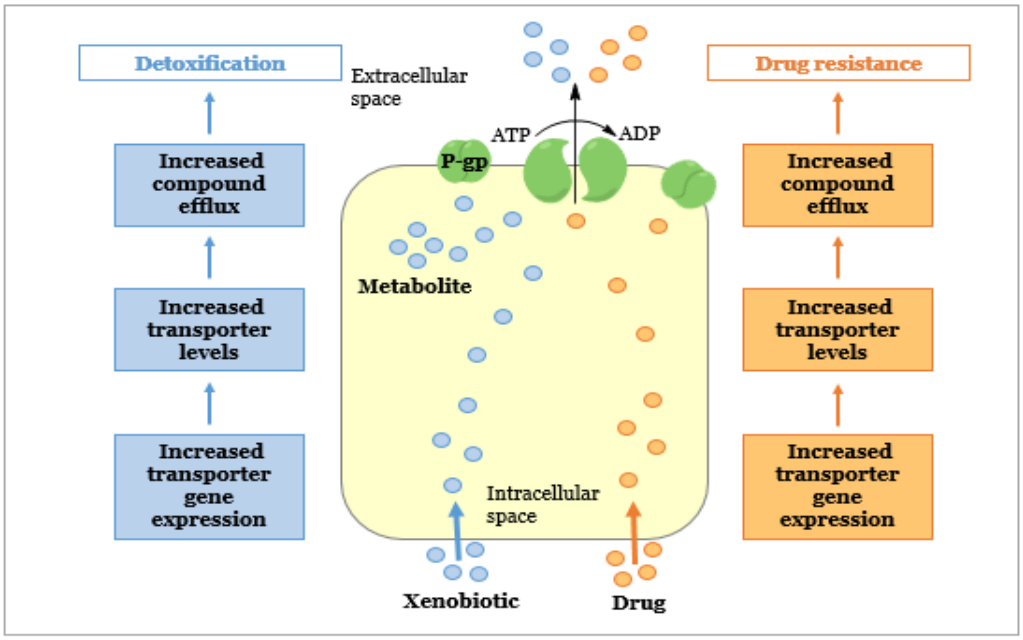

Figure 5 - Mechanism of MDR and detoxification by P-gp. Adapted from (55)

Curiously, the use of P-gp inhibitors was considered and tested, in several studies, and demonstrated to improve the efficiency and pharmacokinetic profile of molecules that interact with P-gp, whereas the use of P-gp inducers or activators has been considered as a potential mechanism of protection against toxic P-gp substrates (6, 25, 26, 31, 32, 39, 40, 43, 46, 56). However, as P-gp is expressed in several organs and plays an important role in absorption, disposition and excretion of several compounds, the modulators need to selectively target P-gp in the target tissues in order to not cause toxicity (32). The great impact of P-gp on the pharmacokinetics of its substrate molecules is consistent with the strategic physiological expression of P-gp in organs that play key roles in the processes of drug absorption and disposition (27).

2. Thioxanthones

Thioxanthones are a group of *S*-heterocycles compounds with a dibenzo-γ-thiopyrone scaffold (Figure 6) showing interesting biological properties (40, 46, 57).

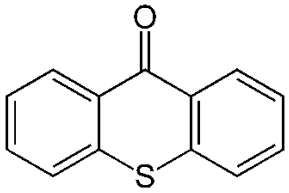

Figure 6 - Thioxanthonic scaffold.

Structurally, similar to xanthones, they are an important class of compounds comprising synthetic derivatives. The first synthesis of a thioxanthone derivative was reported in 1891 (58-61). The biological interest in this class of compounds started when lucanthone (Figure 7 – A) and its metabolite hycanthone (Figure 7 – B) were described for the first time as antischistosomal agents (62, 63). Although the drugs lucanthone and hycanthone were withdrawn from therapy due to mutagenic side effects, in the 1970's, the interest in the mechanisms of action of these thioxanthones and their derivatives continued (63).

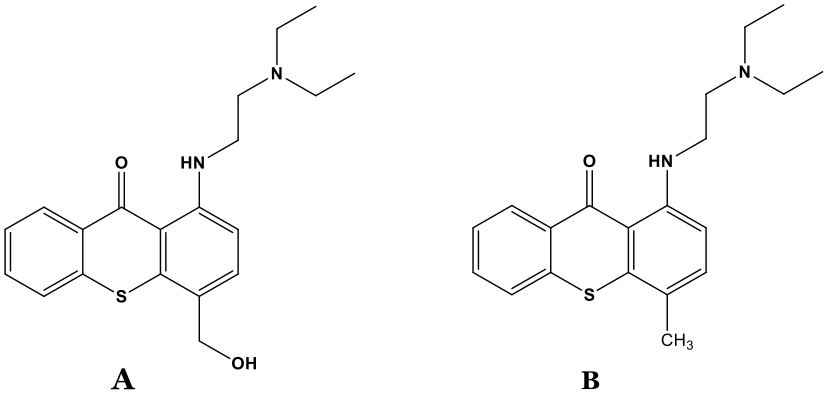

Figure 7 – Structure of (A) lucanthone and (B) hycanthone.

Afterwards, hycanthone was also evaluated as antitumor agent in Phase I and II trials sponsored by the National Cancer Institute, unleashing a big interest in the study of this class of compounds (64).

Over the years, diverse biological activities of thioxanthonic derivatives were described such as P-gp modulation (22, 40, 46), topoisomerase inhibition (65, 66), antitumor activities (43, 59, 67-73), antibiotic activity (67-70), among others (57, 74, 75). The large number of biological activities associated to this class of compounds depends on the nature and/or position of the different substituents in the tricyclic scaffold, reason why several thioxanthonic derivatives have been synthesized and studied (60).

2.1. Synthesis

Several different methodologies have been used to synthesize thioxanthones and their derivatives (57). The selected method for the synthesis of thioxanthonic derivatives depends on the nature and position of the substituents to be introduced on the thioxanthone scaffold (76).

The cyclization of thiosalicylic acid with unsubstituted or corresponding substituted aromatic compounds, in a concentrated sulfuric acid medium, is a traditional approach to prepare thioxanthone and its derivatives (Scheme 1) (57). However, due to some limitations inherent to this one-spot synthesis, such as the requirement of having a thiol and a hydroxyl group at the 6 and 6' position to afford directly the thioxanthone scaffold, other approaches involving typically multistep procedures are used in the synthesis of thioxanthones (57).

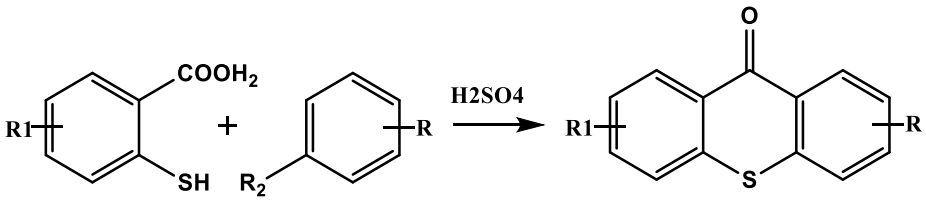

Scheme 1

The synthesis via benzophenone derivative, a diarylthioether (phenylthiobenzoic acid) or a diarylthioester intermediate (Scheme 2), are some these approaches which are usually used to obtain thioxanthonic derivatives (57, 76). The intramolecular electrophilic cyclization of phenylthiobenzoic acid in a concentrated acidic medium (Scheme 2) is the most usual method to obtain the thioxanthone scaffold (77, 78).

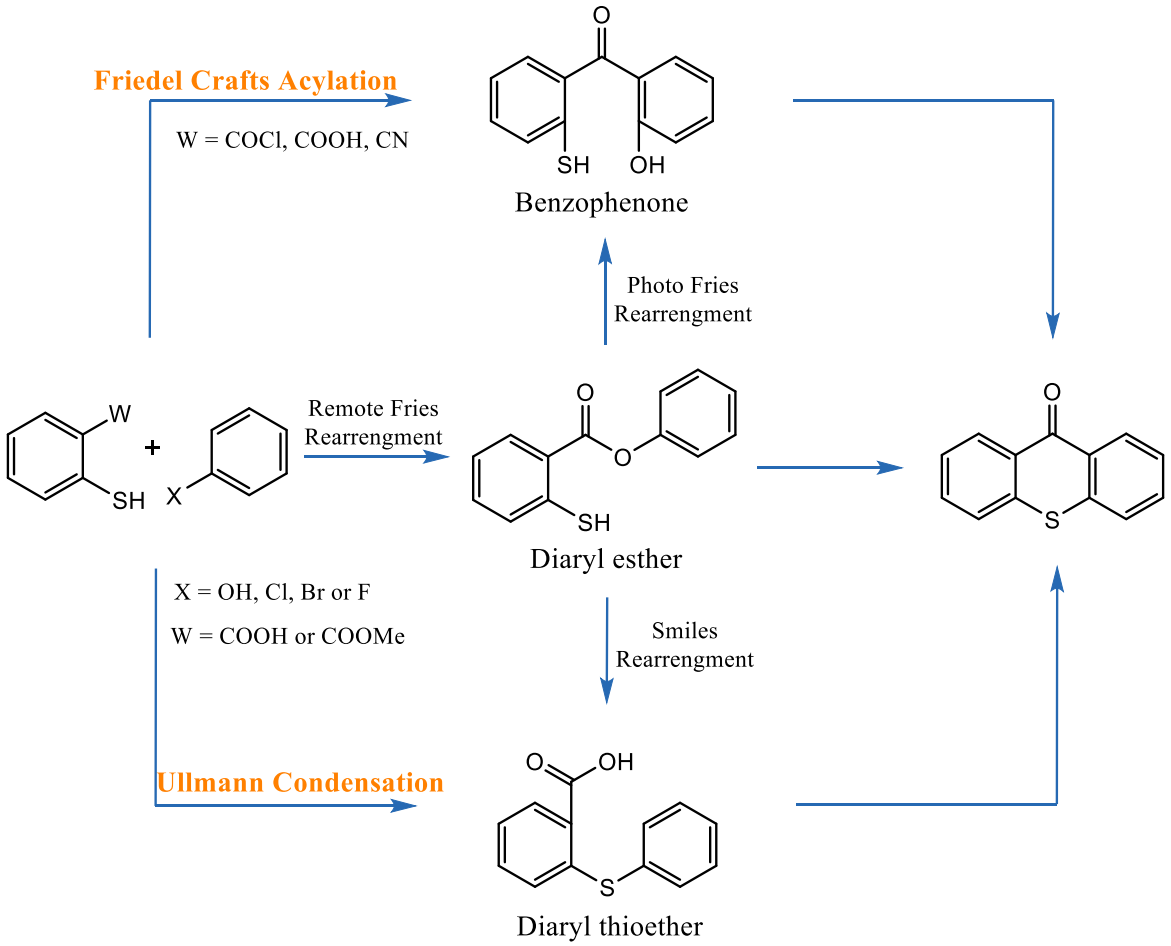

Scheme 2

These traditional methods can often result in low yields of the desired product and in a mixture of by-products which are difficult to separate by conventional techniques (57). Over the years, several reaction conditions were employed in order to optimize the reaction time and yield of the synthesis of thioxanthones and thioxanthonic derivatives, which was revised by Paiva *et al.* (57).

2.2. Thioxanthones as P-gp modulators

Thioxanthones have been found to exhibit P-gp modulation activities (40, 46, 57, 69). A large amount of the studies concerning P-gp modulation were focused on their ability to act as P-gp inhibitors, as well as their behavior as antitumor agents (3, 7, 19, 26, 27, 31, 32, 40). Since the MDR phenomenon in cancer treatment can be a consequence of the overexpression of P-gp in cancer cells, the use of P-gp inhibitors to restore the sensitivity of tumor cells to chemotherapeutic agents was seen as a way to overcome MDR in tumors (3, 32, 39, 57). The combination of P-gp inhibitory properties with antitumor activity in a single molecule was hypothesized to lead towards an improved drug response and, thus, a study

focused on the possibility of thioxanthonic derivatives with known antitumor activity that could also be P-gp inhibitors (40).

In this study, some P-gp activators/inducers were also discovered (40). These derivatives were further investigated and the thioxanthones that promoted an increase the transporter's expression were classified as inducers, while the thioxanthones that increased the P-gp transport function without interfering with the protein expression levels were classified as activators (25). The P-gp inducers are able to act as an effective intracellular protection mechanism since, by increasing the pump expression, they will limit the intracellular accumulation of its substrates and, consequently, their toxicity (20, 56). Indeed, using the Caco-2 cells *in vitro* model, these synthetized thioxanthonic derivatives were studied in order to evaluate their potential to increase P-gp expression and/or activity, and their potential protective effects in Caco-2 cells against the toxicity induced by paraquat (PQ), an extremely toxic herbicide that is a P-gp substrate, in an attempt to develop new antidotes using this efficient antidotal pathway (46).

In Table 4 the thioxanthonic derivatives that showed ability to modulate the P-gp activity are described.

Table 4 - Examples of thioxanthone modulators of P-gp.

Compound	P-gp modulation	Compound	P-gp modulation
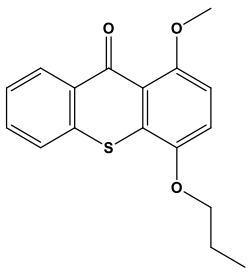 1-methoxy-4-propoxy-9*H*-thioxanthen-9-one	Inhibition	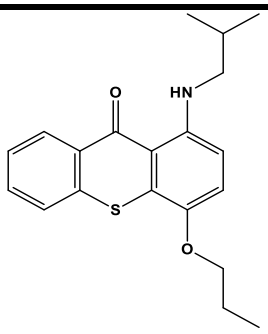 1-(isobutylamino)-4-propoxy-9*H*-thioxanthen-9-one	Activation
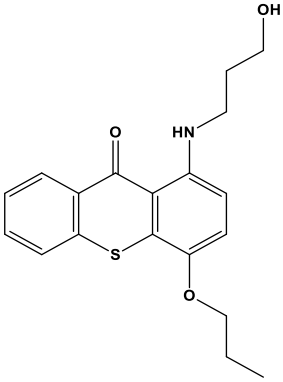	Activation	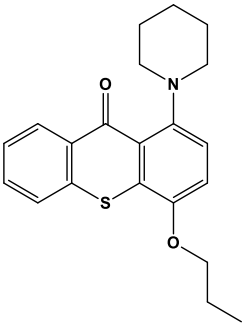	Inhibition

1-((3-hydroxypropyl)amino)-4-propoxy-9*H*-thioxanthen-9-one		1-(piperidin-1-yl)-4-propoxy-9*H*-thioxanthen-9-one	
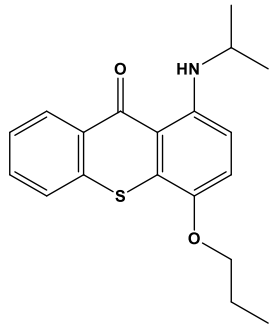 1-(isopropylamino)-4-propoxy-9*H*-thioxanthen-9-one	Activation	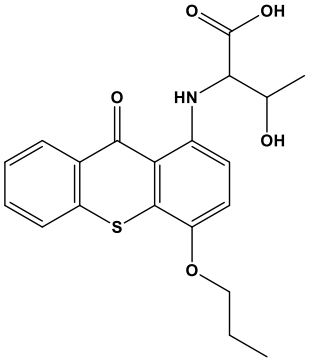 3-hydroxy-2-((9-oxo-4-propoxy-9*H*-thioxanthen-1-yl)amino)butanoic acid	Inhibition
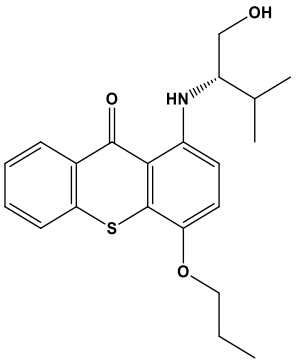 (*S*)-1-((1-hydroxy-3-methylbutan-2-yl)amino)-4-propoxy-9*H*-thioxanthen-9-one	Activation	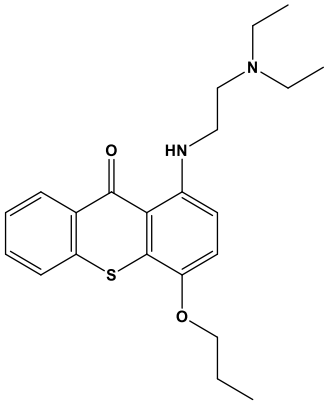 1-((2-(diethylamino)ethyl)amino)-4-propoxy-9*H*-thioxanthen-9-one	Inhibition
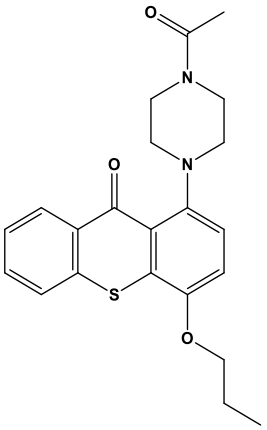 1-(4-acetylpiperazin-1-yl)-4-propoxy-9*H*-thioxanthen-9-one	Inhibition	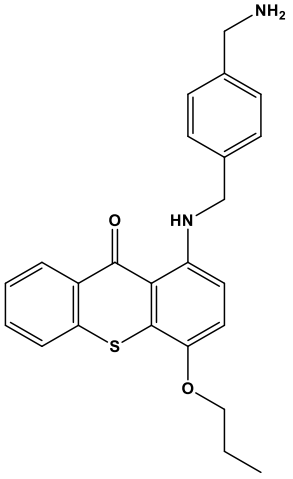 1-{[4-(aminomethyl)benzyl]amino}-4-propoxy-9*H*-thioxanthen-9-one	Activation

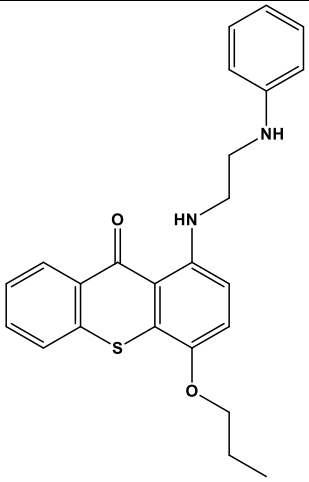 1-{[2-(phenylamino)ethyl]amino}-4-propoxy-9*H*-thioxanthen-9-one	Activation	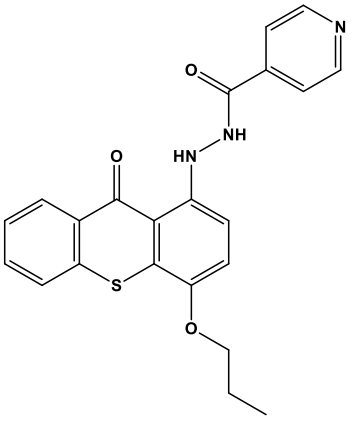 *N*'-(9-oxo-4-propoxy-9*H*-thioxanthen-1-yl)pyridine-4-carbohydrazide	Inhibition
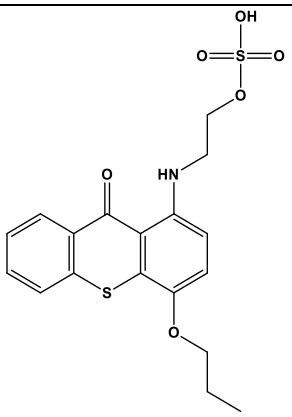 2-[(9-oxo-4-propoxy-9*H*-thioxanthen-1-yl)amino]ethyl hydrogen sulfate	Inhibition	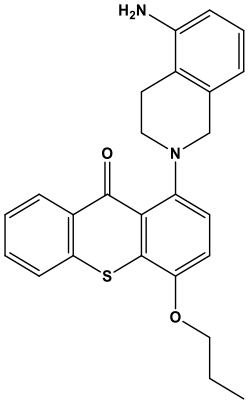 1-(5-amino-3,4-dihydroisoquinolin-2(1*H*)-yl)-4-propoxy-9*H*-thioxanthen-9-one	Inhibition
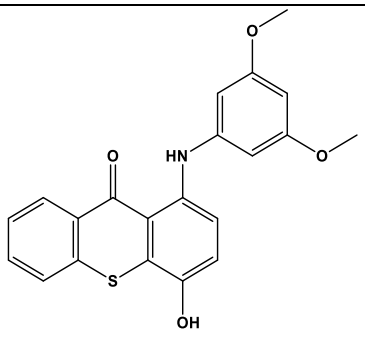 1-[(3,5-dimethoxyphenyl)amino]-4-hydroxy-9*H*-thioxanthen-9-one	Inhibition	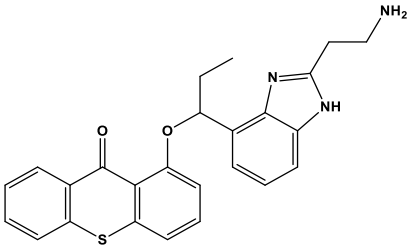 1-[2-(1*H*-benzimidazol-2-yl)ethanamine]-4-propoxy-9*H*-thioxanthen-9-one	Inhibition

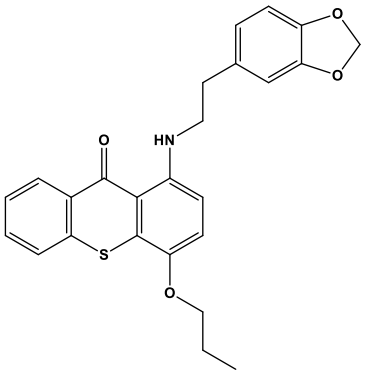 1-{[2-(1,3-benzodioxol-5-yl)ethyl]amino}-4-propoxy-9*H*-thioxanthen-9-one	Activation / Induction	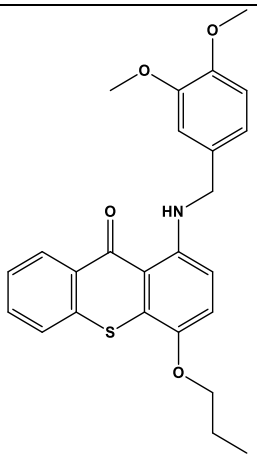 1-[(3,4-dimethoxybenzyl)amino]-4-propoxy-9*H*-thioxanthen-9-one	Activation
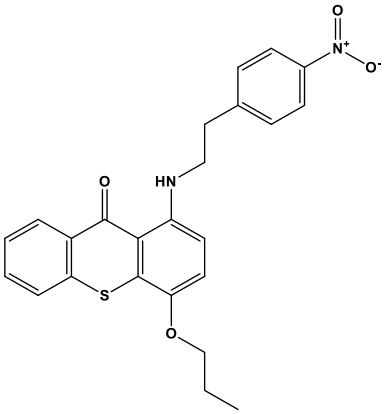 1-{[2-(4-nitrophenyl)ethyl]amino}-4-propoxy-9*H*-thioxanthen-9-one	Inhibition	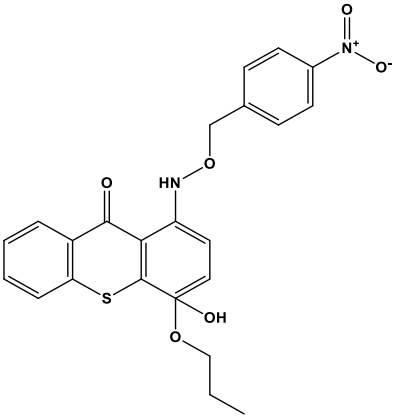 4-hydroxy-1-{[(4-nitrobenzyl)oxy]amino}-4-propoxy-9*H*-thioxanthen-9-one	Inhibition
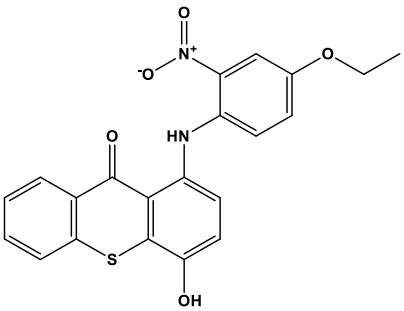 1-[(4-ethoxy-2-nitrophenyl)amino]-4-hydroxy-9*H*-thioxanthen-9-one	Inhibition	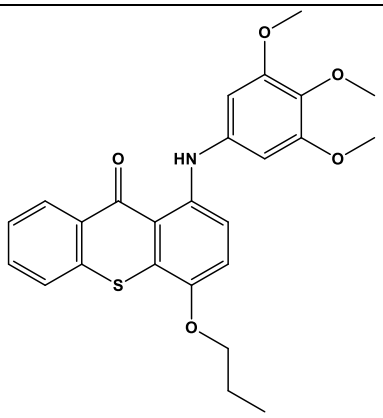 1-[(3,4,5-trimethoxyphenyl)amino]-4-propoxy-9*H*-thioxanthen-9-one	Inhibition

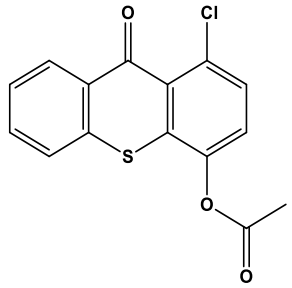 1-chloro-9-oxo-9*H*-thioxanthen-4-yl acetate	Activation	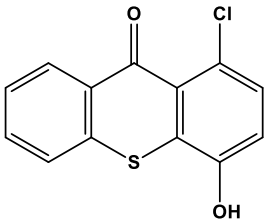 1-Chloro-4-hydroxy-9*H*-thioxanthen-9-one	Activation / Induction
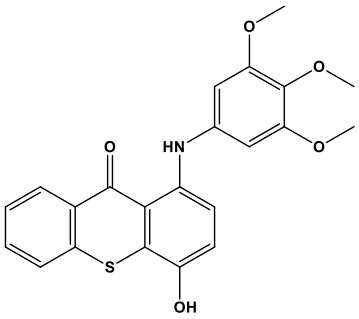 4-hydroxy-1-[(3,4,5-trimethoxyphenyl)amino]-9*H*-thioxanthen-9-one	Inhibition	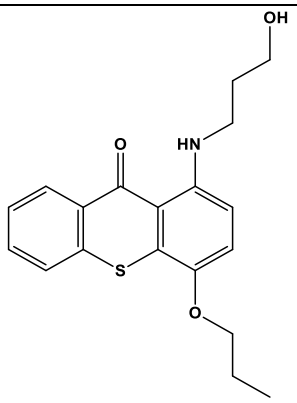 1-[(3-Hydroxypropyl)amino]-4-propoxy-9*H*-thioxanthen-9-one	Activation / Induction
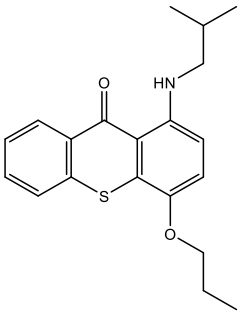 1-[(2-methylpropyl)amino]-4-propoxy-9H-thioxanthen-9-one	Activation / Induction	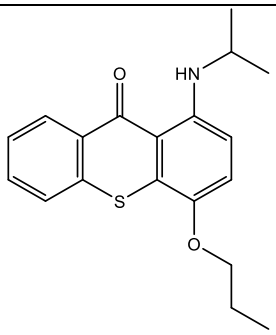 1-(propan-2-ylamino)-4-propoxy-9H-thioxanthen-9-one	Activation / Induction
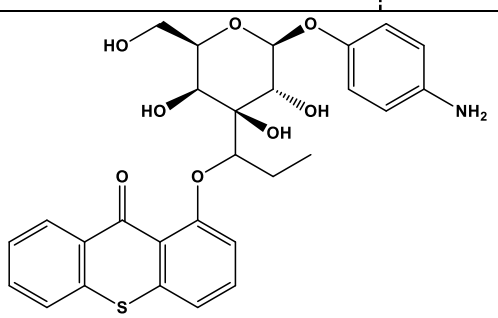 1-(1-((2*S*,3*R*,4*S*,5*S*,6*R*)-2-(4-aminophenoxy)-3,4,5-trihydroxy-6-(hydroxymethyl)tetrahydro-2*H*-pyran-4-yl)propoxy)-9*H*-thioxanthen-9-one		Inhibition	

Data compiled from (40) and (46)

Several aminated thioxanthones (ATx's), presented in table 4, were highly effective at inhibiting P-gp in a chronic myelogenous leukemia cell line, the K562 cells (40). For example, the 1-{[2-(diethylamino)ethyl]amino}-4-propoxy-9*H*-thioxanthen-9-one demonstrated to be the most potent thioxanthone in inhibiting cell growth, as well as a potent inhibitor of tumor cell growth (40). Moreover, 1-[(3-hydroxypropyl)amino]-4-propoxy-9*H*-thioxanthen-9-one, 1-chloro-4-hydroxy-9*H*-thioxanthen-9-one, 1-{[2-(1,3-benzodioxol-5-yl)ethyl]amino}-4-propoxy-9*H*-thioxanthen-9-one, 1-[(2-methylpropyl)amino]-4-propoxy-9*H*-thioxanthen-9-one and 1-(propan-2-ylamino)-4-propoxy-9*H*-thioxanthen-9-one were the compounds tested as possible antidotes against PQ-induced toxicity (46). This last thioxanthonic derivative showed the highest potential in inducing P-gp and, consequently, afforded the highest protection against PQ-induced toxicity (46).

Additionally, computational methods were developed in order to explore, *in silico*, the possible binding modes of the thioxanthonic activators and to build a common pharmacophore for P-gp activators, which can be used to predict new ligands (46). The pharmacophore includes one hydrophobic group, one hydrogen bond acceptor feature and one aromatic ring. Moreover, *in silico,* interactions between thioxanthones and P-gp in the presence of PQ suggested that a co-transport mechanism may be operating. Besides the thioxanthones, some oxygenated xanthones were also recently reported as P-gp activators, by the same group of research (25).

3. Chirality

Chirality is an important and the most defiant property of stereochemistry (79). In other words, it is fundamental in the analysis of static and dynamic characteristics of the three-dimensional shapes of molecules (80). Considering stereochemistry, it is essential to distinguish structural isomerism and stereoisomerism. Structural isomers (or constitutional isomers) have the same molecular formula but different connectivity between their atoms and functional groups (81). On the other hand, stereoisomers (or spatial isomers) are molecules that have the same molecular formula, similar linkages between atoms and similar distance of linkages, but differ in spatial or three-dimensional arrangement (82). The stereoisomers can be enantiomers or diastereomers (Figure 8). When the stereoisomers are mirror images of each other and are nonsuperimposable, they are known as enantiomers (80). In contrast, when they are not mirror images they are called diastereomers (80).

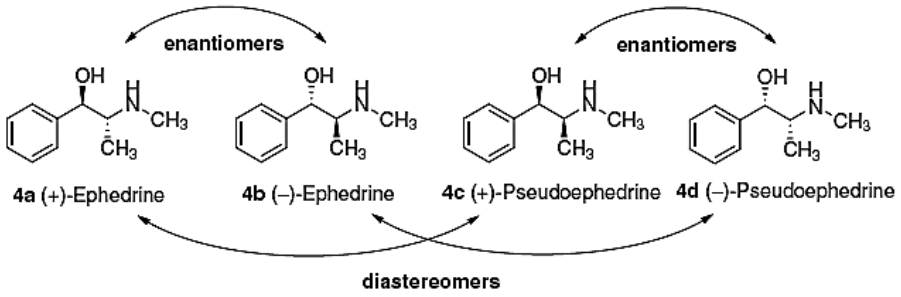

Figure 8 - Example of enantiomers and diastereomers (83).

The spatial relationship between two enantiomers is classically represented by the right and left hands. In Figure 9 the right-handed and left-handed forms of lactic acids are presented (84).

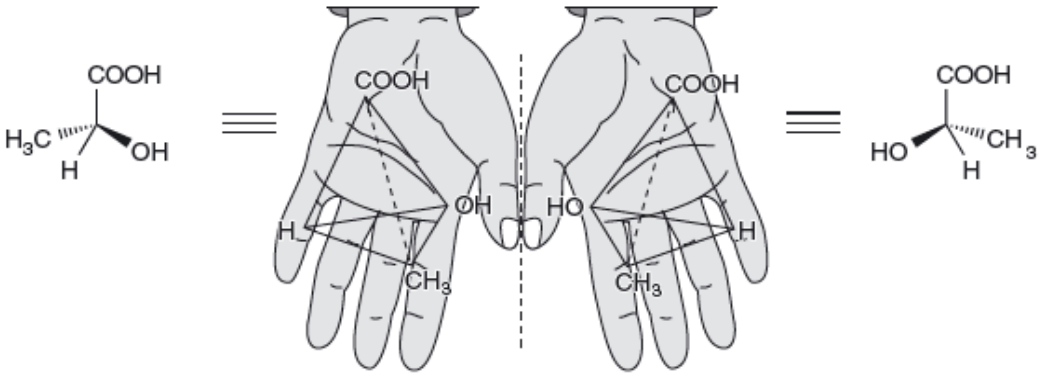

Figure 9 - Mirror images of lactic acid (83).

All compounds that are not overlapping with their own mirror image are called chiral. On the other hand, the compounds that do not fit this definition are achiral (82). More often, the chiral molecules are characterized by the presence of one asymmetric center known as stereogenic center or stereocenter (83). In fact, most chiral organic molecules present central chirality, with one or more stereogenic centers, usually tetravalent carbon atoms bonded to four different substituents (atoms or groups of atoms). In addition to carbon, nitrogen, phosphorus, sulphur, selenium and boron can also produce stereogenic centers (85). Chirality can also be originated by a plane or an axis of chirality (86).

Enantiomers present identical physical and chemical properties such as boiling point and lipophilicity, when they are in an achiral environment (85). However, it is possible to distinguish between them when they interact with chiral systems, and by their optical activity (82). Concerning this physical property, the enantiomers rotate the plane of polarized light in equal amounts but in opposite directions, assigning the symbol (+) or letter "d" to the enantiomers that rotate the plane of polarized light in the clockwise direction (dextrorotatory) and the symbol (-) or letter "l" to the enantiomers that rotate the plane of polarized light in the counterclockwise direction (levorotatory) (83). This is

consistent with absence of optical activity in racemic mixtures or racemates, i.e., equimolar mixtures of enantiomers (82).

The optical activity of enantiomers does not depend necessary from their configuration, i.e., the spatial arrangement of the substituents around the stereogenic center (11). The nomenclature (*R*)/(*S*) or Cahn-Ingold-Prelog (CIP) is the most used system in the chemical community, to distinguish enantiomers based on their configuration (83), setting a framework for an agreed stereochemical pattern (80). This system is based on the application of the CIP priority rules, and subsequent assignment of the (*R*) or (*S*) configuration, taking into account the descending order of higher priority of the groups attached to the stereogenic center. So, is attributed the configuration (*R*) when the order of priority of these groups follows the clockwise direction, and the configuration (*S*) when this sequence follows the counterclockwise direction (83). The D/L system developed by Fisher in order to describe carbohydrate stereisomers, specifically D- and L-glyceraldehyde, is also used for distinguishing enantiomers (83). This system is also commonly used for amino acids, which are named by analogy to glyceraldehyde.

The above mentioned systems are suitable only to determine the relative configuration. X-ray crystallography and chemical conversion of compounds of known stereochemistry are the most commonly used techniques to determine the absolute configuration (83).

3.1. Enantioselectivity

The human organism is a chiral environment since proteins are constituted by L-amino acids, while the carbohydrates are D-isomers of natural sugars (87, 88). Accordingly, the biomacromolecules such as receptors and enzymes, comprising these chiral units, are able to discriminate between the enantiomers, both in pharmacokinetic and pharmacodynamic processes (89). The enantiodiscrimination by biological systems is clinically important when the pharmacological and toxicological effects are significantly different between enantiomeric drugs (90). In such cases, one enantiomer can be responsible for the therapeutic activity while the other enantiomer can be inactive, possess lower activity of interest, or can be an antagonist of the active enantiomer, or has a different activity that could be desirable or undesirable (91). Some examples of well-known stereoselective responses concerning chiral drugs are presented in Table 5.

Table 5 - Examples of stereoselective responses in human concerning chiral drugs.

Drug or group of drugs	Enantiomer	Stereoselective response
Thalidomide	(*S*)-(-)	Teratogenic, inhibits the release of TNF-α from stimulated mononuclear blood cells
	(*R*)-(+)	Sedative
β-Blockers	(*S*)-(-)	100 Times higher antagonistic effect on β-adrenergic receptors than (*R*)-(+)- enantiomer
Barbiturics	(*S*)-(-)	Hypnotic and/or sedative
	(*R*)-(+)	Inactive or excitatory
β-Adrenergic receptor antagonists	(*R*)-(-)	Responsible for the bronchodilatory pharmacological effect
	(*S*)-(+)	No pharmacological effects
Citalopram	(*R*)-(-)	Non active and antagonizes the effect of (*S*)-(+)-enantiomer
	(*S*)-(+)	Pharmacologically active as a selective serotonin reuptake inhibitor
1,4-Dihydropyridines	(*S*)-(-)	Calcium channel agonist, resulting in positive inotropic and vasoconstriction responses
	(*R*)-(+)	Calcium channel antagonist, resulting in vasodilation and, at high doses, negative inotropic effects
Pencillamine	(*S*)-(-)	Anti-arthritic pharmacological action
	(*R*)-(+)	Toxic (mutagenic)
Ibuprofen	(*S*)-(-)	110 times more potent at COX 1 and 2 inhibition than (*R*)-(+)
	(*R*)-(+)	Acts as a pro-drug through chiral inversion

Data adapted of (11).

Also in pharmacokinetics, several examples of stereoselectivity are reported concern the absorption, distribution, metabolism and excretion (ADME) of drugs (12).

The stereoselectivity in metabolism is considered the primary factor responsible for the differences observed in enantioselective drug disposition. This is observed since the stereoselectivity in metabolism results, many times, in the metabolism of enantiomers at different rates and/or different routes, thus yielding alternative products (10). However, changes in the absorption and distribution of chiral compounds caused, for example, by stereoselectivity for binding proteins and transporters, as P-gp, can cause also important changes in the free fraction of drug in the plasma, in the volume of distribution, in the time half-life and the clearance, among others, which can induce toxicity or adverse effects associated to drugs (10). In the excretion, stereoselectivity may arise as a result of selectivity in protein binding and can, consequently, cause changes in glomerular filtration and passive reabsorption, in the active secretion or in the reabsorption. However, in the majority of cases, the selectivity is relatively modest (10).

As a consequence, the use of racemic mixtures typically results in stereoselective drug disposition and may also contribute to the toxicity or adverse effects associated with drugs (89). In fact, the use of stereochemically pure drugs is normally clinically advantageous (90), since it enables a reduction of the total administered dose, enhances the therapeutic window, reduces the intersubjective variability and confers a more precise estimation of dose–response relationships, among other advantages (91).

For these reasons, is essential to study the enantioselectivity in the development of new drugs (86), because the administration of chiral drugs in racemic form might induce toxicity and, in more harsh cases, may be the source of diseases with high mortality rate, as for example cancer (82).

3.2. Importance of chirality in P-gp modulation

The enantiomeric transport is a complex process and depends of different factors, namely enantiomer–enantiomer interactions, interspecies or tissue-specific differences, the concentration-dependent stereoselectivity and opposite stereoselectivity in modulation of drug transporters by the enantiomer (9). The stereoselective binding strength of carriers for drugs can be species- or tissue-specific, concentration-dependent and transporter family member-dependent (10).

For instance, stereoselectivity of P-gp may be a result in differences in the transport of enantiomers (9). A study with pioglitazone, a P-gp substrate, showed that the use of (+)-pioglitazone in enantiomeric pure form may improve clinical efficacy of the drug, because the (+)-pioglitazone levels were clearly higher than (-)-pioglitazone levels in the brains of mice dosed with racemic pioglitazone. The opposite trend was observed in the plasma (92).

The higher presence of (+)-pioglitazone in the brain suggests that can be more distributed to the brain and/or be retained for longer duration in the brain. Thus, the lower presence of (+)-pioglitazone in plasma may translate to fewer undesirable drug effects or drug-induced toxicity in peripheral tissue organs (92).

Furthermore, P-gp can be modulated in a different way by enantiomers (Zhou 2014). When the chiral drugs are P-gp modulators, one isomer can induce the activity of P-gp while its enantiomeric pair can inhibit the activity of the pump (23, 93). An example of this enantioselectivity was observed for mefloquine, a drug used in the prevention and treatment of malaria: (11*R*,12*S*)-(+)-mefloquine presents a much higher human brain penetration than (11*S*,12*R*)-(-)-mefloquine (94). The higher brain penetration of the (11*R*,12*S*)-(+)-enantiomer in humans, when compared to its antipode, was explained by the fact of mefloquine being a P-gp substrate (94). Moreover, the enantioselective inhibition of P-gp by the (-)-isomer of mefloquine was hypothesized to affect the transport of other P-gp substrates, such as cyclosporin and vinblastine (Figure 10).

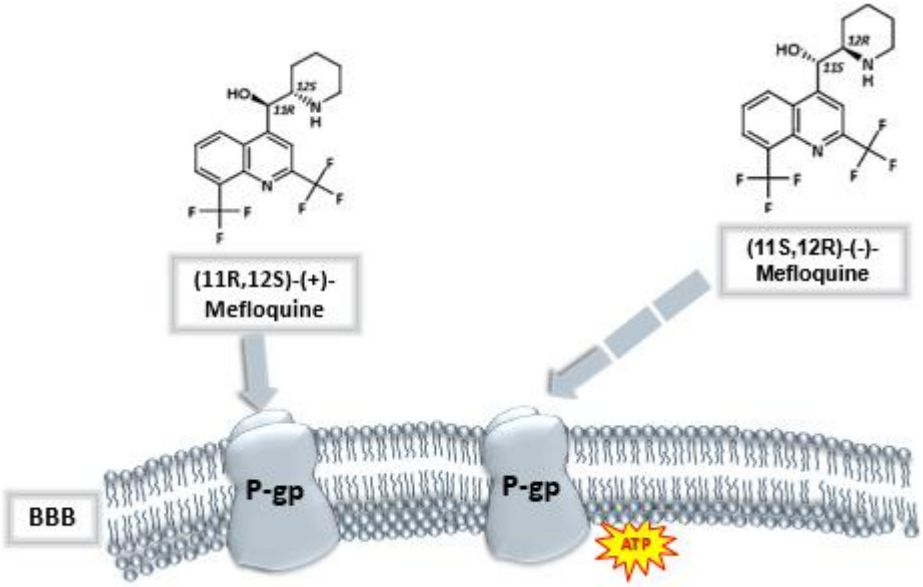

Figure 10 - Enantioselectivity of P-gp by mefloquine enantiomers.

Another interesting example of P-gp enantioselectivity was described for the H1 anti-histaminic cetirizine (Figure 11) (93). The (*R*)-cetirizine upregulates P-gp expression, while (*S*)-cetirizine down-regulates it (82, 93). Moreover, the (*R*)-enantiomer of cetirizine has approximately thirty-fold higher affinity to the human histamine H1-receptors, when compared to the (*S*)-enantiomer (95).

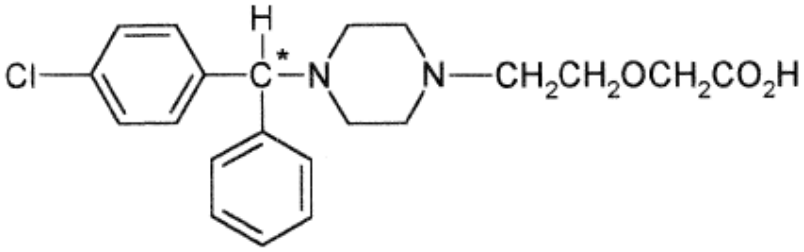

Figure 11 - Structure of cetirizine. The asterisk (*) indicates the stereogenic center

The enantioselective modulation of P-gp can also be concentration-dependent (9). This is the case of clausenamide (CLA), a candidate drug being currently developed to treat memory impairment in neurodegenerative diseases (96), being the isomer (3*S*,4*R*,5*R*,6*S*)-clausenamide [(−)-CLA] the eutomer (97). Results of a study performed in cells expressing P-gp, suggested that (−)-CLA could be a P-gp inhibitor while (+)-CLA could be an inducer of P-gp with concentration-dependent biphasic effects (97). Consequently, CLA shows stereoselective regulation of P-gp activity and possible drug—drug interactions when combined with other P-gp substrate drugs (97). These drug-drug interactions P-gp mediated may contribute for inefficacy or toxicity of drugs, depending if the modulators induce or inhibit the P-gp expression and of the degree of change in the activity of pump (23, 93).

Thus, chirality can have a considerable effect on any barrier, *in vivo*, being an important role not only on the absorption of drugs but also in their distribution and elimination issue in P-gp modulation (10, 12).

CHAPTER 2:

RESULTS AND DISCUSSION

PART I - CHEMISTRY

1.1. Synthesis of thioxanthonic derivatives

Thioxanthones are a class of compounds with interesting biological properties and, recently, have been described as P-glycoprotein (P-gp) modulators (19, 40, 46). Additionally, the modulation of P-gp by this class of compounds has been seen as a possible therapeutic strategy (6), for example against PQ cytotoxicity (25, 46). Moreover, once the chirality is considered as one of the major topics in the development of new drugs (89), it is essential to understand the effects that the enantioselectivity may have in modulation of P-gp by thioxanthonic derivatives.

Accordingly, our aim was the synthesis and characterization of a small library of new enantiomeric pairs of thioxanthonic derivatives, using 1-chloro-4-propoxy-9*H*-thioxanthen-9-one as chemical substrate (Tx) (Figure 12).

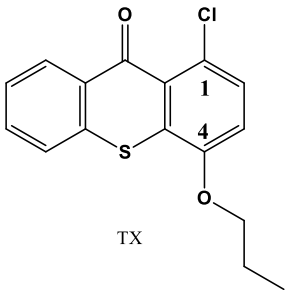

Figure 12 – Structure of the thioxanthone chemical substrate (Tx).

The new chiral thioxanthonic derivatives (ATx's **1-8**) were synthesized by Ullmann cross coupling reaction between the thioxanthone derivative 1-chloro-4-propoxy-9*H*-thioxanthen-9-one (Tx) with eight enantiomerically pure building blocks (A **9-16)** (Figure 13).

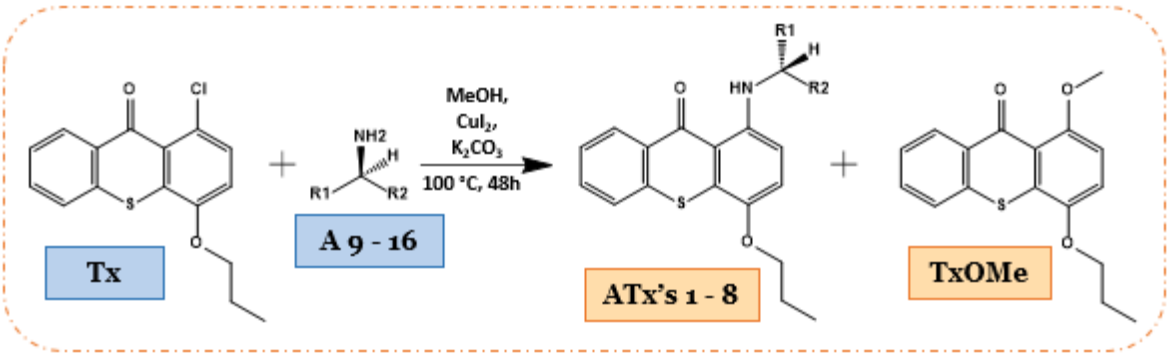

Figure 13 - General scheme of the synthesis of chiral thioxanthonic derivatives.

The conditions used were based on previous described procedures (98). All the synthesis was performed in alkaline medium, in a closed vessel, mixing the chiral amino alcohols (A **9-16**), in excess, with 1-chloro-4-propoxy-9*H*-thioxanthen-9-one (Tx), CuI in catalytic amounts (10% equiv.) in methanol. The reactions were carried out at 100 °C for 48 hours, without stirring.

The structures of the synthesized thioxanthonic derivatives ATx **1-8** and the enantiomerically pure amino alcohols A **9-16** are shown in Figure 14.

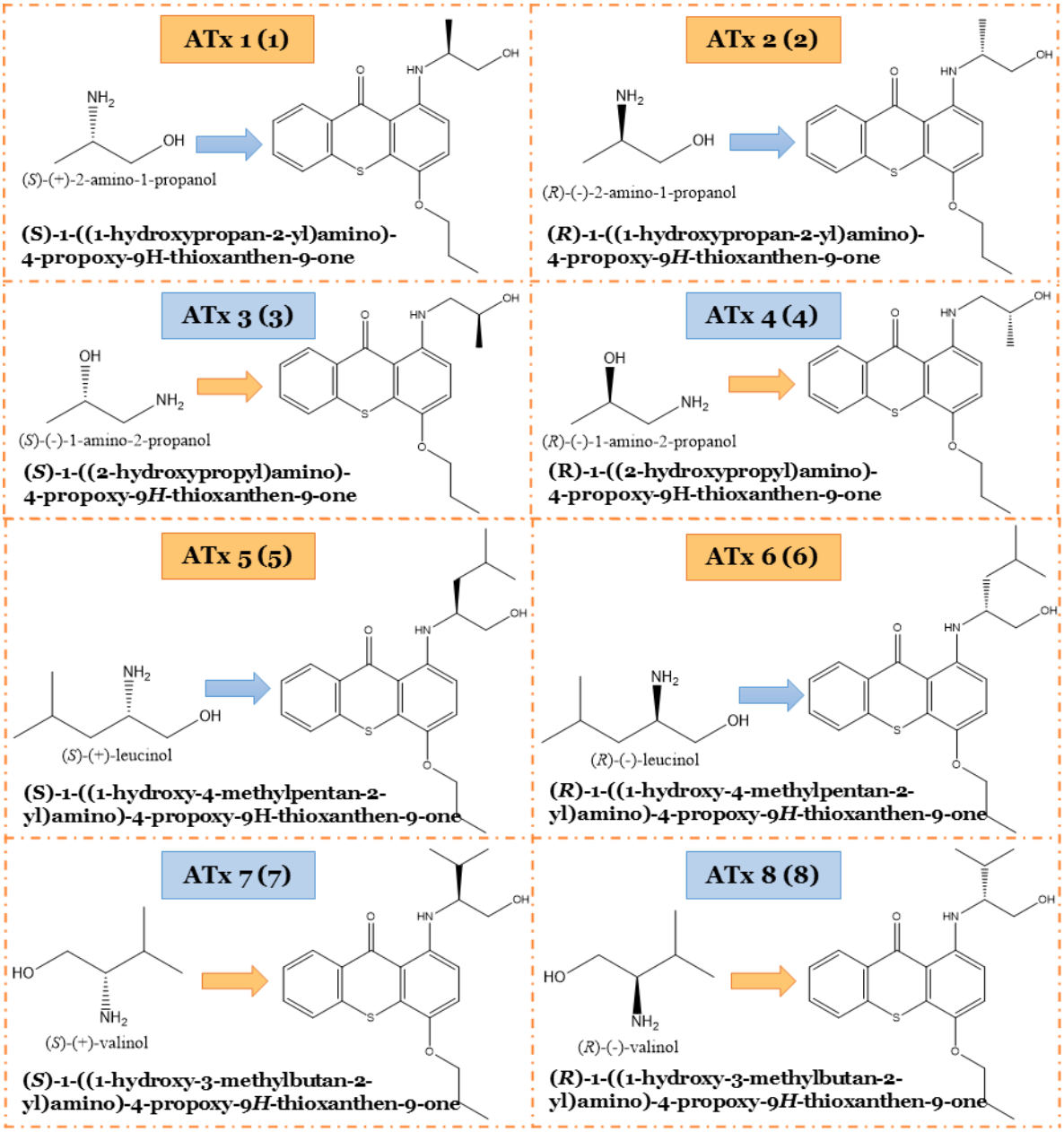

Figure 14 - Structures of the amino alcohols used as building blocks and the correspondent aminated thioxanthones.

The thioxanthone chemical substrate **(**Tx) and all the enantiomerically pure building blocks are commercially available, and were chosen based on a previous work (40) in which

thioxanthonic derivatives comprising the same thioxanthone pattern of substitution, i.e., a propoxy group at position 4 and an chiral amine at position 1 afforded the most interesting results on P-pg modulation. Moreover, in the same study aliphatic amino alcohols were the most promising activators. Therefore, the four enantiomeric pairs represented in Figure 14 were selected for this work. All the amino alcohols, namely (*S*)-(+)-2-amino-1-propanol (**9**), (*R*)-(-)-2-amino-1-propanol (**10**), (*S*)-(+)-1-amino-2-propanol (**11**), (*R*)-(-)-1-amino-2-propanol (**12**), (*S*)-(+)-leucinol (**13**), (*R*)-(-)-leucinol (**14**), (*S*)-(+)-valinol (**15**) and (*R*)-(-)-valinol (**16**), were available in enantiomerically pure form, and no tendency towards racemization or enantiomeric interconversion is expected.

The reactions were accomplished by a nucleophilic aromatic substitution of the chloride on position C-1 of the thioxanthone scaffold by the enantiomerically pure building blocks, affording the desirable chiral thioxanthone (ATx's **1-8**). The main product formed corresponded to the C-N coupling. In all cases, a secondary product, a methoxylated derivative of the thioxanthone (TxOMe) (Figure 13), corresponding to the competition of C-O cross coupling, was observed and identified by thin-layer chromatography (TLC) by the comparison with a standard previously synthesized and characterized, using the same reaction conditions (98). Besides TxOMe, other byproducts were detected in vestigial amounts, so they were not isolated for identified.

The reactions progress was monitored by TLC analysis using chloroform/acetone, 9.7:0.3 (*v/v*) as mobile phase and observed under ultraviolet (UV) light at 254 and 365 nm.

The work-up of the reactions followed a general procedure. After 48 hours, the reaction mixture was first filtered in order to eliminate the CuI. By chemical liquid-liquid extraction with HCl solution most of the acidic/neutral organic impurities were removed in the organic layer. Following, the amines were regenerated with NaOH, extracted and the extract was further subjected to a solid phase extraction (SPE) with a cation exchange cartridge to eliminate remaining impurities (TxOMe and other compounds with similar chromatographic behaviour).

This sequence of purifications was successful for the purification of thioxanthonic derivatives **4**, **5**, **6** and **7**. However, they were insufficient to isolate pure aminated thioxanthones **1**, **2**, **3** and **8**. For thioxanthonic derivatives **3** and **8**, a further purification process by crystallization from chlorophorm/diethyl ether was needed. Thioxanthones **1** and **2** were further purified by flash chromatography from their remaining precursors and following by crystallization from chlorophorm/diethyl ether.

As expected, this synthetic approach yielded the desirable products, as occurred for similar compounds in a previous work (40, 98). However, the obtained isolated yields were low

ranging from 2 to 24 % (Table 6), even in the presence of K_2CO_3 that provided an alkaline media favorable to reaction. This may be a consequence of the formation of the secondary product TxOMe (Figure 13). Despite the low yields, these reactions afforded enough quantity of the desired four enantiomeric pairs of chiral thioxanthonic derivatives for characterization and further biological activity studies.

Table 6 – Yields obtained for each chiral thioxanthone derivative.

Chiral thioxanthonic derivatives	Yield (%)
ATx 1 (1)	1.97
ATx 2 (2)	5.91
ATx 3 (3)	7.86
ATx 4 (4)	23.62
ATx 5 (5)	19.59
ATx 6 (6)	10.40
ATx 7 (7)	10.12
ATx 8 (8)	10.24

The purity of each synthesized chiral thioxanthones was determined by high performance liquid chromatography with diode-array detection (HPLC–DAD) analysis. Figure 15 illustrates a representative chromatogram obtained for ATx **8** (**8**).

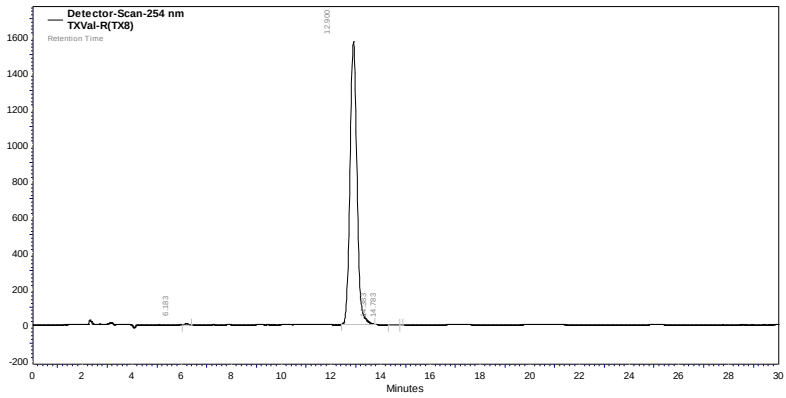

Figure 15 - HPLC chromatogram of ATx **8** (**8**). [λ= 254nm, C18, isocratic elution of methanol and water (80:20 v/v) basified with triethylamine (0.5 %) at a constant flow rate of 1.0 mL/min].

All tested compounds presented a purity of at least 95 %, as described in Table 7.

Table 7 – HPLC purity and melting point (m.p.) of all synthesized compounds.

Compound	Purity (%)	m.p. (°C)	Compound	Purity (%)	m.p. (°C)
ATx 1 (1)	**95.5**	**116 -118**	**ATx 5 (5)**	98.6	82 - 85
ATx 2 (2)	**97.5**	**118 -120**	**ATx 6 (6)**	98.6	80 - 82
ATx 3 (3)	**96.9**	**149 -152**	**ATx 7 (7)**	97.8	100 - 102
ATx 4 (4)	**96.4**	**148 -150**	**ATx 8 (8)**	98.4	102 - 104

As expected, the melting points were similar for both enantiomers of each enantiomeric pair (85).

1.2. Structure Elucidation

The structure elucidation of all new thioxanthonic derivatives (ATx's **1-8**) was established by spectroscopic methods: infrared (IR), ^{1}H and ^{13}C nuclear magnetic resonance (NMR), and bidimentional heteronuclear single quantum correlation (HSQC) and heteronuclear multiple bond correlation (HMBC). Since these determinations were performed in achiral environments, no significant differences were noted for each pair of enantiomers obtained, as expected.

The IR data of the synthesized thioxanthonic derivatives are presented in Table 8.

Table 8 - IR data of the synthesized thioxanthonic derivatives.

Compound	Bond	Vmax (cm^{-1})
ATx 1 (1)	O-H	3419
	N-H	3270
	C-H	2962, 2925, 2873
	C=O	1618
	C-C	1568, 1507, 1435
	C-N	1252
	C-O	1225, 1070
ATx 2 (2)	O-H	3447
	N-H	3282
	C-H	2963, 2927, 2874
	C=O	1611
	C-C	1595, 1569, 1506, 1436
	C-N	1252
	C-O	1226, 1072

ATx 3 (3)	OH	3460
	N-H	3320
	C-H	2965, 2933, 2875
	C=O	1607
	C-C	1566, 1556, 1501, 1450
	C-N	1249
	C-O	1227, 1060
ATx 4 (4)	O-H	3460
	N-H	3323
	C-H	2966, 2932, 2875
	C=O	1606
	C-C	1566, 1556, 1501, 1451
	C-N	1249
	C-O	1227, 1060
ATx 5 (5)	O-H	3457
	N-H	3290
	C-H	2955, 2923, 2870
	C=O	1613
	C-C	1595, 1566, 1505, 1435
	C-N	1265
	C-O	1224, 1067
ATx 6 (6)	O-H	3459
	N-H	3291
	C-H	2954, 2925, 2871
	C=O	1613
	C-C	1595, 1566, 1505, 1435
	C-N	1266
	C-O	1224, 1072
ATx 7 (7)	O-H	3385
	N-H	3256
	C-H	2960, 2926, 2873
	C=O	1614
	C-C	1569, 1514, 1463, 1434
	C-N	1249

	C-O	1225, 1070
ATx 8 (8)	O-H	3423
	N-H	3272
	C-H	2959, 2925, 2872
	C=O	1611
	C-C	1570, 1511, 1463, 1435
	C-N	1251
	C-O	1226, 1068

As expected, the IR spectra of the eight thioxanthonic derivatives showed the presence of absorptions bands corresponding to N-H bond (3270-3323 cm^{-1}) and to O-H bond (3385 - 3460 cm^{-1}), which allowed to hypothesize the binding of the chiral building blocks to the thioxanthone scaffold by an amine group. Moreover, considering the thioxanthonic scaffold, the IR data indicate the presence of an absorption band corresponding to C=O (1606 - 1628 cm^{-1}). It is also important to highlighted the presence of two absorption bands corresponding to C-O (1060-1072 and 1224-1227 cm-*1*), associated with the carbonyl group of carbon 9 and to ether group of aliphatic chain of carbon 4, respectively. Additional bands corresponding to the aromatic carbons (C-C bonds: 1434 – 1595 cm-*1*), typical of thioxanthonic compounds, could be found.

The ^{1}H and ^{13}C NMR data for aminated thioxanthones **1-8** are presented in Tables 9 - 12.

All the synthesised thioxanthonic derivatives showed similar NMR profiles with respect to the six aromatic protons of the thioxanthonic scaffold and to the protons of the propoxy group, with similar chemical shifts and coupling constants as the building block values.

Regarding the ^{1}H NMR spectra (Table 9 and 10), the signals corresponding to the six aromatic protons, namely H-2, H3, H-5, H-6, H-7, and H-8, present a range of chemical shifts between 6.73 and 8.56 ppm. The highest chemical shift value for proton H-8 is due to the magnetic anisotropy of carbonyl group (C-9) that deshields this proton.

Concerning the signals of the aliphatic chain at C-4, the chemical shifts of H-a, H-b and H-c were comprised between 1.11 and 4.10 ppm, with small variations between the different compounds.

Table 9 - ^{1}H NMR data for ATx **1** (1), ATx **2** (2), ATx **3** (3) and ATx **4** (4).

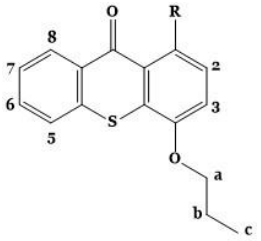	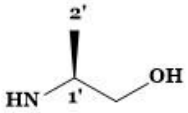	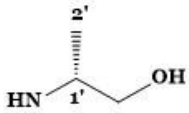	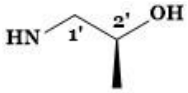	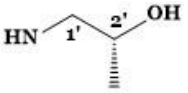
	ATx 1 (1)	**ATx 2 (2)**	**ATx 3 (3)**	**ATx 4 (4)**
	δH (ppm)			
1'	3.81, 1H, m	3.78, 1H, m	3.30, 2H, m	3.29, 2H, m
2'	1.32, 3H, d, *J* = 6.2 Hz	1.33, 3H, d, *J* = 6.3 Hz	4.26, 1H, m	4.22, 1H, m
C<u>H</u>$_2$OH /CH3	3.81, 2H, m	3.78, 2H, m	1.35, 3H, d, *J* = 6.3 Hz	1.35, 3H, d, *J* = 6.3 Hz
2	6.85, 1H, d, *J* = 9.0 Hz	6.82, 1H, d, *J* = 9.1 Hz	6.78, 1H, d, *J* = 9.0 Hz	6.73, 1H, d, *J* = 9.0 Hz
3	7.13, 1H, d, *J* = 9.0 Hz	7.13, 1H, d, *J* = 9.1 Hz	7.13, 1H, d, *J* = 9.0 Hz	7.12, 1H, d, *J* = 9.0 Hz
5	7.56, 1H, m	7.56, 1H, m	7.56, 1H, m	7.50, 1H, m
6	7.56, 1H, m	7.56, 1H, m	7.56, 1H, m	7.50, 1H, m
7	7.43, 1H, m	7.42, 1H, m	7.42, 1H, m	7.41, 1H, m
8	8.50, 1H, d, *J* = 8.0 Hz	8.50, 1H, d, *J* = 8.1 Hz	8.52, 1H, d, *J* = 8.1 Hz	8.51, 1H, d, *J* = 8.0 Hz
a	4.03, 2H, t, *J* = 6.5 Hz	4.04, 2H, t, *J* = 6.5 Hz	4.03, 2H, t, *J* = 6.5 Hz	4.03, 2H, t, *J* = 6.4 Hz
b	1.90, 2H, m	1.90, 2H, m	1.90, 2H, m	1.90, 2H, m
c	1.12, 3H, t, *J* = 7.4 Hz	1.11, 3H, m	1.12, 3H, t, *J* = 7.4 Hz	1.12, 3H, t, *J* = 7.4 Hz

*Values in ppm (δH) relative to (CH3)4Si as an internal reference.

The ^{1}H-NMR spectrum of both enantiomers ATx's **1** and **2** (1 and 2) and ATx's **3** and **4** (3 and 4) exhibited characteristic signals for the different protons of the aminated chain, however the signal corresponding to the NH of the amine could not be observed. The signals corresponding to the aminated chain of ATx **1** (1) appear at $\delta_{H\text{-}1'}$: 3.81, $\delta_{C\underline{H}_2OH}$: 3.81, and $\delta_{H\text{-}2'}$: 1.32 ppm. As expected the signals of ATx **2** (2) are similar.

In the case of the ^{1}H NMR spectrum of ATx **3** (3) and ATx **4** (4), the signals corresponding to chiral moieties arise at $\delta_{H\text{-}1'}$: 3.30, $\delta_{H\text{-}2'}$: 4.26 and $\delta_{H\text{–}CH_3}$: 1.35 ppm.

The ^{1}H NMR data of ATx **5** (5), ATx **6** (6), ATx **7** (7) and ATx **8** (8) are described in Table 10.

Table 10 - ^{1}H NMR data* for ATx **5** (5), ATx **6** (6), ATx **7** (7) and ATx **8** (8).

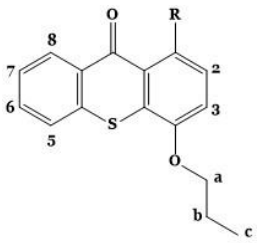

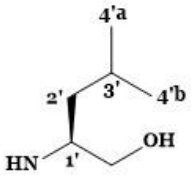

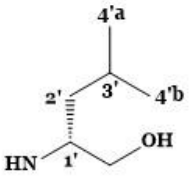

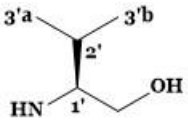

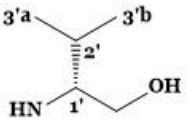

	ATx 5 (5)	ATx 6 (6)	ATx 7 (7)	ATx 8 (8)
	δH (ppm)			
1'	3.88, 1H, dd, *J* = 3.12 and *J* = 3.03 Hz	3.85, 1H, dd, *J* = 3.78 and *J* =3.27 Hz	3.53, 1H, m	3.50, 1H, m
2'	1.57, 2H, t, *J* = 6.9 Hz	1.57, 2H, t, *J* = 6.9 Hz	2.08, 1H, m	2.10, 1H, m
3'	1.78, 1H, m	1.76, 1H, m	-	-
4'a / 3'a	0.94, 3H, d, *J* = 6.5 Hz	0.96, 3H, d, *J* = 6.5 Hz	1.05, 3H, d, *J* = 6.9 Hz	1.02, 3H, d, *J* = 6.9 Hz
4'b / 3'b	0.89, 3H, d, *J* = 6.5 Hz	0.89, 3H, d, *J* = 6.5 Hz	0.87, 3H, d, *J* = 6.9 Hz	0.98, 3H, d, *J* = 6.9 Hz
C$\underline{H}_2$OH	3.71, 2H, m	3.72, 2H, m	3.86, 2H, m	3.90, 2H, m
2	6.93, 1H, d, *J* = 9.0 Hz	6.86, 1H, d, *J* = 9.1 Hz	7.07, 1H, d, *J* = 9.1 Hz	7.17, 1H, d, *J* = 8.9 Hz
3	7.13, 1H, d, *J* = 9.0 Hz	7.12, 1H, d, *J* = 9.1 Hz	7.14, 1H, d, *J* = 9.1 Hz	7.34, 1H, d, *J* = 8.9 Hz
5	7.57, 1H, m	7.55, 1H, m	7.59, 1H, m	7.64, 1H, m
6	7.57, 1H, m	7.55, 1H, m	7.59, 1H, m	7.64, 1H, m
7	7.42, 1H, m	7.42, 1H, m	7.45, 1H, m	7.49, 1H, m
8	8.51, 1H, d, *J* = 8.1 Hz	8.51, 1H, d, *J* = 8.1 Hz	8.54, 1H, d, *J* = 8.0 Hz	8.56, 1H, d, *J* = 8.0 Hz
a	4.04, 2H, t, *J* = 6.5 Hz	4.03, 2H, t, *J* = 6.5 Hz	4.06, 2H, t, *J* = 6.4 Hz	4.10, 2H, t, *J* = 6.4 Hz
b	1.85, 2H, m	1.83, 2H, m	1.91, 2H, m	1.91, 2H, m
c	1.12, 3H, t, *J* = 7.4 Hz	1.12, 3H, t, *J* = 7.4 Hz	1.12, 3H, m	1.14, 3H, m

*Values in ppm (δH) relative to (CH3)4Si as an internal reference.

The most deshielded protons of the chiral moieties of both enantiomers Tx **5** and **6** (5 and 6) are close to the amine (($\delta_{H\text{-}1'}$: 3.88 and 3.85 ppm) and alcohol groups ($\delta_{H\text{-}CH_2OH}$: 3.71 and

3.72ppm). The four signals remaining that characterize the chiral moieties of these compounds, showed values of δ ranging from 0.89 to 3.88 ppm.

The ^{1}H RMN data of ATx **7** (7) and ATx **8** (8) showed the presence of five signal corresponding to the chiral moiety. The most deshielded protons are close to the the OH ($\delta_{H\text{-}CH_2OH}$: 3.86 and 3.90 ppm), and NH groups ($\delta_{H\text{-}C1'}$: 3.53 and 3.50 ppm).

The ^{13}C NMR data of all chiral thioxanthonic derivatives (Table 11 and 12) showed the presence of one signal with the highest chemical shift value corresponding to the carbon of carbonyl group ($\delta_{C\text{-}9}$: 183.46 - 183.65 ppm) of the thioxanthone scaffold. Moreover, signals corresponding to the carbons linked to the ether chain ($\delta_{C\text{-}4}$: 145.00 – 147.74 ppm) and amine groups ($\delta_{C\text{-}1}$: 141.53 – 144.02 ppm) are also present. The lowest values shifts ($\delta_{C\text{-}a\text{-}C\text{-}c}$: 10.14 - 72.52 ppm) correspond to the three carbons of the propoxy groups. The signals corresponding to the remaining ten carbons of the thioxanthone scaffold presented values ranging from 108.42 to 137.16 ppm.

Table 11 - ^{13}C NMR data* for ATx **1** (1), ATx **2** (2), ATx **3** (3) and ATx **4** (4).

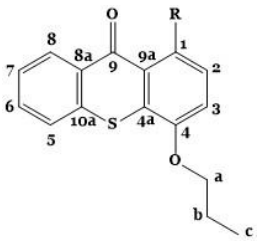	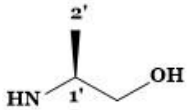	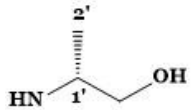	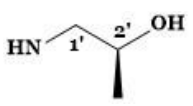	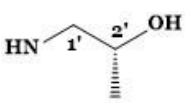
	ATx 1 (1)	**ATx 2 (2)**	**ATx 3 (3)**	**ATx 4 (4)**
	δC (ppm)			
1'	51.91	51.55	54.12	52.07
2'	16.86	17.00	65.58	66.11
C$\underline{H_2}$OH / CH3	65.96	66.04	20.97	21.02
1	144.02	144.00	144.01	143.91
2	109.80	109.02	111.83	108.42
3	119.12	119.35	117.94	119.25
4	146.50	146.80	146.18	147.48
4a	129.85	129.91	129.54	129.92
5	125.20	125.20	126.10	125.95
6	136.85	136.82	136.98	136.81
7	125.98	125.97	126.32	126.02
8	126.08	126.05	127.19	129.26
8a	131.92	131.87	133.27	131.83
9	183.55	183.56	183.46	183.46
9a	129.24	129.22	129.43	129.85
10a	114.10	114.00	115.36	113.95

a	72.48	72.52	72.31	72.47
b	22.66	22.70	22.74	22.85
c	10.71	10.71	14.15	10.71

*Values in ppm (δC) relative to $(CH_3)_4Si$ as an internal reference.

The presence of the chiral moieties in thioxanthones **1-8** were evidenced, in ^{13}C RMN data, by the presence of the signals corresponding to C-1', C-2' and C-CH_2OH/CH_3.

Table 12 - ^{13}C NMR data* for ATx **5** (5), ATx **6** (6), ATx **7** (7) and ATx **8** (8).

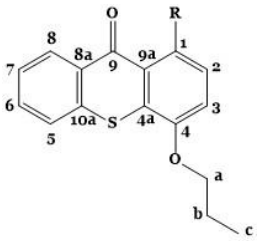

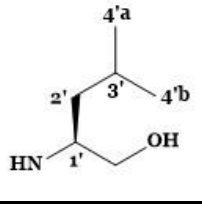

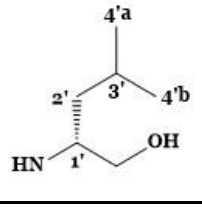

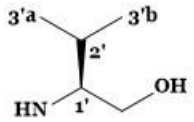

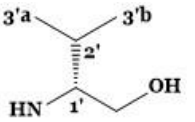

	ATx 5 (5)	**ATx 6 (6)**	**ATx 7 (7)**	**ATx 8 (8)**
	δC (ppm)			
1'	64.62	64.87	63.93	67.02
2'	40.44	40.71	28.83	28.87
3'	24.90	24.92	-	-
4'a / 3'a	22.86	22.96	18.53	19.31
4'b / 3'b	22.83	22.86	18.41	18.58
C$\underline{H_2}$OH	55.01	54.35	61.56	61.17
1	142.80	142.80	142.8	141.53
2	111.02	108.80	111.6	115.38
3	119.05	119.42	117.82	117.12
4	145.00	145.00	145.0	147.74
4a	129.97	129.93	129.53	130.43
5	126.00	125.97	125.51	126.19
6	136.7	136.82	136.43	137.16
7	126.11	126.03	125.70	126.52
8	129.28	128.80	128.84	129.21
8a	131.98	131.87	131.66	132.60
9	183.61	183.61	183.43	183.65
9a	129.83	129.24	129.03	129.52
10a	114.43	113.94	114.71	116.69
a	72.45	72.49	71.80	72.19
b	22.61	22.55	22.21	22.65
c	10.71	10.71	10.14	10.69

*Values in ppm (δ_C) relative to $(CH_3)_4Si$ as an internal reference.

The ^{13}C NMR data of ATx **5** (5) and ATx **6** (6) showed the presence of six signals corresponding to the chiral moiety with similar values ($\delta_{C\text{-}1'}$: 64.62, $\delta_{C\text{-}2'}$:40.44, $\delta_{C\text{-}3'}$: 24.90, $\delta_{C\text{-}4'a}$: 22.86$\delta_{C\text{-}4'b}$: 22.8 and $\delta_{C\text{-}CH_2OH}$: 55.01 ppm for ATx **5** (5)).

In the case of both enantiomers of ATx **7** and **8**, it should be noted the presence of five signals corresponding to chiral moieties ($\delta_{C\text{-}1'}$: 63.93, $\delta_{C\text{-}2'}$:28.83 and 28.87, $\delta_{C\text{-}3'a}$: 18.53, $\delta_{C\text{-}3'b}$: 18.41 and $\delta_{C\text{-}CH_2OH}$: 61.56 ppm for ATx **7** (7); ATx **8** (8) presented similar signals).

The ^{13}C NMR assignments were made by HSQC and HMBC experiments and by comparison with assignments of similar molecules. The HMBC data were important to deduce the chemical shifts of quaternary carbons and confirm the C-N coupling product.

The main connectivity of HMBC for ATx **2** (2) and ATx **4** (4) can be seen in Figure 16.

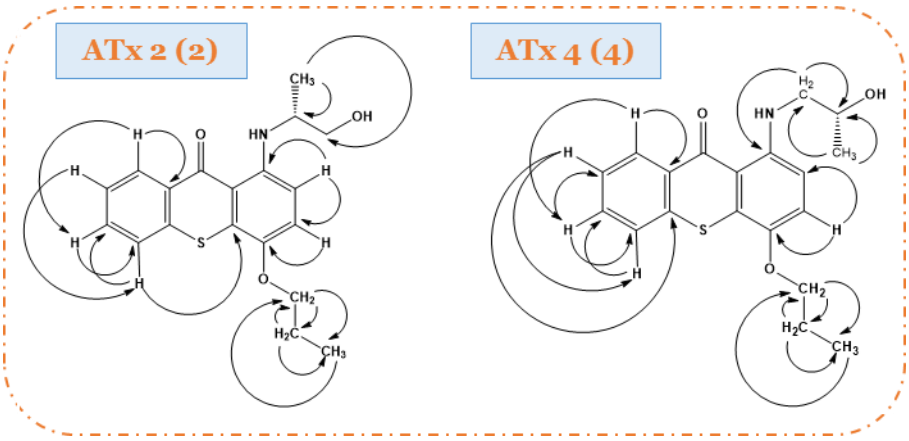

Figure 16 - Correlations between carbons and protons in HMBC spectrum of ATx **2** and ATx **4**.

The connectivities of HMBC for ATx **6** (6) and ATx **7** (7) are presented in Figure 17.

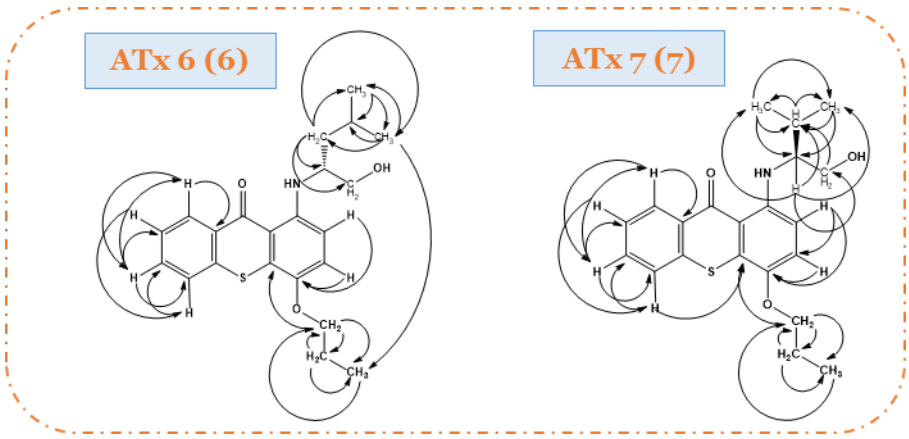

Figure 17 - Correlations between carbons and protons in HMBC spectrum of ATx **6** and ATx **7**.

For example, the formation of the amine linkage at the carbon 1 with the amino alcohol building block to afford ATx **4** could be confirmed by HMBC by the correlation between the

H-1' and carbons C-1 and C-2' (Figure 16). The data provided by HMBC spectrum are consistent with the structure of the ATx **6** and ATx **7**.

Considering that the synthesized compounds are chiral, the determination of their specific rotation was also performed. The results of measured rotation obtained with a polarimeter and the specific rotation are present in Table 13**.**

Table 13 - Specific rotation data for the synthesized thioxanthonic derivatives.

Compound	**C (g/mL) ***	**α (⁰)**	$[\propto]_D^{25^\circ C}$ **(⁰)**	**Compound**	**C (g/mL) ***	**α (⁰)**	$[\propto]_D^{25^\circ C}$ **(⁰)**
ATx1 (1)	3.4×10^{-3}	+0.38	+112	**ATx 5 (5)**	6.75×10^{-3}	-0.46	-68
ATx 2 (2)	3.4×10^{-3}	-0.38	-112	**ATx 6 (6)**	6.75×10^{-3}	+0.38	+56
ATx 3 (3)	6.67×10^{-3}	-0.08	-12	**ATx 7 (7)**	6.80×10^{-3}	-0.18	-26
ATx 4 (4)	6.67×10^{-3}	+0.08	+12	**ATx 8 (8)**	6.80×10^{-3}	+0.18	+26

* Dichloromethane

As expected, both enantiomers of the same enantiomeric pair of thioxanthonic derivatives (ATx's **1-8**) presented similar absolute values of specific rotation but with opposite signals.

These results confirmed that the synthesis occurred without racemization, and allowed to stablish which of the enantiomers is the dextrorotatory and the levorotatory.

PART II - BIOLOGICAL ACTIVITY

2.1. Cytotoxicity Assay

Thioxanthones cytotoxicity (ATx **1-8**) was evaluated by the NR uptake assay, in order to select a noncytotoxic working concentration to be used in the subsequent studies that aim to evaluate their potential to induce and/or activate P-gp. After 24 hours of incubation, significant cytotoxicity was observed for the 50 μM concentration of aminated thioxanthones **1**, **2**, **6**, **7** and **8** (Figure 18). For the other tested aminated thioxanthones (ATx's **3**, **4**, and **5**), no cytotoxicity was observed after 24 hours of incubation within the tested concentration range (0-50 μM). Therefore, ATx's effect on P-gp expression and activity was further evaluated using a noncytotoxic concentration of 20 μM.

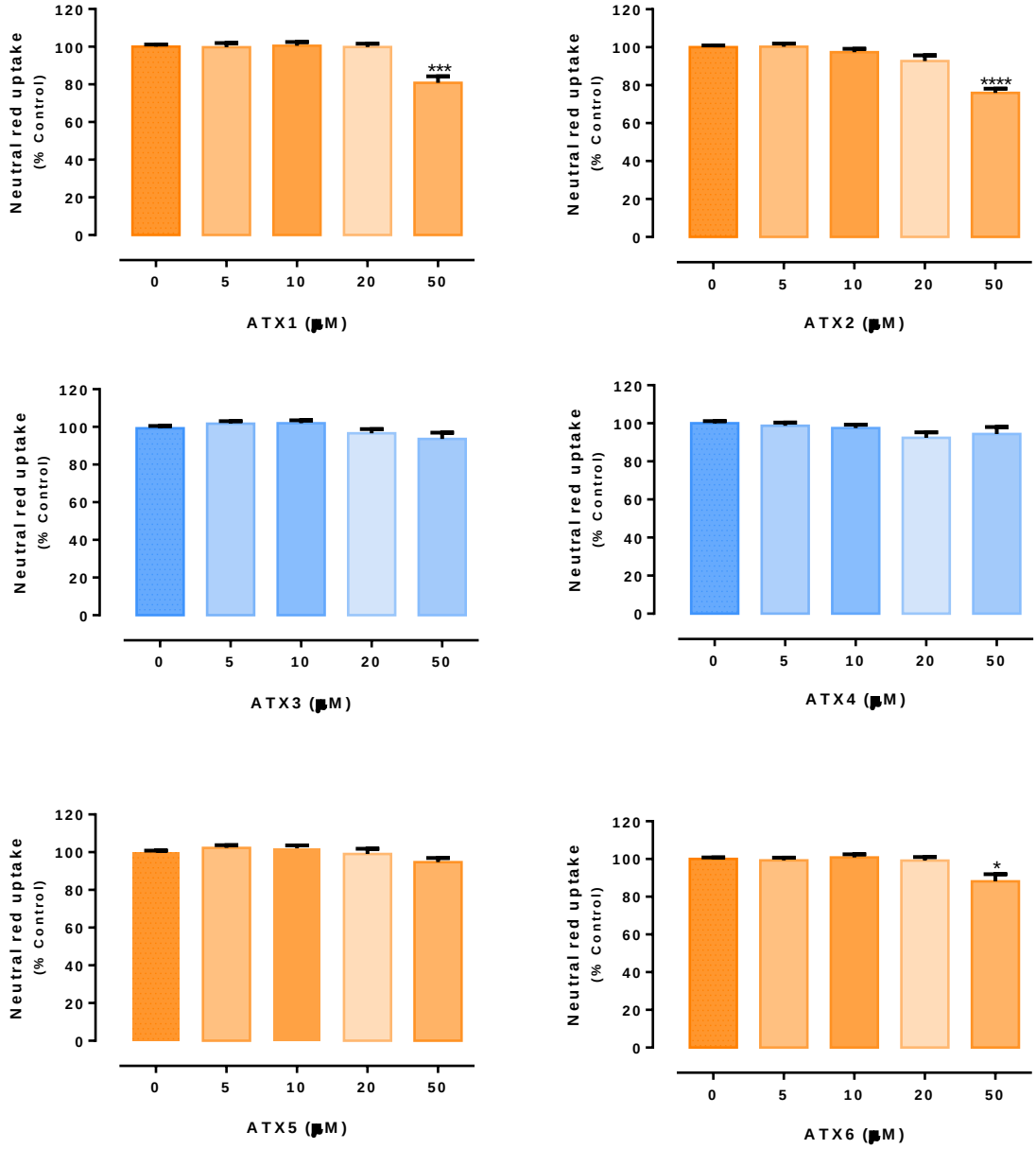

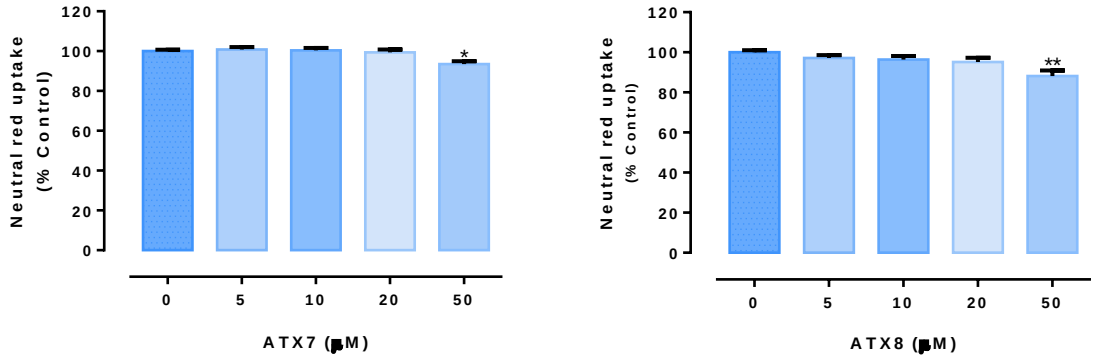

Figure 18 - Aminated thioxanthones ATx **1** - ATx **8** (0 – 50 μM) cytotoxicity in Caco-2 cells evaluated by the Neutral Red uptake assay, 24 hours after exposure. Results are presented as mean ± standard error mean (SEM) from at least 5 independent experiments (performed in triplicate) . Statistical comparisons were estimated using the nonparametric method of Kruskal–Wallis (one-way ANOVA on ranks), followed by the Dunn's multiple comparisons post hoc test [*p < 0.05; **p < 0.01; ***p < 0.001; ****p < 0.0001 *vs*. control (0 μM)].

2.2. Flow cytometry analysis of P-glycoprotein expression

The ability of the tested ATx's to induce P-gp expression in Caco-2 cells was evaluated by flow cytometry, using a P-gp monoclonal antibody [UIC2] conjugated with PE.

As shown in Figure 19, ATx **2** and ATx **6** significantly increased P-gp expression to 131 and 130%, respectively, when compared to control cells. For ATX **1** and ATX **5**, although a slight increase in P-gp expression was observed, no significance was obtained when compared to control cells. Furthermore, for ATx **3**, ATx **4**, ATx **7** and ATx **8**, no significant effect on P-gp expression was observed after 24 hours of incubation.

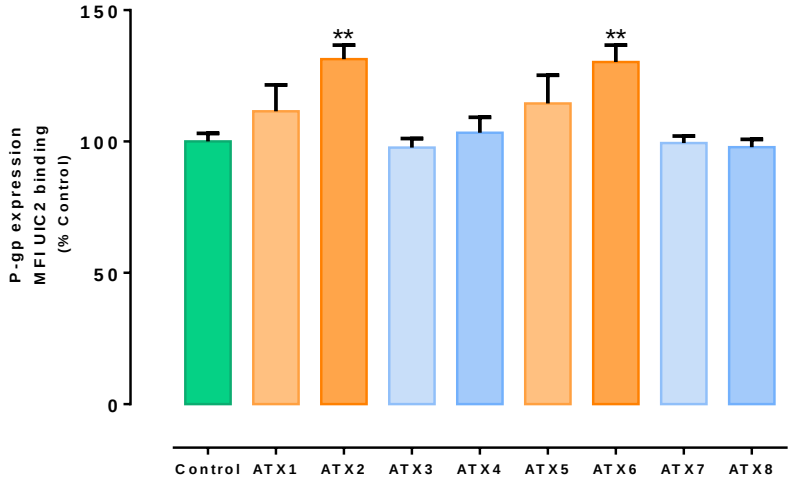

Figure 19 - Flow cytometry analysis of P-glycoprotein expression levels in Caco-2 cells exposed to ATx's **1-8** (20 μM) for 24 hours. Results are presented as mean ± standard error mean (SEM) from 2 independent experiments (performed in duplicate). Statistical comparisons were made using One-way ANOVA, followed by Tukey's multiple comparisons test [**p < 0.01 *vs*. control (0 μM)].

2.3. Evaluation of P-glycoprotein transport activity

The evaluation of P-gp transport activity was determined by flow cytometry using rhodamine (RHO) 123, a P-gp fluorescent substrate (20, 40). Two different approaches were performed.

In the first approach, RHO 123 accumulation was evaluated in the presence of the tested ATx's **1-8** (20 μM) during the RHO 123 accumulation phase that lasted 60 minutes, in order to evaluate the potential immediate effects of the tested compounds on P-gp activity as a result of a direct activation of the pump. P-gp activity was evaluated through the ratio between the mean intracellular RHO123 fluorescence intensity (MFI) obtained under P-gp inhibition (IA) and the MFI observed in normal conditions (NA, in the absence of P-gp inhibition). A higher ratio results from a smaller MFI NA, which is a consequence of a higher P-gp activity as the dye is being pumped out of the cells during the accumulation phase.

As observed in Figure 20, all the tested compounds induced a significant increase in P-gp activity, when compared to control cells. From the tested ATx's, ATx **2** and ATx **7** were the most efficient P-gp activators, as revealed by the increased P-gp activity that resulted from an increased RHO 123 efflux (P-gp activity significantly increased to 132 and 131 %, respectively, when compared to control cells).

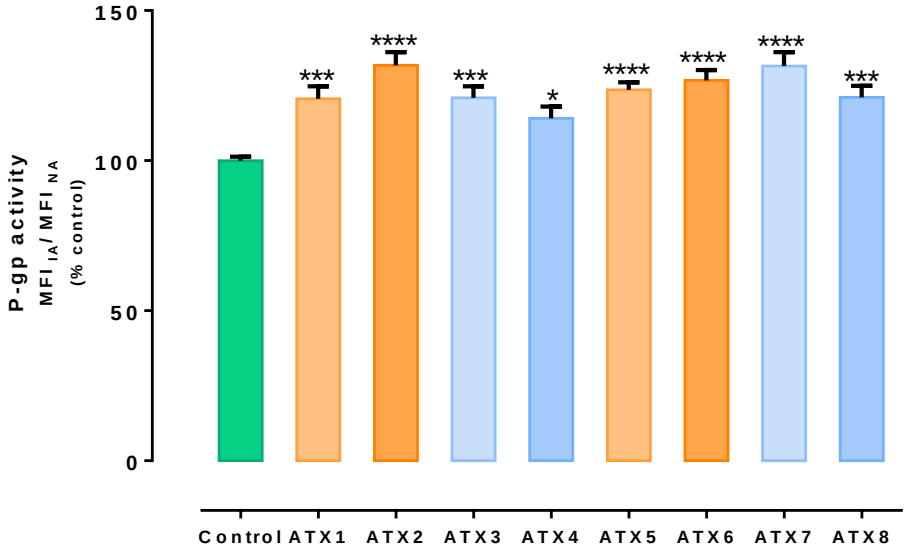

Figure 20 - P-glycoprotein activity evaluated through the RHO 123 accumulation in the presence of ATx's (20 μM) during the RHO123 accumulation phase. Results are presented as mean ± SEM from 5 independent experiments (performed in triplicate). Statistical comparisons were estimated using One-way ANOVA, followed by Tukey's multiple comparisons test [*p < 0.05; ***p < 0.001; ****p < 0.0001 *vs.* control (0 μM)].

In the second approach, RHO 123 accumulation was evaluated in Caco-2 cells pre-exposed to the tested ATx's (20 μM) for 24 hours. With this second protocol, it is possible to evaluate whether the increased P-gp expression induced by the ATx's is accompanied by the corresponding increases in P-gp activity, given that an increased protein expression does

not necessarily translates into an increased transport activity (Silva et al. 2014a; Takara et al. 2009).

The obtained results (Figure 21) demonstrated a significant increase in P-gp activity for seven of the tested compounds, namely ATx **1**, ATx **2**, ATx **4**, ATx **5**, ATx **6**, ATx **7** and ATx **8**. In fact, P-gp activity increased to 163, 167, 147, 176, 169, 167 and 165 % for ATx **1**, ATx **2**, ATx **4**, ATx **5**, ATx **6**, ATx **7** and ATx **8**, respectively.

For ATx **3**, no significant increase in P-gp activity was observed when compared to control cells (P-gp activity increased only to 115 %).

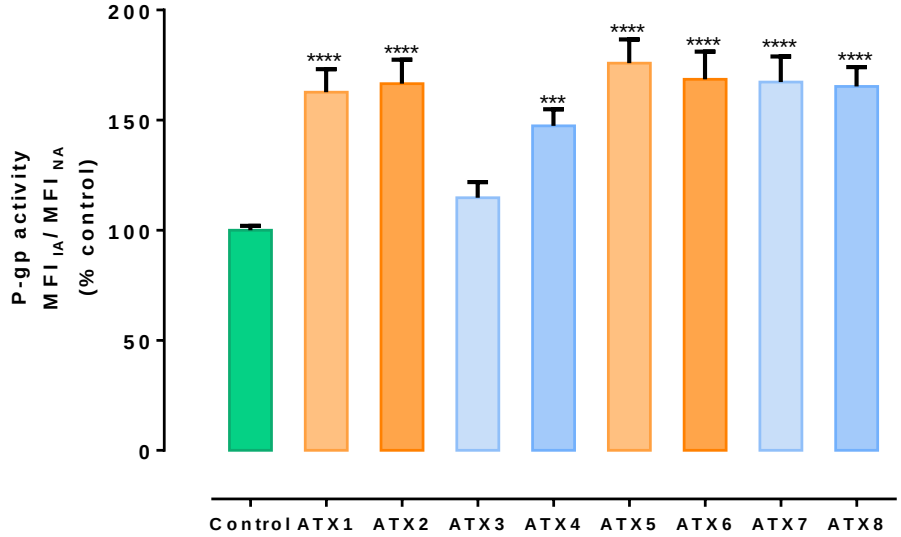

Figure 21 - P-glycoprotein activity evaluated through the RHO 123 accumulation in Caco-2 cells exposed to ATx's (20 μM) for 24 hours. Results are presented as mean ± SEM from 4 independent experiments (performed in duplicate). Statistical comparisons were estimated using One-way ANOVA, followed by Tukey's multiple comparisons test [***p < 0.001; ****p < 0.0001 *vs.* control (0 μM)].

2.4. Determination of ATPase activity

The effects of ATx's **1-8** on the ATPase activity of P-gp was evaluated through of detection and quantification of the unmetabolized ATP, as a luciferase-generated luminescent signal, in human P-gp-enriched membranes. P-gp-dependent decreases in luminescence reflect ATP consumption by P-gp and, consequently, a decrease in the obtained signal reflects the presence of a compound that stimulates P-gp ATPase activity.

In the present study, Na3VO4 (sodium orthovanadate) was used as a selective P-gp inhibitor and, thus, samples treated with Na3VO4 have no P-gp ATPase activity. Consequently, the difference in luminescent signal between Na3VO4-treated samples and untreated samples (ΔRLU_{basal}) reflects the basal P-gp ATPase activity, whereas the difference in luminescent signal between Na3VO4-treated samples and samples treated with the test compound (TC)

(ΔRLU_{TC}) represents the P-gp ATPase activity in the presence of the test compound. Therefore, the test compound can be a stimulator of P-gp ATPase activity, if $\Delta RLU_{TC} > \Delta RLU_{basal}$; can be an inhibitor of P-gp ATPase activity, if $\Delta RLU_{TC} < \Delta RLU_{basal}$; or can have no effect on P-gp ATPase activity , if $\Delta RLU_{TC} = \Delta RLU_{basal}$. Verapamil was used in the present assay as a positive control since it is a substrate for P-gp-mediated transport thus stimulating P-gp ATPase activity.The results for the eight tested compounds and verapamil (Ver) are shown in Figure 22, as well as the basal P-gp ATPase activity.

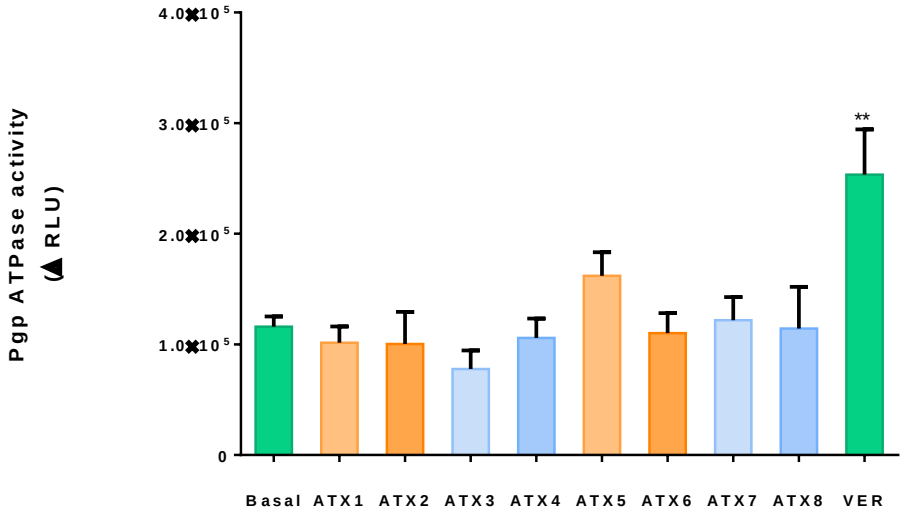

Figure 22 – P-gp ATPase activity in the presence of ATx's **1-8**. Results are expressed as mean ± SEM from 3 independent experiments (performed in triplicate). Statistical comparisons were estimated using One-way ANOVA, followed by Tukey's multiple comparisons test [**p < 0.01 vs. basal P-gp ATPase activity].

None compound tested (ATx's **1-8**) caused a significant change in the Δ RLU in relation to the basal P-gp ATPase activity.

2.5. Discussion

Caco-2 cells express P-gp at levels like those found in normal human jejunum (99) and they were already validated as a suitable *in vitro* model for the evaluation of P-gp modulation (20, 25).

P-gp plays an important role in the pharmacokinetics of a large range of drugs and, consequently, the level of expression and functionality of this efflux transporter can greatly affect the therapeutic effectiveness of many drugs. Accordingly, is essential to study the influence of P-gp expression and activity levels in drug discovery and development.

Thioxanthones are a class of interesting compounds due the numerous demonstrated biological properties, namely the P-gp modulation ability. Although the studies on their ability to modulate P-gp expression and activity are still sparse, some compounds of this class were already reported to increase or decrease P-gp expression/activity (40, 46).

In order to find dual inhibitors of P-gp and tumor cell growth, the P-gp activity in cells exposed to different thioxanthonic derivatives was previously analysed. In those studies, for fifteen of the investigated compounds it was observed an effect compatible with P-gp inhibition, three of them with an effect similar to that elicited by the known P-gp inhibitor, quinidine, and higher than the known thioxanthone hycanthone. In opposition, twelve derivatives showed a significant decrease in the RHO123 accumulation, an effect compatible with P-gp activation. Furthermore, several aminated thioxanthones demonstrated to be highly effective at inhibiting P-gp in a chronic myelogenous leukemia cell line, K562 cells, suggesting a potential use in reducing multi-drug resistance (40).

More recently, in a study focused on P-gp induction as an antidotal strategy to prevent PQ-mediated cytotoxicity, it was evaluated the ability of five thioxanthones to act as P-gp inducers and also their ability to immediately increase the pump activity as a consequence of a direct activation of the pump (46). In this study, all the tested ATx's significantly increased both P-gp expression and activity in Caco-2 cells, 24 hours after exposure, being the first report on the ability of such compounds to act as P-gp inducers. Moreover, although it is known that increases in protein expression may not necessarily result in proportional increases in the pump activity, for these compounds, the detected increases in the cell surface P-gp expression (since the UIC2 monoclonal antibody used in the experiments recognizes an external P-gp epitope) were accompanied by similar increases in its transport activity. An important aspect to note among the obtained data was the ability of all the tested thioxanthonic compounds to rapidly and significantly increase P-gp activity, without interfering with its expression, an effect compatible with a P-gp activation phenomenon.

Contrarily to what was observed in the previously mentioned study, in the present work, the data obtained for the eight tested compounds demonstrated that, although not all aminated thioxanthones (ATx's **1-8**) caused a significant increase in P-gp expression 24 hours after exposure, all the tested compounds significantly increased P-gp activity. In fact, and as previously mentioned, it is known that increases in protein expression may not result necessarily in proportional increases in pump activity, and that increases in activity can be observed independently of the level of expression.

Furthermore, the tested ATx's **1-8** demonstrated to be P-gp activators since they were able to significantly increase P-gp transport function without interfering with the protein

expression levels, such as demonstrated by the data obtained in the RHO 123 accumulation assay performed in the presence of the ATx's during a short 60 minutes' accumulation phase. The RHO 123 accumulation evaluated using this protocol does not reflects a possible contribution of an increased P-gp expression in the increased activity due to the short duration of the contact between the ATx's and the cells during the RHO 123 accumulation phase.

Curiously, although ATx **1**, **4**, **5**, **7** and **8** were not able to significantly increase P-gp expression 24 hours after exposure, a significant increased P-gp activity was observed in Caco-2 cells pre-exposed to the tested compounds for this incubation period. Therefore, since these compounds demonstrated to be P-gp activators (as demonstrated by the significant differences observed in the RHO123 accumulation assay performed with the compounds present only the short RHO123 accumulation phase), the observed increases in the pump activity may result from a direct pump activation, instead of an increased P-gp expression. The observed P-gp activation may be caused by the compound that remains intracellularly, once the cells are pre-exposed to the tested compounds for 24 h, and then washed (to remove the tested compounds) prior to the evaluation of P-gp activity by the RHO123 accumulation assay. In what concerns to P-gp ATPase activity, no significant differences were observed between the P-gp ATPase activity observed in the presence of the tested compounds and the basal P-gp ATPase activity. Therefore, as ATx's **1-8** seem to not affect the P-gp ATPase activity, there are unlikely to be substrates for P-gp-mediated transport, since P-gp substrates, like verapamil, typically stimulate its ATPase activity.

All compounds tested were synthesized in enantiomeric pure form in order to study the effect of the enantioselectivity in P-gp modulation.

It is known that stereoselectivity of P-gp may be a result of differences in the transport of enantiomers, and may, consequently, affect the effectiveness and safety of several drugs (9).

Although, until the present date, no studies were reported focusing the stereoselectivity of thioxanthones in modulating P-gp, some examples of enantioselective modulation of P-gp with other scaffolds have already been described (92-94, 97).

An interesting example of this enantioselectivity is observed with mefloquine, since (11R,12S)-(+)-mefloquine presents a much higher human brain penetration than (11S,12R)-(-)-mefloquine (94). Furthermore, P-gp can be modulated in a different way by enantiomers as described for cetirizine, which up-regulated P-gp expression with the (*R*)-enantiomer and down-regulates by it with treatment with (*S*)-cetirizine (82, 93).

Comparing the results obtained for the studied enantiomeric pairs (ATx **1** and ATx **2**, ATx **3** and ATx **4**, ATx **5** and ATx **6**, and ATx **7** and ATx **8**), no significant differences in P-gp

expression neither in P-gp activity were observed. Consequently, this library of compounds did not put in evidence the stereoselective modulation of P-gp as previously observed for other substrates, such as for mefloquine enantiomers. Future *in silico* studies will be performed and may help to explain the obtained experimental results.

CHAPTER 3:

CONCLUSIONS

Conclusions

Thioxanthonic derivatives and, particularly, aminated thioxanthones, have been characterized as P-gp modulators. Since the pharmacokinetics, efficacy and safety of drugs that are P-gp substrates depend on the level of expression and functionality of P-gp, and can be affected by the chirality, it is important to better understand the effect that enantioselectivity may have in P-gp modulation.

Therefore, in order to accomplish the main aim of this study, four enantiomeric pairs of thioxanthonic derivatives were synthesized, in an enantiomerically pure form. The reaction conditions used in the Ullmann cross coupling reaction between a suitable functionalize thioxanthone with chiral building blocks allowed a successful synthesis of the desirable thioxanthones.

Spectroscopic methods (IR, ^{1}H NMR, ^{13}C NMR, and bidimensional HSQC and HMBC) allowed the unambiguous elucidation of all the thioxanthonic derivatives (ATx **1-8**) and the absolute values of specific rotation confirmed that no racemization occurred under these reaction conditions. Moreover, the purification process applied allowed to obtain the desirable thioxanthones with a purity of at least 95 % and with enough amounts to proceed with the evaluation of their biological activity.

The assay carried out for evaluation of the biological activity of the tested ATx's **1-8** have the ability the increase the P-gp activity without interfering with its levels of expression and, therefore, can be characterized as P-gp activators. ATx **2** and ATx **7** demonstrated to be the more efficient P-gp activators, among all the aminated thioxanthones tested.

Comparing the results obtained with enantiomers (R) and (*S)*, no significant enantioselectivity was observed for all the tested enantiomeric pairs.

CHAPTER 4:

EXPERIMENTAL

PART I – CHEMISTRY

1.1. General methods

All reagents and solvents were purchased from Sigma Aldrich, and had no further purification process. Solvents were evaporated using rotary evaporator under reduced pressure, Buchi Waterchath B-480.

Reactions were performed in a muffle for 48 hours at 100º C. All reactions were monitored by TLC carried out on precoated plates with 0.2 mm of thickness using Merck silica gel 60 (GF254). The UV light at 254 and 365 nm or/and chemical.

Flash column chromatography using Merck silica gel 60 (0.040-0.063 mm), flash cartridge chromatography (GraceResolv®, Grace Company, Deerfield, IL, USA), and Discovery® DSC-SCX SPE cationic exchange cartridge were used in the purification of the synthesized compounds.

Melting points (m.p.) were obtained in a Köfler microscope and are uncorrected. Infrared (IR) spectra were obtained in KBr microplates in a Fourier transform infrared spectroscopy spectrometer Nicolet iS10 from Thermo Scientific with Smart OMNI-Transmisson accessory (Software OMNIC 8.3) (cm^{-1}).

Optical rotation measurements were carried out on a Polartronic Universal polarimeter using dichloromethane as solvent.

NMR spectra were performed in University of Aveiro, Department of Chemistry, and were taken in CDCl3 (Deutero GmbH) at room temperature on Bruker Avance 300 spectrometer (300.13 MHz for ^{1}H and 75.47 MHz for ^{13}C). ^{13}C NMR assignments were made by bidimentional HSQC and HMBC experiments (long-range C, H coupling constants were optimized to 7 and 1 Hz) or by comparison with the assignments of similar molecules.

HPLC analyses were performed by Dr. Sara Cravo, Department of Chemistry, Laboratory of Organic and Pharmaceutical Chemistry, Faculty of Pharmacy, University of Porto. The HPLC analysis was performed on a Finnigan Surveyor equiped with diode array detector TSP UV8000LP. Chromatographic separation was carried out on 250 × 4.6 mm i.d. FortisBIO C18 column (5 μM) with the mobile phase MeOH:H_2O:TEA (80:20:0.5 *v/v/v*). The flow rate was 1 ml/min. An aliquot of 20 μL of each synthesized tioxanthone derivative (ATx's **1-8**) was injected into the HPLC system.

1.2. Synthesis of thioxanthonic derivatives

1.2.1 General procedure

The 1-chloro-4-propoxy-9*H*-thioxanthen-9-one (Tx, 450 mg, 1.48 mmol) and suitable chiral amino alcohol precursor (A **10-17**, 1.72 mmol) were dissolved in methanol (30 mL) and CuI (0.15 mmol) and K_2CO_3 (1.92 mmol) were added. The reaction mixture was heated at 100º C in a muffle for 48 hours, and monitored by TLC using the mobile phase chloroform/acetone 9.7:0.3 (*v/v*). After the completion of the reaction, the crude material was filtrated, washed with dichloromethane and was dried and concentrated under reduced pressure. Then, the solid was dissolved in 50 mL of dichloromethane and extracted with HCl 1M (3 × 50mL). The aqueous layer was basified with NaOH 20% and extracted with dichloromethane (3 × 100 mL). The organic layers were gathered, washed with water (50 mL), dried over anhydrous sodium sulphate and concentrated under reduced pressure.

Then, a solid phase extraction with a cation exchange cartridge Discovery ® DSC-SCX was applied to the extract material, as following: activation of the cartridge with dichloromethane (50 mL); loading the cartridge with the sample (previously incorporated in silica); elution with dichloromethane; elution with a mixture of dichloromethane/methanol 5:5 (*v/v*); elution with methanol 100%; elution with NH3 2% in methanol. All the fractions were controlled by TLC using as mobile phase chloroform/ acetone 9.7: 1.3. The fractions containing the thioxanthonic derivatives were gathered and concentrated under reduced pressure. The solids obtained was subjected to different work-up strategies as described below.

1.2.2. Synthesis of (*S*)-1-((1-hydroxypropan-2-yl)amino)-4-propoxy-9*H*-thioxanthen-9-one (ATx 1) (1)

The solid obtained following the general procedure (section 1.2.1.) was then purified by a flash column chromatography with *n*-hexane/ ethyl acetate in gradient and crystallized from chloroform and petroleum ether (4:1). The procedure allowed obtaining the desirable compound ATx **1** (1) as a red solid in 1.97 % yield (10.0 mg).

ATx **1** (1): m.p: 116 - 118 ºC; $[\alpha]_D^{25^\circ C}$ +112° (c = 3.4 x 10^{-3}g/mL in dichloromethane).

IR (KBr) v $_{max}$: 3419, 3270, 2962, 2925, 2873, 2359, 2341, 1618, 1568, 1507, 1435, 1293, 1269, 1252, 1225, 746 cm^{-1}.

^{1}H NMR (300.13 MHz, $CDCl_3$): δ: 8.50 (1H, d, *J* = 8.0 Hz, H-8), δ: 7.56 (2H, m, H-5 and H-6), δ: 7.43 (1H, m, H-7), δ: 7.13 (1H, d, *J* = 9.0 Hz, H-3), δ: 6.85 (1H, d, *J* = 9.0 Hz, H-2), δ: 4.03 (2H, t, *J* = 6.5 Hz, H-a), δ: 3.81 (3H, m, H-1' and C<u>H$_2$</u>OH), δ: 1.90 (2H, m, H-b), δ: 1.32 (3H, d, *J* = 6.2 Hz, H-2'), δ: 1.12 (3H, t, *J* = 7.4 Hz, H-c).

^{13}C NMR (75.47 MHz, $CDCl_3$): δ: 183.55 (C-9), 146.50 (C-4), 144.02 (C-1), 136.85 (C-6), 131.92 (C-8a), 129.85 (C-4a), 129.24 (C-9a), 126.08 (C-8), 125.98 (C-7), 125.20 (C-5), 119.12 (C-3), 114.10 (C-10a), 109.80 (C-2), 72.48 (C-a), 65.96 (C-CH_2OH), 51.91 (C-1'), 22.66 (C-b), 16.86 (C-2'), 10.71 (C-c).

1.2.3. Synthesis of (*R*)-1-((1-hydroxypropan-2-yl)amino)-4-propoxy-9*H*-thioxanthen-9-one (ATx 2) (2)

The solid obtained with the general procedure (section 1.2.1.) was subject to the same purification procedures as described above for the ATx **1** (1), allowing to obtain the desirable compound 2 as a red solid in 5.91 % yield (30.0 mg).

ATx **2** (2): m.p: 118 - 120 °C; $[\alpha]_D^{25°C}$ - 112° (c = 3.4 x 10^{-3}g/mL in dichloromethane).

IR (KBr) v $_{max}$: 3447, 3282, 2963, 2927, 2874, 1611, 1595, 1569, 1506, 1436, 1290, 1270, 1252, 1226, 1072, 795, 746 cm^{-1}.

^{1}H NMR (300.13 MHz, $CDCl_3$): δ: 8.50 (1H, d, *J* = 8.1 Hz, H-8), δ: 7.56 (2H, m, H-5 and H-6), δ: 7.42 (1H, m, H-7), δ: 7.13 (1H, d, *J* = 9.1 Hz, H-3), δ: 6.82 (1H, d, *J* = 9.1 Hz, H-2), δ: 4.04 (2H, t, *J* = 6.5 Hz, H-a), δ: 3.78 (3H, m, H-1' and C$\underline{H_2}$OH), δ: 1.90 (2H, m, H-b), δ: 1.33 (3H, d, *J* = 6.3 Hz, H-2'), δ: 1.11 (3H, m, H-c).

^{13}C NMR (75.47 MHz, $CDCl_3$): δ: 183.56 (C-9), 146.80 (C-4), 144.00 (C-1), 136.82 (C-6), 131.87 (C-8a), 129.91 (C-4a), 129.22 (C-9a), 126.05 (C-8), 125.97 (C-7), 125.20 (C-5), 119.35 (C-3), 114.00 (C-10a), 109.02 (C-2), 72.52 (C-a), 66.04 (C-CH_2OH), 51.55 (C-1'), 22.70 (C-b), 17.00 (C-2'), 10.71 (C-c).

1.2.4. (*S*)-1-((2-hydroxypropyl)amino)-4-propoxy-9*H*-thioxanthen-9-one (ATx 3) (3)

The solid obtained with the general procedure (section 1.2.1.) was then crystallized from chloroform and petroleum ether, to obtain the desirable compound 3 as a red solid in 7.86 % yield (40.0 mg).

ATx **3** (3): m.p: 149-152 °C; $[\alpha]_D^{25°C}$ - 12° (c = 6.67 x 10^{-3}g/mL in dichloromethane).

IR (KBr) v $_{max}$: 3460, 3320, 2965, 2933, 2875, 1607, 1566, 1556, 1502, 1450, 1434, 1286, 1269, 1249, 1227, 1158, 1133, 1060, 744 cm^{-1}.

^{1}H NMR (300.13 MHz, $CDCl_3$): δ: 8.52 (1H, d, *J* = 8.1 Hz, H-8), δ: 7.56 (2H, m, H-5 and H-6), δ: 7.42 (1H, m, H-7), δ: 7.13 (1H, d, *J* = 9.0 Hz, H-3), δ: 6.78 (1H, d, *J* = 9.0 Hz, H-2), δ: 4.26 (1H, m, H-2'), δ: 4.03 (2H, t, *J* = 6.5 Hz, H-a), δ: 3.30 (2H, m, H-1'), δ: 1.90 (2H, m, H-b), δ: 1.35 (3H, d, *J* = 6.3, CH_3), δ: 1.12 (3H, t, *J* = 7.4, H-c).

^{13}C NMR (75.47 MHz, $CDCl_3$): δ: 183.46 (C-9), 146.18 (C-4), 144.01 (C-1), 136.98 (C-6), 133.27 (C-8a), 129.54 (C-4a), 129.43 (C-9a), 127.19 (C-8), 126.32 (C-7), 126.10 (C-5), 117.94 (C-3), 115.36 (C-10a), 111.83 (C-2), 72.31 (C-a), 65.58 (C-2'), 54.12 (C-1'), 22.74 (C-b), 20.97 (C-CH_3), 14.15 (C-c).

1.2.5. (*R*)-1-((2-hydroxypropyl)amino)-4-propoxy-9*H*-thioxanthen-9-one (ATx 4) (4)

The general procedure (section 1.2.1.) allowed to obtain the desirable compound 4 as a red solid in 23.62 % yield (120.0 mg).

ATx **4** (4): m.p: 145-150 ℃; $[\alpha]_D^{25℃}$ + 12° (c = 6.67 x 10^{-3}g/mL in dichloromethane).

IR (KBr) ν_{max}: 3460, 3323, 2966, 2932, 2875, 1606, 1566, 1556, 1501, 1451, 1434, 1328, 1286, 1270, 1249, 1227, 1158, 1133, 1102, 1060, 972, 744 cm^{-1}.

^{1}H NMR (300.13 MHz, $CDCl_3$): δ: 8.51 (1H, d, *J* = 8.0 Hz, H-8), δ: 7.50 (2H, m, H-5 and H-6), δ: 7.41 (1H, m, H-7), δ: 7.12 (1H, d, *J* = 9.0 Hz, H-3), δ: 6.73 (1H, d, *J* = 9.0 Hz, H-2), δ: 4.22 (1H, m, H-2'), δ: 4.03 (2H, t, *J* = 6.4 Hz, H-a), δ: 3.29 (2H, m, H-1'), δ: 1.90 (2H, m, H-b), δ: 1.35 (3H, d, *J* = 6.3, CH_3), δ: 1.12 (3H, t, *J* = 7.4, H-c).

^{13}C NMR (75.47 MHz, $CDCl_3$): δ: 183.46 (C-9), 147.48 (C-4), 143.91 (C-1), 136.81 (C-6), 131.83 (C-8a), 129.92 (C-4a), 129.85 (C-9a), 129.26 (C-8), 126.02 (C-7), 125.95 (C-5), 119.25 (C-3), 113.95 (C-10a), 108.42 (C-2), 72.47 (C-a), 66.11 (C-2'), 52.07 (C-1'), 22.85 (C-b), 21.02 (C-CH_3), 10.71 (C-c).

1.2.6. (*S*)-1-((1-hydroxy-4-methylpentan-2-yl)amino)-4-propoxy-9*H*-thioxanthen-9-one (ATx **5**) (5)

The general procedure (section 1.2.1.) allowed obtaining the desirable compound 5 as a red solid in 19.59 % yield (111.8 mg).

ATx **5** (5): m.p: 82-85 ℃; $[\alpha]_D^{25℃}$ - 68° (c = 6.75 x 10^{-3}g/mL in dichloromethane).

IR (KBr) ν_{max}: 3457, 3290, 2955, 2923, 2870, 1613, 1595, 1566, 1505, 1464, 1435, 1386, 1265, 1224, 1107, 1067, 1018, 745 cm^{-1}.

^{1}H NMR (300.13 MHz, $CDCl_3$): δ: 8.51 (1H, d, *J* = 8.1 Hz, H-8), δ: 7.57 (2H, m, H-5 and H-6), δ: 7.42 (1H, m, H-7), δ: 7.13 (1H, d, *J* = 9.0 Hz, H-3), δ: 6.93 (1H, d, *J* = 9.0 Hz, H-2), δ: 4.04 (2H, t, *J* = 6.5 Hz, H-a), δ: 3.88 (1H, dd, *J* = 10.1 Hz, H-1'), δ: 3.71 (2H, m, $C\underline{H_2}OH$), δ: 1.85 (4H, m, H-b), δ:1.78 (1H, m, H-3'), δ: 1.57 (1H, t, *J* = 6.9 Hz, H-2'), δ: 1.12 (3H, t, *J* = 7.4 Hz, H-c), δ: 0.94 (3H, d, *J* = 6.5 Hz, H-4'a), δ: 0.89 (3H, d, *J* = 6.5 Hz, H-4'b).

^{13}C NMR (75.47 MHz, $CDCl_3$): δ: 183.61 (C-9), 145.00 (C-4), 142.80 (C-1), 136.7 (C-6), 131.98 (C-8a), 129.97 (C-4a), 129.83 (C-9a), 129.28 (C-8), 126.11 (C-7), 126.00 (C-5), 119.05 (C-3), 114.43 (C-10a), 111.02 (C-2), 72.45 (C-a), 64.62 (C-1'), 55.01 ($C\text{-}CH_2OH$), 40.44 (C-2'), 24.90 (C-3'), 22.86 (C-4'a), 22.83 (C-4'b), 22.61 (C-b), 10.71 (C-c).

1.2.7. (*R*)-1-((1-hydroxy-4-methylpentan-2-yl)amino)-4-propoxy-9*H*-thioxanthen-9-one (ATx 6) (6)

The general procedure (section 1.2.1.) allowed to obtain the desirable compound 6 as a red solid in 10.40 % yield (59.3 mg).

ATx **6** (6): m.p: 80-82 ℃; $[\alpha]_D^{25℃}$ +56 ° (c = 6.75 x 10^{-3}g/mL in dichloromethane).

IR (KBr) ν_{max}: 3459, 3291, 2954, 2925, 2871, 1613, 1595, 1566, 1505, 1480, 1435, 1386, 1266, 1224, 1108, 1072, 1018, 746 cm^{-1}.

^{1}H NMR (300.13 MHz, $CDCl_3$): δ: 8.51 (1H, d, *J* = 8.1 Hz, H-8), δ: 7.55 (2H, m, H-5 and H-6), δ: 7.42 (1H, m, H-7), δ: 7.12 (1H, d, *J* = 9.1 Hz, H-3), δ: 6.86 (1H, d, *J* = 9.1 Hz, H-2), δ: 4.03 (2H, t, *J* = 6.5 Hz, H-a), δ: 3.85 (1H, dd, *J* = 10.5 , H-1'), δ: 3.72 (2H, m, $C\underline{H_2}OH$), δ: 1.83 (4H, m, H-b), δ: 1.76 (1H, m, H-3'), δ: 1.57 (1H, t, *J* = 6.9 Hz, H-3'), δ: 1.12 (3H, t, *J* = 7.4 Hz, H-c), δ: 0.96 (3H, d, *J* = 6.5 Hz, H-4'a), δ: 0.89 (3H, d, *J* = 6.5 Hz, H-4'b).

^{13}C NMR (75.47 MHz, $CDCl_3$): δ: 183.61 (C-9), 145.00 (C-4), 142.80 (C-1), 136.82 (C-6), 131.87 (C-8a), 129.93 (C-4a), 129.24 (C-9a), 128.80 (C-8), 126.03 (C-7), 125.97 (C-5), 119.42 (C-3), 113.94 (C-10a), 108.80 (C-2), 72.49 (C-a), 64.87 (C-1'), 40.71 (C-2'), 24.92 (C-3'), 22.96 (C-4'a), 22.86 (C-4'b), 22.55 (C-b), 10.71 (C-c).

1.2.8. (*S*)-1-((1-hydroxy-3-methylbutan-2-yl)amino)-4-propoxy-9*H*-thioxanthen-9-one (ATx 7) (7)

The general procedure allowed (section 1.2.1.) to obtain the desirable compound 7 as a red solid in 10.12 % yield (55.6 mg).

ATx **7** (7): m.p: 98-102 °C; $[\alpha]_D^{25°C}$ - 26° (c = 6.80 x 10^{-3}g/mL in dichloromethane).

IR (KBr) v $_{max}$: 3385, 3256, 2960, 2926, 2873, 2360, 1614, 1569, 1514, 1463, 1434, 1386, 1329, 1267, 1249, 1225, 1165, 1070, 1021, 744 cm^{-1}.

^{1}H NMR (300.13 MHz, $CDCl_3$): δ: 8.54 (1H, d, *J* = 8.0 Hz, H-8), δ: 7.59 (2H, m, H-5 and H-6), δ: 7.45 (1H, m, H-7), δ: 7.14 (1H, d, *J* = 9.1 Hz, H-3), δ: 7.07 (1H, d, *J* = 9.1 Hz, H-2), δ: 4.06 (2H, t, *J* = 6.4 Hz, H-a), δ: 3.86 (2H, m, C$\underline{H_2}$OH), δ: 3.53 (1H, m, H-1'), δ: 2.08 (1H, m, H-2') δ: 1.91 (2H, m, H-b), δ: 1.05 (3H, d, *J* = 6.9 Hz, H-3'a), δ: 0.87 (3H, d, *J* = 6.9 Hz, H-3'b), δ: 1.12 (3H, t, m, H-c).

^{13}C NMR (75.47 MHz, $CDCl_3$): δ: 183.43 (C-9), 145.0 (C-4), 142.8 (C-1), 136.43 (C-6), 131.66 (C-8a), 129.53 (C-4a), 129.03 (C-9a), 128.84 (C-8), 125.70 (C-7), 125.51 (C-5), 117.82 (C-3), 114.71 (C-10a), 111.6 (C-2), 71.80 (C-a), 63.93 (C-1'), 61.56 (C-CH_2OH), 29.15 (C-2'), 22.21 (C-b), 18.53 (C-3'a), 18.41 (C-3'b), 10.14 (C-c).

1.2.9. (*R*)-1-((1-hydroxy-3-methylbutan-2-yl)amino)-4-propoxy-9*H*-thioxanthen-9-one (ATx 8) (8)

After the general procedure (section 1.2.1.), the solid obtained was crystallized using an identical procedure of section 1.2.4, allowing to obtain the desirable compound 8 as a red solid in 10.24 % yield (75.0 mg).

ATx **8** (8): m.p: 98-104 °C; $[\alpha]_D^{25°C}$ + 26° (c = 6.80 x 10^{-3}g/mL in dichloromethane).

IR (KBr) v $_{max}$: 3423, 3272, 2959, 2925, 2872, 1611, 1570, 1511, 1463, 1435, 1385, 1251, 1226, 1161, 1068, 1022, 747 cm^{-1}.

^{1}H NMR (300.13 MHz, $CDCl_3$): δ: 8.56 (1H, d, *J* = 8.0 Hz, H-8), δ: 7.64 (2H, m, H-5 and H-6), δ: 7.49 (1H, m, H-7), δ: 7.34 (1H, d, *J* = 8.9 Hz, H-3), δ: 7.17 (1H, d, *J* = 8.9 Hz, H-2), δ: 4.10 (2H, t, *J* = 6.4 Hz, H-a), δ: 3.90 (2H, m, C$\underline{H_2}$OH), δ: 3.50 (1H, m, H-1'), δ: 2.10 (1H, m, H-2') δ: 1.91 (2H, m, H-b), δ: 1.02 (3H, d, *J* = 6.9 Hz, H-3'a), δ: 0.98 (3H, d, *J* = 6.9 Hz, H-3'b), δ: 1.14 (3H, t, m, H-c);

^{13}C NMR (75.47 MHz, $CDCl_3$): δ: 183.65 (C-9), 147.74 (C-4), 141.53 (C-1), 137.16 (C-6), 132.60 (C-8a), 130.43 (C-4a), 129.52 (C-9a), 129.21 (C-8), 126.52 (C-7), 126.19 (C-5), 117.12 (C-3), 116.69 (C-10a), 115.38 (C-2), 72.19 (C-a), 67.02 (C-1'), 61.17 (CH_2OH), 28.87 (C-2'), 22.65 (C-b), 19.31 (C-3'a), 18.58 (C-3'b), 10.69 (C-c).

PART II - BIOLOGICAL ACTIVITY

2.1. Material

Dulbecco's modified Eagle's medium (high glucose), RHO 123, elacridar and neutral red (NR) solution were obtained from Sigma (St. Louis, MO, USA).

Reagents used in cell culture, including nonessential amino acids (NEAA), heat inactivated fetal bovine serum (FBS), 0.25% trypsin/1 mM EDTA, antibiotic (10,000 U/mL penicillin, 10,000 µg/mL streptomycin) and human transferrin (4 mg/mL) were purchased from Gibco Laboratories (Lenexa, KS, USA). P-glycoprotein monoclonal antibody (clone UIC2) conjugated with with phycoerythrin (PE) was purchased from Abcam (Cambridge, United Kingdom). Flow cytometry reagents (sheath fluid, cleaning solution, decontamination solution, extended flow cell clean) were purchased from BD Bioscience Pgp-Glo™ Assay System was purchased from Promega Corporation (Madison, USA). All the reagents used were of analytical grade or of the highest grade available.

2.2 Caco-2 cell culture

Caco-2 cells, derived from human colorectal adenocarcinoma, were routinely cultured in 75 cm^2 flasks using Dulbecco's modified Eagle's medium (DMEM) supplemented with 10 % heat-inactivated fetal bovine serum (FBS), 100 µM nonessential amino acids (NEAA), 100 U/mL penicillin, 100 µg/mL streptomycin and 6 µg/mL transferrin.

Cells were maintained in a 5 % CO2-95 % air atmosphere, at 37 °C, and the medium was changed every 2 to 3 days. Cultures were passaged weekly by trypsinization (0.25 % trypsin/1 mM EDTA). The cells used for all the experiments were taken between the 27^{th} and 36^{th} passages.

For the cytotoxicity assays, the cells were seeded in 96-well plates at a density of 60,000 cells/cm^2 and used 3 days after seeding, when confluence was reached.

For the experiments performed for the evaluation of P-glycoprotein expression and P-glycoprotein transport activity, the cells were seeded in 12-well plates at a density of 60,000 cells/cm^2 and used 3 days after seeding.

2.3. Cytotoxicity assays

The NR uptake assay is based on the ability of viable cells to incorporate and bind the supravital dye NR in the lysosomes, thus providing a quantitative estimation of the number of viable cells in a culture (46).

Aminated thioxanthones **1-8** (0–50 μM) cytotoxicity was evaluated, 24 hours after exposure, by the NR uptake assay. Briefly, the cells were seeded onto 96-well plates at a density of 60,000 cells/cm^2, and exposed, after reaching confluence, to the eight tested ATx's (0–50 μM) in fresh cell culture medium. Twenty-four hours after exposure, the cells were incubated with NR (40 μg/mL in cell culture medium) at 37 °C, in a humidified, 5 % CO2-95 % air atmosphere, for 60 minutes. After this incubation period, the cell culture medium was removed, the dye absorbed only by viable cells extracted [with absolute ethyl alcohol/distilled water (1:1) containing 5 % acetic acid] and the absorbance measured at 540 nm in a multiwall plate reader (BioTek Synergy™ HT, BioTek Instruments). The percentage of NR uptake relative to that of the control cells was used as the cytotoxicity measure.

2.4. Flow cytometry analysis of P-glycoprotein expression

For the *in vitro* evaluation of P-gp expression, the cells were seeded onto 12-well plates, at a density of 60,000 cells/ cm^2 and exposed, three days after seeding, to the eight tested ATx's **1-8** (20 μM) in fresh cell culture medium for 24 hours.

After the incubation period, the cells were washed with HBSS buffer and harvested by trypsinization (0.25 % trypsin/1 mM EDTA) to obtain a cellular suspension. The cells were then centrifuged (300*g*, for 10 min, at 4 °C) and suspended in HBSS buffer containing the P-gp antibody [UIC2] conjugated with PE. The antibody dilution used in this experiment was applied according to the manufacturer's instructions for flow cytometry. The cells were then incubated, for 30 min, at 37 °C in the dark.

After this incubation period, the cells were washed twice with HBSS containing 10 % heat-inactivated FBS, centrifuged (300*g* for 10 min), suspended in ice-cold HBSS buffer and kept on ice until analysis. Fluorescence measurements of isolated cells were performed with a flow cytometer (BD Accuri™ C6).

The fluorescence of the PE-UIC2 antibody was measure by a 585 ± 40 nm band-pass filter (FL2). The logarithmic fluorescence was recorded and displayed as a single parameter histogram, and based on the acquisition of data for 20,000 cells.

The mean of fluorescence intensity (MFI) was the parameter used for comparison [calculated as percentage of control (0 μM)]. Nonlabeled cells (with or without ATx's) were also analyzed in each experiment by a 585 ± 40 nm band-pass filter (FL2) in order to detect a possible contribution from cells autofluorescence to the analyzed fluorescence signals.

2.5. Evaluation of P-glycoprotein transport activity

The P-gp transport activity was evaluated by flow cytometry using RHO 123 (2 μM) as a P-gp fluorescent substrate. P-gp transport activity was evaluated through the analysis of RHO 123 accumulation using two different experimental designs:

- RHO 123 accumulation assay in the presence (IA) and absence (NA) of a P-gp inhibitor, elacridar (10 μM), and with or without exposure to the tested thioxanthonic compounds (20 μM) only during the RHO 123 accumulation phase;
- RHO 123 accumulation assay, in the presence (IA) and absence (NA) of a P-gp inhibitor, elacridar (10 μM), and with or without pre-exposure to the tested thioxanthones (20 μM) for 24h.

2.5.1. RHO 123 accumulation assay in the presence of thioxanthones

Caco-2 cells were seeded onto 75 cm^2 flasks and, after reaching confluence, washed with HBSS and harvested by trypsinization (0.25 % trypsin/1 mM EDTA) to obtain a cellular suspension. This cell suspension was then divided into several aliquots of 300,000 cells, which were submitted to the following procedures:

i. Normal rhodamine accumulation (NA): the cells were centrifuged (300 g for 10 minutes), suspended in HBSS containing 10% heat-inactivated FBS and 2 μM RHO123, with and without 20 μM thioxanthones, and incubated at 37º C for 60 min in the absence of the P-gp inhibitor (elacridar). After the incubation period the cells were washed twice with ice-cold HBSS with 10% heat-inactivated FBS, centrifuged (300 g for 10 min) at 4° C and kept on ice until flow cytometry analysis;

ii. Inhibited rhodamine accumulation (IA): the cells were centrifuged (300 g for 10 min), suspended in HBSS containing 10% heat-inactivated FBS, 2 μM RHO 123 and the P-gp inhibitor elacridar (10 μM), with and without 20 μM thioxanthones, and incubated at 37ºC for 60 min. After the accumulation of the fluorescent substrate, the cells were washed twice with ice-cold HBBS with 10% heat-inactivated FBS, centrifuged (300 g for 10 min) at 4ºC and kept on ice until flow cytometry analysis.

Fluorescence measurements of isolated cells were performed as described in section "Evaluation of P-gp expression". The green intracellular fluorescence of RHO 123 was measured by a 530 ± 15 nm band-pass filter (FL1). The results were calculated according to the ratio defined in Equation 1 and expressed as percentage of control (0 μM).

$$\textbf{\textit{RHO 123 Accumulation}} = \frac{\text{MFI inhibited rhodamine accumulation (IA)}}{\text{MFI normal rhodamine accumulation (NA)}}$$

Equation 1. P-gp activity evaluated through rhodamine 123 accumulation ratio.

When P-gp activity increases, the amount of RHO 123 effluxed from the cells is higher and accompanied by a decrease in the intracellular fluorescence intensity due to the corresponding decrease in the intracellular RHO 123 content. Thus, a higher ratio results from a smaller MFI NA, which is a consequence of a higher P-gp activity as the dye is being pumped out of the cells during the accumulation phase.

2.5.2. RHO 123 accumulation assay in Caco-2 cells pre-expose to thioxanthones for 24 hours

Caco-2 cells were seeded onto 12-well plates, at a density of 60,000 cells/cm², to obtain confluent monolayers at the day of the experiment. Three days after seeding, the cells were exposed to ATx's (20 μM), in fresh cell culture medium, for 24 h. After this incubation period, the cells were washed with HBSS and harvested by trypsinization (0.25 % trypsin/1 mM EDTA) to obtain a cell suspension. The cells of each well were divided into two aliquots. The first aliquot was submitted to a RHO 123 accumulation phase performed under inhibited conditions (RHO 123 accumulation performed in the presence of the P-gp inhibitor, elacridar — IA). The second aliquot was submitted to a RHO 123 accumulation phase performed under normal conditions (RHO 123 accumulation performed in the absence of P-gp inhibitor—NA). For IA accumulation, the cells were centrifuged (300 g for 10 minutes), suspended in HBSS buffer (pH 7.4) containing 10% heat-inactivated FBS, 2 μM RHO 123 and the P-gp inhibitor elacridar (10.0 μM), and incubated at 37 ºC for 60 min to allow RHO 123 accumulation. For NA accumulation, a similar incubation was performed but in the absence of the P-gp inhibitor. After this accumulation period, the cells were washed twice with ice-cold HBSS buffer containing 10 % heat-inactivated FBS and suspended in ice-cold wash solution immediately before analysis. The fluorescence measurements of isolated cells were performed as described in "Flow cytometry analysis of P-glycoprotein expression" section. The green intracellular fluorescence of RHO 123 was measured by a 530 ± 15 nm band-pass filter (FL1). The results were calculated according to the ratio defined in Equation 1 and expressed as percentage of control values.

2.6. Determination of ATPase activity

The effects of the tested thioxanthones on P-gp ATPase activity were evaluated using the luminescen Pgp-Glo™ Assay (Promega), according to the manufacturer's protocol, using recombinant human P-gp-enriched membranes.

Briefly, recombinant human P-gp-enriched membranes (25 μg/ well) were incubated with 20 μM ATx's or sodium vanadate at 100 μM (positive control for P-gp ATPase activity inhibition) or verapamil at 200 μM (positive control for P-gp ATPase activity stimulation) in assay buffer, and 5 mM MgATP for exactly 60 min at 37 °C. After the incubation, the reaction was stopped and the remaining ATP detected after a 20 min signal-developing period at room temperature, as a luciferase-generated luminescent signal in a multi-well plate reader (BioTek Synergy™ HT).

The decreased luminescence of the untreated (NT) incubations relative to Na3VO4-treated incubations reflects basal Pgp ATPase activity. The decreased luminescence of incubations performed with the positive control drug verapamil relative to Na3VO4-treated reactions reflects verapamil-stimulated Pgp ATPase activity. The luminescence of the ATx's performed incubations relative to that of the Na3VO4-treated reactions reflects the effect, if any, of that compounds on P-gp ATPase activity (i.e. a decrease in luminescence reflects a stimulated Pgp ATPase activity). Therefore, for data analysis, the following equations were thus used to calculate the change in luminescence (ΔRLU) signals:

1. $\mathbf{\Delta RLU_{basal}}$ = $RLUNa_3VO_4 - RLU_{NT}$, reflecting basal P-gp ATPase activity

2. $\mathbf{\Delta RLU_{TC}}$ = $RLUNa_3VO_4 - RLU_{TC}$, reflecting P-gp ATPase activity in the presence of a test compound (TC).

Three independent experiments were performed in triplicate for this assay and the results expressed as Mean ± SEM.

2.7. Statistical analysis

All statistical calculations were performed with the GraphPad Prism version 6.00 for Windows (GraphPad Software, San Diego California, USA). Normality of the data distribution was assessed by three different tests (KS normality test, D'Agostino & Pearson omnibus normality test and Shapiro-Wilk normality test).

Data obtained from the thioxanthones cytotoxicity assays are expressed as mean ± SEM from at least 5 independent experiments (performed in triplicate) and the statistical

comparisons were estimated using the nonparametric method of Kruskal–Wallis, followed by the Dunn's post hoc test. Data from the P-gp expression assays are presented as mean ± SEM from 2 independent experiments (performed in duplicate) and the statistical comparisons were made using One-way ANOVA, followed by theTukey's multiple comparisons test. Results from the P-gp transport activity assays performed in the presence of ATx's during the RHO123 accumulation phase are presented as mean ± SEM from 5 independent experiments (performed in triplicate) and the statistical comparisons were estimated using One-way ANOVA, followed by the Tukey's multiple comparisons test. Results from the P-gp transport activity assays performed in cells pre-exposed to ATx's for 24 h are presented as mean ± SEM from 4 independent experiments (performed in duplicate) and the statistical comparisons were estimated using One-way ANOVA, followed by the Tukey's multiple comparisons test. Results from the P-gp ATPase activity are presented as mean ± SEM from 3 independent experiments (performed in triplicate) and the statistical comparisons were estimated using One-way ANOVA, followed by the Tukey's multiple comparisons test. In all cases, p values lower than 0.05 were considered significant. In all cases, p values lower than 0.05 were considered significant.

CHAPTER 5:

REFERENCES

REFERENCES

1. Sosnik A. Reversal of multidrug resistance by the inhibition of ATP-binding cassette pumps employing “Generally Recognized As Safe” (GRAS) nanopharmaceuticals: A review. Advanced Drug Delivery Reviews. 2013;65(13–14):1828-51.
2. Huang Y, Sadee W. Membrane transporters and channels in chemoresistance and -sensitivity of tumor cells. Cancer Letters. 2006;239(2):168-82.
3. Chen Z, Shi T, Zhang L, Zhu P, Deng M, Huang C, et al. Mammalian drug efflux transporters of the ATP binding cassette (ABC) family in multidrug resistance: A review of the past decade. Cancer Letters. 2016;370(1):153-64.
4. Sharom FJ. The P-glycoprotein multidrug transporter: interactions with membrane lipids, and their modulation of activity. Biochemical Society transactions. 1997;25(3):1088-96.
5. Eckford PD, Sharom FJ. ABC efflux pump-based resistance to chemotherapy drugs. Chemical reviews. 2009;109(7):2989-3011.
6. Silva R, Vilas-Boas V, Carmo H, Dinis-Oliveira RJ, Carvalho F, de Lourdes Bastos M, et al. Modulation of P-glycoprotein efflux pump: Induction and activation as a therapeutic strategy. Pharmacology & Therapeutics. 2015(0).
7. Leslie EM, Deeley RG, Cole SPC. Multidrug resistance proteins: role of P-glycoprotein, MRP1, MRP2, and BCRP (ABCG2) in tissue defense. Toxicology and Applied Pharmacology. 2005;204(3):216-37.
8. Doull’s C. Toxicology. 2013.
9. Zhou Q, Yu LS, Zeng S. Stereoselectivity of chiral drug transport: A focus on enantiomer- transporter interaction. Drug Metab Reviews. 2014;46(3):283-90.
10. Dekker M. Chirality in drug design and development. Copyright; 2004.
11. Evans SE, Kasprzyk-Hordern B. Applications of chiral chromatography coupled with mass spectrometry in the analysis of chiral pharmaceuticals in the environment. Trends in Environmental Analytical Chemistry. 2014;1(0):e34-e51.
12. Kerns EH, Li D. Drug-like Properties: Concepts, Structure Design and Methods: from ADME to Toxicity Optimization. Elsevier: Copyright; 2008.
13. Capparelli E, Zinzi L, Cantore M, Contino M, Perrone MG, Luurtsema G, et al. SAR Studies on tetrahydroisoquinoline derivatives: The role of flexibility and bioisosterism to raise potency and selectivity toward P-glycoprotein. Journal of Medicinal Chemistry. 2014;57(23):9983-94.
14. Thiebaut F, Tsuruo T, Hamada H, Gottesman MM, Pastan I, Willingham MC. Cellular localization of the multidrug-resistance gene product P-glycoprotein in normal human tissues. Proceedings of the National Academy of Sciences of the United States of America. 1987;84(21):7735-8.
15. Varma MVS, Ashokraj Y, Dey CS, Panchagnula R. P-glycoprotein inhibitors and their screening: a perspective from bioavailability enhancement. Pharmacological Research. 2003;48(4):347-59.
16. Sharom FJ. The P-glycoprotein multidrug transporter. Essays in biochemistry. 2011;50(1):161-78.
17. Katayama K, Kapoor K, Ohnuma S, Patel A, Swaim W, Ambudkar IS, et al. Revealing the fate of cell surface human P-glycoprotein (ABCB1): The lysosomal degradation pathway. Biochimica et Biophysica Acta (BBA) - Molecular Cell Research. 2015;1853(10, Part A):2361-70.
18. Ambudkar SV, Dey S, Hrycyna CA, Ramachandra M, Pastan I, Gottesman MM. Biochemical, cellular, and pharmacological aspects of the multidrug transporter. Annual review of pharmacology and toxicology. 1999;39:361-98.
19. Palmeira A, Sousa E, Vasconcelos MH, Pinto MM. Three Decades of P-gp Inhibitors: Skimming Through Several Generations and Scaffolds. Current medicinal chemistry. 2012;19(13):1946-2025.

20. Silva R, Carmo H, Dinis-Oliveira R, Cordeiro-da-Silva A, Lima SC, Carvalho F, et al. In vitro study of P-glycoprotein induction as an antidotal pathway to prevent cytotoxicity in Caco-2 cells. Archives of toxicology. 2011 Apr; 85(4):[315-26 pp.].
21. Hennessy M, Spiers JP. A primer on the mechanics of P-glycoprotein the multidrug transporter. Pharmacological Research. 2007;55(1):1-15.
22. Juliano RL, Ling V. A surface glycoprotein modulating drug permeability in Chinese hamster ovary cell mutants. Biochim Biophys Acta. 1976;455(1):152-62.
23. Choong E, Dobrinas M, Carrupt PA, Eap CB. The permeability P-glycoprotein: a focus on enantioselectivity and brain distribution. Expert opinion on drug metabolism & toxicology. 2010;6(8):953-65.
24. Fojo AT, Ueda K, Slamon DJ, Poplack DG, Gottesman MM, Pastan I. Expression of a multidrug-resistance gene in human tumors and tissues. Proceedings of the National Academy of Sciences of the United States of America. 1987;84(1):265-9.
25. Silva R, Sousa E, Carmo H, Palmeira A, Barbosa DJ, Gameiro M, et al. Induction and activation of P-glycoprotein by dihydroxylated xanthones protect against the cytotoxicity of the P-glycoprotein substrate paraquat. Archives of toxicology. 2014;88(4):937-51.
26. Kobori T, Harada S, Nakamoto K, Tokuyama S. Mechanisms of P-glycoprotein alteration during anticancer treatment: Role in the pharmacokinetic and pharmacological effects of various substrate drugs. Journal of Pharmacological Sciences. 2014;125(3):242-54.
27. Ferreira A, Pousinho S, Fortuna A, Falcão A, Alves G. Flavonoid compounds as reversal agents of the P-glycoprotein-mediated multidrug resistance: biology, chemistry and pharmacology. Phytochemistry Reviews. 2015;14(2):233-72.
28. Wessler JD, Grip LT, Mendell J, Giugliano RP. The P-Glycoprotein Transport System and Cardiovascular Drugs. Journal of the American College of Cardiology. 2013;61(25):2495-502.
29. Higgins CF, Gottesman MM. Is the multidrug transporter a flippase? Trends in Biochemical Sciences. 1992;17(1):18-21.
30. Stouch TR, Gudmundsson O. Progress in understanding the structure–activity relationships of P-glycoprotein. Advanced Drug Delivery Reviews. 2002;54(3):315-28.
31. Coley HM. Overcoming multidrug resistance in cancer: clinical studies of p-glycoprotein inhibitors. Methods in molecular biology (Clifton, NJ). 2010;596:341-58.
32. Bansal T, Jaggi M, Khar RK, Talegaonkar S. Emerging significance of flavonoids as P-glycoprotein inhibitors in cancer chemotherapy. Journal of pharmacy & pharmaceutical sciences : a publication of the Canadian Society for Pharmaceutical Sciences, Societe canadienne des sciences pharmaceutiques. 2009;12(1):46-78.
33. Zhou SF. Structure, function and regulation of P-glycoprotein and its clinical relevance in drug disposition. Xenobiotica. 2008;38(7-8):802-32.
34. Qosa H, Miller DS, Pasinelli P, Trotti D. Regulation of ABC efflux transporters at blood-brain barrier in health and neurological disorders. Brain Research. 2015.
35. Bundgaard C, Eneberg E, Sánchez C. P-glycoprotein differentially affects escitalopram, levomilnacipran, vilazodone and vortioxetine transport at the mouse blood–brain barrier in vivo. Neuropharmacology. 2016;103:104-11.
36. Miller DS, Bauer B, Hartz AM. Modulation of P-glycoprotein at the blood-brain barrier: opportunities to improve central nervous system pharmacotherapy. Pharmacological reviews. 2008;60(2):196-209.
37. Limtrakul P, Chearwae W, Shukla S, Phisalphong C, Ambudkar SV. Modulation of function of three ABC drug transporters, P-glycoprotein (ABCB1), mitoxantrone resistance protein (ABCG2) and multidrug resistance protein 1 (ABCC1) by tetrahydrocurcumin, a major metabolite of curcumin. Molecular and cellular biochemistry. 2007;296(1-2):85-95.
38. Juliano RL, Ling V. A surface glycoprotein modulating drug permeability in Chinese hamster ovary cell mutants. Biochimica et Biophysica Acta. 1976;445(1):152-62.
39. Krishna R, Mayer LD. Multidrug resistance (MDR) in cancer: Mechanisms, reversal using modulators of MDR and the role of MDR modulators in influencing the pharmacokinetics of anticancer drugs. European Journal of Pharmaceutical Sciences. 2000;11(4):265-83.

40. Palmeira A, Vasconcelos MH, Paiva A, Fernandes MX, Pinto M, Sousa E. Dual inhibitors of P-glycoprotein and tumor cell growth: (Re)discovering thioxanthones. Biochemical Pharmacology. 2012;83(1):57-68.
41. Palmeira A, Rodrigues F, Sousa E, Pinto M, Vasconcelos MH, Fernandes MX. New uses for old drugs: pharmacophore-based screening for the discovery of P-glycoprotein inhibitors. Chemical biology & drug design. 2011;78(1):57-72.
42. McDevitt CA, Callaghan R. How can we best use structural information on P-glycoprotein to design inhibitors? Pharmacology & Therapeutics. 2007;113(2):429-41.
43. Fernandes C, Masawang K, Tiritan ME, Sousa E, de Lima V, Afonso C, et al. New chiral derivatives of xanthones: Synthesis and investigation of enantioselectivity as inhibitors of growth of human tumor cell lines. Bioorganic & Medicinal Chemistry. 2014;22(3):1049-62.
44. Wang RB, Kuo CL, Lien LL, Lien EJ. Structure-activity relationship: analyses of p-glycoprotein substrates and inhibitors. Journal of clinical pharmacy and therapeutics. 2003;28(3):203-28.
45. Vilas-Boas V, Silva R, Palmeira A, Sousa E, Ferreira LM, Branco PS, et al. Development of novel rifampicin-derived P-glycoprotein activators/inducers. synthesis, in silico analysis and application in the RBE4 cell model, using paraquat as substrate. PLoS One. 2013;8(8):e74425.
46. Silva R, Palmeira A, Carmo H, Barbosa DJ, Gameiro M, Gomes A, et al. P-glycoprotein induction in Caco-2 cells by newly synthetized thioxanthones prevents paraquat cytotoxicity. Archives of toxicology. 2015;89(10):1783-800.
47. Mizuno N, Sugiyama Y. Drug transporters: their role and importance in the selection and development of new drugs. Drug metabolism and pharmacokinetics. 2002;17(2):93-108.
48. DeGorter MK, Xia CQ, Yang JJ, Kim RB. Drug Transporters in Drug Efficacy and Toxicity. In: Insel PA, Amara SG, Blaschke TF, editors. Annual Review of Pharmacology and Toxicology, Vol 52. Annual Review of Pharmacology and Toxicology. 52. Palo Alto: Annual Reviews; 2012. p. 249-73.
49. Constantinides PP, Wasan KM. Lipid formulation strategies for enhancing intestinal transport and absorption of P-glycoprotein (P-gp) substrate drugs: In vitro/in vivo case studies. Journal of Pharmaceutical Sciences. 2007;96(2):235-48.
50. Endicott JA, Ling V. The biochemistry of P-glycoprotein-mediated multidrug resistance. Annual review of biochemistry. 1989;58:137-71.
51. Ferte J. Analysis of the tangled relationships between P-glycoprotein-mediated multidrug resistance and the lipid phase of the cell membrane. European journal of biochemistry / FEBS. 2000;267(2):277-94.
52. Loo TW, Clarke DM. Mapping the binding site of the inhibitor tariquidar that stabilizes the first transmembrane domain of P-glycoprotein. Journal of Biological Chemistry. 2015;290(49):29389-401.
53. Silva R, Carmo H, Vilas-Boas V, Barbosa DJ, Palmeira A, Sousa E, et al. Colchicine effect on P-glycoprotein expression and activity: In silico and in vitro studies. Chemico-Biological Interactions. 2014;218:50-62.
54. Takara K, Hayashi R, Kokufu M, Yamamoto K, Kitada N, Ohnishi N, et al. Effects of nonsteroidal anti-inflammatory drugs on the expression and function of P-glycoprotein/MDR1 in Caco-2 cells. Drug and chemical toxicology. 2009;32(4):332-7.
55. Fletcher JI, Haber M, Henderson MJ, Norris MD. ABC transporters in cancer: more than just drug efflux pumps. Nat Rev Cancer. 2010;10(2):147-56.
56. Silva R, Carmo H, Vilas-Boas V, Pinho PGd, Dinis-Oliveira RJ, Carvalho F, et al. Doxorubicin decreases paraquat accumulation and toxicity in Caco-2 cells. Toxicology Letters. 2013;217(1):34-41.
57. Paiva AM, Pinto MM, Sousa E. A century of thioxanthones: through synthesis and biological applications. Current medicinal chemistry. 2013;20(19):2438-57.
58. Graebe C, Schultess O. 1. Ueber Thioxanthon. Justus Liebigs Annalen der Chemie. 1891;263(1):1-15.

59. Castanheiro R, Silva A, Campos N, Nascimento M, Pinto M. Antitumor Activity of Some Prenylated Xanthones. Pharmaceuticals. 2009;2(2):33.
60. Pinto MM, Sousa ME, Nascimento MS. Xanthone derivatives: new insights in biological activities. Current medicinal chemistry. 2005;12(21):2517-38.
61. Verbanac D, Jain SC, Jain N, Chand M, Čipčić Paljetak H, Matijašić M, et al. An efficient and convenient microwave-assisted chemical synthesis of (thio)xanthones with additional in vitro and in silico characterization. Bioorganic & Medicinal Chemistry. 2012;20(10):3180-5.
62. Rosi D, Peruzzotti G, Dennis EW, Berberian DA, Freele H, Archer S. A new active metabolite of "Miracil D". Nature. 1965;208(5014):1005-6.
63. Cioli D, Pica-Mattoccia L, Archer S. Antischistosomal drugs: Past, present ... and future? Pharmacology & Therapeutics. 1995;68(1):35-85.
64. Foster BJ, Wiegand RA, Pugh S, LoRusso PM, Rake J, Corbett TH. Pharmacokinetic studies in mice of two new thioxanthenones (183577 and 232759) that showed preferential solid tumor activity. Clinical cancer research : an official journal of the American Association for Cancer Research. 1997;3(11):2047-53.
65. Bases RE, Mendez F. Topoisomerase inhibition by lucanthone, an adjuvant in radiation therapy. International Journal of Radiation Oncology*Biology*Physics. 1997;37(5):1133-7.
66. Sangwook Woo, Da-hye Kang, Jungsook Kim, Chong-Soon Lee, Eung-Seok Lee, Yurngdong Jahng, et al. Synthesis, Cytotoxicity and Topoisomerase II Inhibition Study of New Thioxanthone Analogues. Bulletin of Korean Chemical Society. 2008;29(2):471-4.
67. Kostakis IK, Pouli N, Marakos P, Mikros E, Skaltsounis A-L, Leonce S, et al. Synthesis, cytotoxic activity, NMR study and stereochemical effects of some new pyrano[3,2-b]thioxanthen-6-ones and Pyrano[2,3-c]thioxanthen-7-ones. Bioorganic & Medicinal Chemistry. 2001;9(11):2793-802.
68. Chen C-L, Chen T-C, Lee C-C, Shih L-C, Lin C-Y, Hsieh Y-Y, et al. Synthesis and evaluation of new 3-substituted-4-chloro-thioxanthone derivatives as potent anti-breast cancer agents. Arabian Journal of Chemistry. 2015.
69. Palmeira A, Sousa E, Fernandes MX, Pinto MM, Vasconcelos MH. Multidrug resistance reversal effects of aminated thioxanthones and interaction with cytochrome P450 3A4. Journal of pharmacy & pharmaceutical sciences : a publication of the Canadian Society for Pharmaceutical Sciences, Societe canadienne des sciences pharmaceutiques. 2012;15(1):31-45.
70. Horwitz JP, Massova I, Wiese TE, Besler BH, Corbett TH. Comparative Molecular Field Analysis of the Antitumor Activity of 9H-Thiioxanthen-9-one Derivatives against Pancreatic Ductal Carcinoma 03. Journal of Medicinal Chemistry. 1994;37(6):781-6.
71. Corbett TH, Panchapor C, Polin L, Lowichik N, Pugh S, White K, et al. Preclinical efficacy of thioxanthone SR271425 against transplanted solid tumors of mouse and human origin. Investigational new drugs. 1999;17(1):17-27.
72. Varvaresou A, Tsotinis A, Papadaki-Valiraki A, Siatra-Papastaikoudi T. New aza-thioxanthones: Synthesis and cytotoxicity. Bioorganic & Medicinal Chemistry Letters. 1996;6(7):861-4.
73. G. Neumann M, H. Gehlen M, V. Encinas M, S. Allen N, Corrales T, Peinado C, et al. Photophysics and photoreactivity of substituted thioxanthones. Journal of the Chemical Society, Faraday Transactions. 1997;93(8):1517-21.
74. Belal F, Hefnawy MM, Aly FA. Analysis of pharmaceutically-important thioxanthene derivatives. Journal of Pharmaceutical and Biomedical Analysis. 1997;16(3):369-76.
75. Lory PMJ, Estrella-Jimenez ME, Shashack MJ, Lokesh GL, Natarajan A, Gilbertson SR. Synthesis and screening of 3-substituted thioxanthen-9-one-10,10-dioxides. Bioorganic & Medicinal Chemistry Letters. 2007;17(21):5940-3.
76. Zhao J, Larock RC. Synthesis of xanthones, thioxanthones, and acridones by the coupling of arynes and substituted benzoates. Journal of Organic Chemistry. 2007;72(2):583-8.
77. Okabayashi I, Fujiwara H, Tanaka C. Synthesis of 1,8-, 1,6- and 3,6-dichloro-9H-thioxanthen-9-ones. Journal of Heterocyclic Chemistry. 1991;28(8):1977-9.

78. Okabayashi I, Murakami N, Sekiya K. Synthesis of 1, 5- and 1, 7-dichloro-9H-thioxanthen-9-ones. Journal of Heterocyclic Chemistry. 1989;26(3):635-7.
79. Gal J. Molecular Chirality in Chemistry and Biology: Historical Milestones. Helvetica Chimica Acta. 2013;96:1617-57.
80. Eric V. Anslyn, Dougherty DA. Modern Physical Organic Chemistry: University Science Books; 2006.
81. Zelewsky AV. Stereochemistry of coordination compounds. from alfred werner to the 21st century. Chimia. 2014;68(5):297-8.
82. Smith SW. Chiral toxicology: it's the same thing...only different. Toxicol Sci. 2009;110(1):4-30.
83. Guo-Qiang Lin J-GZ, Jie-Fei Cheng. Overview of chirality and chiral drugs In: Guo-Qiang Lin Q-DYaJ-FC, editor. Chiral Drugs: Chemistry and Biological Action: John Wiley & Sons, Inc.; 2011. p. 3-21.
84. Lin G-Q, Zhang J-G, Cheng J-F. Overview of Chirality and Chiral Drugs. Chiral Drugs: John Wiley & Sons, Inc.; 2011. p. 3-28.
85. Brocks DR. Drug Disposition in Three Dimensions: An Update on Stereoselectivity in Pharmacokinetics. Biopharmaceutics & Drug Disposition. 2006;27:387–406.
86. Ribeiro AR, Maia AS, Cass QB, Tiritan ME. Enantioseparation of chiral pharmaceuticals in biomedical and environmental analyses by liquid chromatography: An overview. Journal of Chromatography B. 2014;968(0):8-21.
87. Nerkar AG, Lade KS, Gadhave NA, Sawant SD. Chiral switches: A Review. Journal of Pharmacy Research. 2011;4(4):1300-3.
88. Lees P, Hunter RP, Reeves PT, Toutain PL. Pharmacokinetics and pharmacodynamics of stereoisomeric drugs with particular reference to bioequivalence determination. Journal of Veterinary Pharmacology & Therapeutics. 2012;35:17-29.
89. Caslavska J, Thormann W. Stereoselective determination of drugs and metabolites in body fluids, tissues and microsomal preparations by capillary electrophoresis (2000–2010). Journal of Chromatography A. 2011;1218(4):588-601.
90. Tsuchiya H, Mizogami M. The membrane interaction of drugs as one of mechanisms for their enantioselective effects. Medical Hypotheses. 2012;79(1):65-7.
91. Caner H, Groner E, Levy L, Agranat I. Trends in the development of chiral drugs. Drug Discovery Today. 2004;9(3):105-10.
92. Chang KL, Pee HN, Yang S, Ho PC. Influence of drug transporters and stereoselectivity on the brain penetration of pioglitazone as a potential medicine against Alzheimer's disease. Scientific reports. 2015;5:9000.
93. Shen S, He Y, Zeng S. Stereoselective regulation of MDR1 expression in Caco-2 cells by cetirizine enantiomers. Chirality. 2007;19(6):485-90.
94. Pham Y-T, Régina A, Farinotti R, Couraud P-O, Wainer IW, Roux F, et al. Interactions of racemic mefloquine and its enantiomers with P-glycoprotein in an immortalised rat brain capillary endothelial cell line, GPNT. Biochimica et Biophysica Acta (BBA) - General Subjects. 2000;1524(2–3):212-9.
95. Kang SW, Jang HJ, Moore VS, Park J-Y, Kim K-A, Youm J-R, et al. Enantioselective determination of cetirizine in human plasma by normal-phase liquid chromatography–atmospheric pressure chemical ionization–tandem mass spectrometry. Journal of Chromatography B. 2010;878(32):3351-7.
96. Chu S, Liu S, Duan W, Cheng Y, Jiang X, Zhu C, et al. The anti-dementia drug candidate, (−)-clausenamide, improves memory impairment through its multi-target effect. Pharmacology & Therapeutics. 2016;162:179-87.
97. Zhu C-j, Hua F, Zhu X-l, Li M, Wang H-x, Yu X-m, et al. Stereoselective Regulation of P-gp Activity by Clausenamide Enantiomers in Caco-2, KB/KBv and Brain Microvessel Endothelial Cells. PLoS ONE. 2015;10(8):e0135866.
98. Sousa EL, A.; Gomes, A.; Cravo, S.; Pinto, M. Synthesis of Aminated Xanthones: Exploiting Chemical Routes to Reach for Bioactive Compounds. In Proceedings of the 1st Int Electron Conf Med Chem 2015;1.
99. Taipalensuu J, Tornblom H, Lindberg G, Einarsson C, Sjoqvist F, Melhus H, et al. Correlation of gene expression of ten drug efflux proteins of the ATP-binding cassette

transporter family in normal human jejunum and in human intestinal epithelial Caco-2 cell monolayers. The Journal of pharmacology and experimental therapeutics. 2001;299(1):164-70.

CHAPTER 6:

APPENDIX

Table 14 - The chemical structures of the synthesized chiral thioxanthones.

Synthesized chiral thioxanthones	Chemical structures
ATx 1 (1) (*S*)-1-((1-hydroxypropan-2-yl)amino)-4-propoxy-9*H*-thioxanthen-9-one	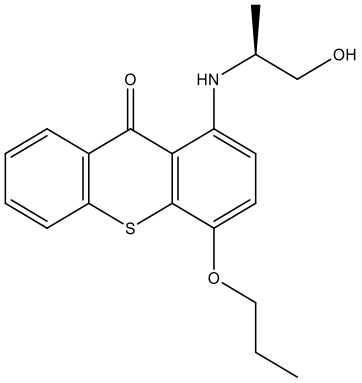
ATx 2 (2) (*R*)-1-((1-hydroxypropan-2-yl)amino)-4-propoxy-9*H*-thioxanthen-9-one	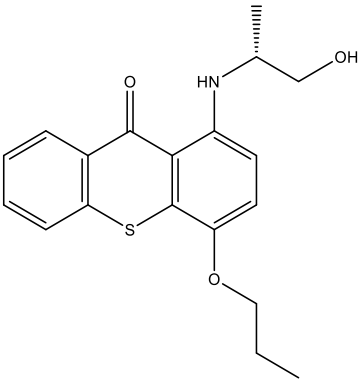
ATx 3 (3) (*S*)-1-((2-hydroxypropyl)amino)-4-propoxy-9*H*-thioxanthen-9-one	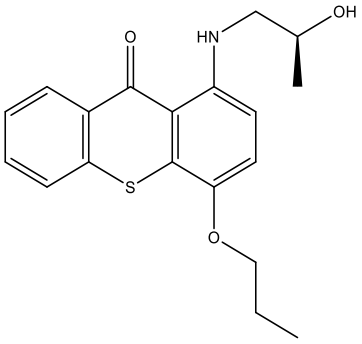
ATx 4 (4) (*R*)-1-((2-hydroxypropyl)amino)-4-propoxy-9*H*-thioxanthen-9-one	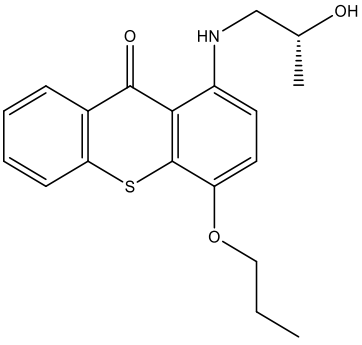

ATx 5 (5) (*S*)-1-((1-hydroxy-4-methylpentan-2-yl)amino)-4-propoxy-9*H*-thioxanthen-9-one	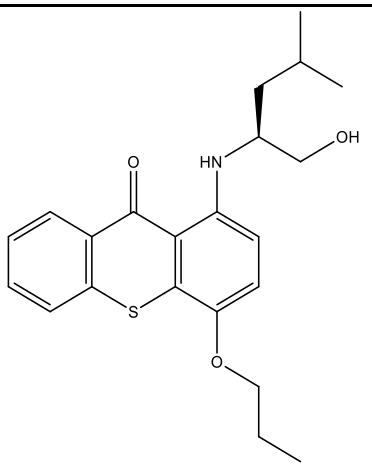
ATx 6 (6) (*R*)-1-((1-hydroxy-4-methylpentan-2-yl)amino)-4-propoxy-9*H*-thioxanthen-9-one	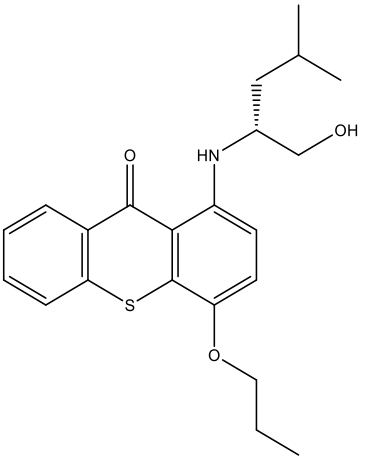
ATx 7 (7) (*S*)-1-((1-hydroxy-3-methylbutan-2-yl)amino)-4-propoxy-9*H*-thioxanthen-9-one	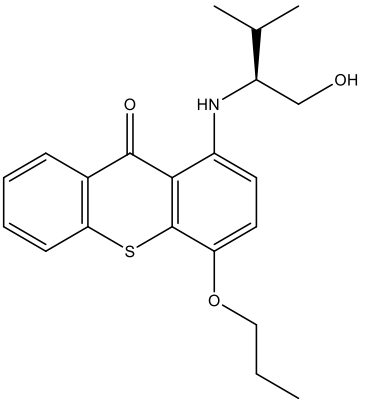
ATx 8 (8) (*R*)-1-((1-hydroxy-3-methylbutan-2-yl)amino)-4-propoxy-9*H*-thioxanthen-9-one